

# Reliable Chain-of-Thought via Prefix Consistency

Naoto Iwase<sup>1</sup> Yuki Ichihara<sup>2,3</sup> Mohammad Atif Quamar<sup>3</sup> Junpei Komiyama<sup>3,4</sup>

<sup>1</sup>Nagoya University <sup>2</sup>Nara Institute of Science and Technology

<sup>3</sup>Mohamed bin Zayed University of Artificial Intelligence <sup>4</sup>RIKEN AIP

naoto@iwase.dev {yuki.ichihara, mohammad.atif}@mbzuai.ac.ae junpei@komiyama.info

Project Page: <https://naoto-iwase.github.io/prefix-consistency-page>

## Abstract

Large Language Models often improve accuracy on reasoning tasks by sampling multiple Chain-of-Thought (CoT) traces and aggregating them with majority voting (MV), a test-time technique called self-consistency. When we truncate a CoT partway through and regenerate the remainder, we observe that traces with correct answers reproduce their original answer more often than traces with wrong answers. We use this difference as a reliability signal, **prefix consistency**, that weights each candidate answer by how often it reappears under regeneration. It requires no access to token log-probabilities or self-rating prompts. Across five reasoning models and four math and science benchmarks, prefix consistency is the best correctness predictor in most settings, and reweighting votes by it reaches Standard MV plateau accuracy at up to 21× fewer tokens (median 4.6×). Our code is available at <https://github.com/naoto-iwase/prefix-consistency>.

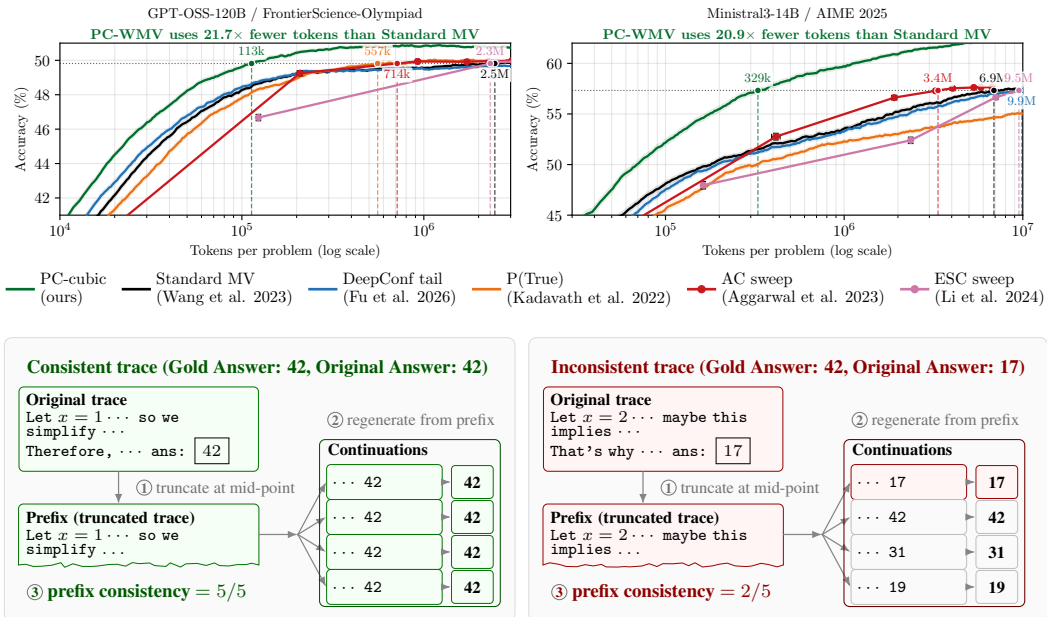


Figure 1: **Overview of prefix-consistency-weighted majority voting (PC-WMV).** *Top:* cost-equivalent accuracy on two models and benchmark settings. Shaded bands and error bars are  $\pm 2\sigma$  confidence intervals. *Bottom:* Overview of our proposed method (prefix consistency). Correct reasoning traces exhibit greater reproducibility under regeneration.

# 1 Introduction

Large Language Models (LLMs) have shown strong reasoning ability when allowed to produce Chain-of-Thought (CoT) reasoning [Kojima et al., 2022, Wei et al., 2022]. Generating intermediate reasoning steps substantially improves performance on challenging tasks such as math [Zhou et al., 2023, Fu et al., 2023], scientific reasoning [Lu et al., 2022, Wang et al., 2024], and knowledge-intensive question answering [Trivedi et al., 2023, Wang et al., 2023a].

A simple and effective way to further improve the accuracy of the final answer is majority voting (MV, also known as self-consistency), which samples a diverse set of CoTs and returns the most frequent answer [Wang et al., 2023b]. A limitation is that Standard MV treats all CoT outputs equally and still fails when the correct answer is in the minority.

To improve MV, the standard approach has been to use weighted majority voting (WMV). WMV refines MV by weighting each generation according to its quality. The more reliable a generation is, the greater the signal it receives. Existing WMV methods derive a per-sample reliability signal from the generated trace, including response probability [Wang et al., 2023b], self-certainty [Kang et al., 2025], DeepConf [Fu et al., 2026], verbalized confidence elicited in text [Lin et al., 2022, Taubenfeld et al., 2025], and P(True) [Kadavath et al., 2022]. Previous studies have demonstrated that these reliability-aware aggregation methods outperform Standard MV. However, these signals often fail to separate correct from wrong traces on difficult problems, the regime where Standard MV most needs improvement (Figure 2).

We introduce a novel reliability signal, **prefix consistency**, and incorporate it into WMV. This signal is motivated by the observation that correct reasoning traces tend to be more reproducible under regeneration than incorrect ones. We truncate each sample’s CoT at a specified fraction and regenerate continuations from the prefix (Figure 1). Prefix consistency requires no access to token log-probabilities. Since regenerated answers also participate in voting, our method recovers correct answers absent from the initial samples.

Our contributions are:

1. We propose *prefix consistency*, a reliability signal that truncates each sample’s CoT and regenerates from the prefix, and use it to form prefix-consistency-weighted majority voting (PC-WMV). PC-WMV requires no access to token log-probabilities.
2. Across 4 benchmarks and 5 model scales, prefix consistency outperforms existing WMV baselines (e.g. DeepConf, P(True), Self-certainty) as a correctness predictor (best macro-averaged AUROC on 15 out of 20 (model, benchmark) cells, .63–.80). On many problems with Pass@1 below 50%, where Standard MV fails by default, prefix consistency still discriminates correct from wrong traces (Section 4.4), leaving room for PC-WMV to find the correct answer.
3. In cost-equivalent comparison against the primary WMV baselines (DeepConf tail, P(True), Self-certainty) and adaptive-stopping baselines (AC, ESC), PC-WMV is the most cost-efficient on the majority of the 20 (model, benchmark) settings, reaching Standard MV plateau at a median  $4.6\times$  fewer tokens (up to  $21\times$  vs. Standard MV and  $10\times$  vs. AC sweep, Figure 1 and Table 4).

## 2 Preliminary

We consider a benchmark  $\mathcal{Q}$ , a set of problems. For each problem  $q \in \mathcal{Q}$ , we have an answer space  $\mathcal{A}$  and a correct answer  $a_q^* \in \mathcal{A}$ . Given  $q$ , an LLM generates a trace  $y$ , i.e., a sequence of tokens that represents a CoT followed by a final summary, from which we parse the final answer  $a \in \mathcal{A}$ . We write  $(y, a) \sim \text{LLM}(\cdot | q)$ . We write  $\text{Pass}@1_q := \Pr_{(y,a) \sim \text{LLM}(\cdot | q)}[a = a_q^*]$  for the per-problem single-sample success probability, and report the macro-average over  $\mathcal{Q}$  as the benchmark-level Pass@1. When the context is clear, we suppress  $q$  in the notation (e.g.,  $a^*$  instead of  $a_q^*$ ).

To improve the accuracy over Pass@1 at test time, we draw  $N$  independent samples  $\{(y_i, a_i)\}_{i=1}^N$  and aggregate them into a single output. A standard method that aggregates the  $N$  answers is *majority voting* (MV, also known as self-consistency), which returns the most frequent answer:

$$\hat{a}_N^{\text{MV}} = \arg \max_{a \in \mathcal{A}} \sum_{i=1}^N \mathbf{1}[a_i = a]. \quad (1)$$

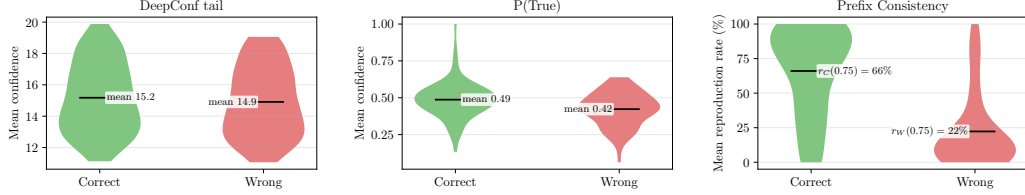


Figure 2: **Per-problem reliability signal distributions for correct vs. wrong traces** on FrontierScience-Olympiad with GPT-OSS-120B. Each violin shows the distribution of per-problem mean signal values across the 73 problems that have at least one correct and one wrong trace. On this difficult benchmark (Pass@1  $\approx$  .34), the baseline methods DeepConf tail and P(True) place correct and wrong traces in nearly overlapping ranges, while prefix consistency separates them. The same baselines have some discriminative ability on easier (model, benchmark) settings (Table 2). The point is that they fail precisely in the regime where reweighting matters most.

We refer to this unweighted aggregator as *Standard MV* (Eq. (1)). Standard MV treats all samples equally and fails when the correct answer is not the mode of the answer distribution, typically observed when an LLM faces challenging problems where Pass@1 accuracy is below 50%. A natural extension is *weighted majority voting* (WMV), where each sample  $i$  contributes a weighted vote  $v_i(a) \geq 0$  for answer  $a$ :

$$\hat{a}_N^{\text{WMV}} = \arg \max_{a \in \mathcal{A}} \sum_{i=1}^N v_i(a). \quad (2)$$

For sample  $i$ , let  $\ell_i$  denote the model’s token-level log-probabilities available to the signal. Prior WMV methods extract a confidence signal  $s(y_i, \ell_i) \geq 0$  from the trace and apply a weighting function  $w: \mathbb{R}_{\geq 0} \rightarrow \mathbb{R}_{\geq 0}$  to it:

$$v_i(a) = w(s(y_i, \ell_i)) \cdot \mathbf{1}[a_i = a]. \quad (3)$$

Another class of WMV methods adopts verbalized signals that require no log-probability access ( $\ell_i = \emptyset$ ), where  $s$  depends only on the text of  $y_i$ . Other methods (Self-certainty, DeepConf, Response probability) set  $\ell_i$  to the per-token log-probabilities along  $y_i$ . P(True) sets  $\ell_i$  to the log-probability of the “True” token under a self-rating prompt. Appendix E gives the explicit form of  $s$  and  $w$  for each baseline. However, such confidence signals often fail to separate correct traces from wrong traces on difficult problems. We next introduce prefix consistency, a signal that requires no log-probability access ( $\ell_i = \emptyset$ ).

### 3 Prefix Consistency

We propose prefix consistency, a reliability signal: truncate each sample’s CoT at an intermediate point and regenerate its continuation, treating samples whose initial answer reappears as more reliable than those whose answer changes (Figure 1).

#### 3.1 Prefix Consistency as a Reliability Signal

For each sample  $(y_i, a_i)$ , let  $|y_i|$  denote the number of tokens in  $y_i$ . We truncate  $y_i$  after its first  $\lceil \tau |y_i| \rceil$  tokens for a fixed fraction  $\tau \in (0, 1)$ , and regenerate  $K$  continuations from this prefix, yielding the multiset:

$$A_i^{(\tau, K)} = \{a_i, \tilde{a}_{i,1}^{(\tau)}, \dots, \tilde{a}_{i,K}^{(\tau)}\}. \quad (4)$$

We refer to  $A_i^{(\tau, K)}$  as the  $i$ -th *group*. For the following discussion, we focus on the case when  $K = 1$ . We will write  $A_i^{(\tau)}$  for  $A_i^{(\tau, 1)}$  and write  $\tilde{a}_i^{(\tau)}$  for  $\tilde{a}_{i,1}^{(\tau)}$ . Extending this to arbitrary  $K$  is straightforward.

The key empirical phenomenon is a *reproduction-rate asymmetry*: a regenerated answer is more likely to match the initial answer when the initial answer is correct. Let  $r_C(\tau)$  and  $r_W(\tau)$  denote the probabilities of reproducing the initial answer, conditioned on whether it is correct or wrong:

$$r_C(\tau) := \Pr[\tilde{a}_i^{(\tau)} = a_i \mid a_i = a^*], \quad r_W(\tau) := \Pr[\tilde{a}_i^{(\tau)} = a_i \mid a_i \neq a^*] \quad (5)$$

---

**Algorithm 1** Prefix-Consistency-Weighted Majority Voting (PC-WMV)

---

**Require:** Problem  $q$ , #groups  $N$ , truncation fraction  $\tau$ , #regenerations per group  $K$ , weighting  $w$

```
1: votes  $\leftarrow \emptyset$  {map from answer to accumulated votes}
2: for  $i = 1$  to  $N$  do
3:    $y_i \leftarrow \text{GENERATE TRACE}(q)$ 
4:    $a_i \leftarrow \text{EXTRACT ANSWER}(y_i)$ 
5:    $y_i[:\lceil \tau |y_i| \rceil] \leftarrow \text{TRUNCATE}(y_i, \tau)$  {shared prefix}
6:    $A_i^{(\tau, K)} \leftarrow [a_i]$  {multiset of answers for  $i$ -th group}
7:   for  $k = 1$  to  $K$  do
8:      $\tilde{y}_{i,k}^{(\tau)} \leftarrow \text{CONTINUE FROM PREFIX}(q, y_i[:\lceil \tau |y_i| \rceil])$ 
9:      $\tilde{a}_{i,k}^{(\tau)} \leftarrow \text{EXTRACT ANSWER}(\tilde{y}_{i,k}^{(\tau)})$ 
10:    append  $\tilde{a}_{i,k}^{(\tau)}$  to  $A_i^{(\tau, K)}$ 
11:   end for
12:   for each distinct  $a$  in  $A_i^{(\tau, K)}$  do
13:      $c_i^{(\tau, K)}(a) \leftarrow |\{a' \in A_i^{(\tau, K)} : a' = a\}| / (K+1)$  {general- $K$  form of Eq. (7)}
14:     votes[ $a$ ]  $\leftarrow$  votes[ $a$ ] +  $w(c_i^{(\tau, K)}(a))$ 
15:   end for
16: end for
17: return  $\arg \max_{a \in \mathcal{A}} \text{votes}[a]$ 
```

---

Across models and benchmarks, we consistently observe the following inequality (Table 1):

$$r_C(\tau) > r_W(\tau). \quad (6)$$

In other words, when the initial answer is correct, regeneration from its prefix tends to produce the same answer. When the initial answer is incorrect, regeneration more often produces a different incorrect answer than the same incorrect answer. Figure 2 illustrates this asymmetry on FrontierScience-Olympiad with GPT-OSS-120B and contrasts it with two baseline signals (DeepConf tail and  $P(\text{True})$ ) that fail to distinguish between correct and incorrect traces.

To exploit this observation, we score each candidate  $a \in A_i^{(\tau)}$  by its reproducibility within the group:

$$c_i^{(\tau)}(a) := \frac{|\{a' \in A_i^{(\tau)} : a' = a\}|}{2}. \quad (7)$$

We denote the *prefix consistency score* of  $a$  in group  $i$  by  $c_i^{(\tau)}(a) \in \{0, 1/2, 1\}$ . Unlike conventional per-sample reliability signals (e.g., DeepConf tail,  $P(\text{True})$ ), which assign a single scalar to each sample’s initial answer,  $c_i^{(\tau)}(a)$  is defined for every candidate  $a \in A_i^{(\tau)}$ , including regenerated answers that did not appear among the initial answers.

### 3.2 Prefix-Consistency-Weighted Majority Voting (Algorithm 1)

We set the WMV weight in Eq. (2) using Eq. (7):

$$v_i(a) = w\left(c_i^{(\tau)}(a)\right) \quad (8)$$

where  $w: [0, 1] \rightarrow \mathbb{R}_{\geq 0}$  with  $w(0) = 0$ .

We refer to this method as **prefix-consistency-weighted majority voting (PC-WMV)** (Algorithm 1). Since Eq. (8) weights every distinct  $a \in A_i^{(\tau)}$  rather than only the initial answer  $a_i$ , PC-WMV’s aggregated vote  $\sum_i v_i(a)$  can be positive for regenerated answers absent from the initial  $N$  samples. This is the operational consequence of using a per-candidate signal rather than a per-sample one.

We now demonstrate that this additional flexibility results in a clear advantage over Standard MV in situations where Standard MV is proven to fail. Standard MV fails when the correct answer occurs less frequently than a wrong answer. The following theorem, in the simplest case of a binary answer space, demonstrates how PC-WMV uses the reproduction-rate asymmetry to recover the correct answer in this regime.

**Theorem 1** (PC-WMV strictly improves over Standard MV when  $r_C(\tau) > r_W(\tau)$ ). Fix  $\tau \in (0, 1)$  and  $K = 1$ . Let  $\mathcal{A} = \{a^*, a'\}$ , where  $a^*$  is the correct answer and  $a'$  is the only wrong answer. Assume the  $N$  groups are i.i.d., and let  $\pi(a^*) := \Pr[a_i = a^*]$  denote the Pass@1. Assume  $r_C(\tau) > r_W(\tau) > 0$ . For any weighting function  $w$  with  $w(0) = 0$  and  $w(1) > 0$ , in the limit of  $N \rightarrow \infty$ , PC-WMV converges to  $a^*$  iff

$$\pi(a^*) > \frac{r_W(\tau)}{r_C(\tau) + r_W(\tau)}. \quad (9)$$

In contrast, Standard MV converges to  $a^*$  if and only if  $\pi(a^*) > \frac{1}{2}$ . Therefore, PC-WMV converges to  $a^*$  on the interval where Standard MV does not:

$$\pi(a^*) \in \left( \frac{r_W(\tau)}{r_C(\tau) + r_W(\tau)}, \frac{1}{2} \right], \quad (10)$$

of width

$$\frac{D(\tau)}{2(r_C(\tau) + r_W(\tau))} \quad (D(\tau) := r_C(\tau) - r_W(\tau)). \quad (11)$$

The formal proof of Theorem 1 is in Appendix C.3.

*Interpretation.* The key quantity in our analysis is  $D(\tau)$ , which we call the *discrimination gap*. Theorem 1 considers the simple case of two answer candidates, correct and wrong: when  $D(\tau) > 0$ , PC-WMV recovers the correct answer in cases where the majority is wrong, provided that Pass@1 falls within the interval of Eq. (10). The larger  $D(\tau)$  is, the wider the region in which PC-WMV outperforms Standard MV. Our benchmarks (Table 1) show that  $D(\tau)$  is substantially larger than 0 across models and benchmarks, so PC-WMV is effective in practice.

**Hyperparameters.** Prefix consistency has two hyperparameters: the truncation fraction  $\tau \in (0, 1)$  and the number of regenerations per group  $K \in \mathbb{N}$ . PC-WMV adds a third, the weighting function  $w: [0, 1] \rightarrow \mathbb{R}_{\geq 0}$  with  $w(0) = 0$ .

## 4 Experiments

We conduct experiments on science (FrontierScience-Olympiad [Wang et al., 2025]) and math (HMMT Feb 2026, AIME 2025, Brumo 2025 [Balunović et al., 2025]) datasets. We evaluate on five reasoning LLMs: GPT-OSS-120B, GPT-OSS-20B [OpenAI, 2025], Nemotron3-30B (NVIDIA-Nemotron-3-Nano-30B-A3B-BF16) [NVIDIA, 2025a], Nemotron2-9B (NVIDIA-Nemotron-Nano-9B-v2) [NVIDIA, 2025b], and Ministral3-14B (Ministral-3-14B-Reasoning-2512) [Mistral AI, 2026].

We compare our proposed methods against Standard MV, three primary WMV baselines (Self-certainty [Kang et al., 2025], DeepConf tail [Fu et al., 2026], and P(True) [Kadavath et al., 2022, Taubenfeld et al., 2025]), and two adaptive-stopping rules over MV (Adaptive Consistency, AC [Aggarwal et al., 2023], and Early-Stopping Self-Consistency, ESC [Li et al., 2024]). The details of these methods are documented in Appendix E.

**Hyperparameters of prefix consistency.** Unless otherwise specified, we fix the truncation fraction at  $\tau = 0.75$ . The results in the main paper use  $K = 1$  throughout. We accordingly suppress  $\tau$  in the notation and write  $c_i(a), r_C, r_W, D$  for  $c_i^{(\tau)}(a), r_C(\tau), r_W(\tau), D(\tau)$ .

### 4.1 Prefix Consistency as a Correctness Predictor

We report  $\overline{\text{AUROC}}$ , the macro-averaged AUROC over problems with at least one correct and one wrong initial sample (formal definition in Appendix G.2).

Note that some previous work [Xiong et al., 2024, Fadeeva et al., 2024] adopted AUROC pooled across problems, which differs from  $\overline{\text{AUROC}}$ . However, as argued in Taubenfeld et al. [2025], such an

Table 1: **Reproduction rates  $r_C, r_W$  and discrimination gap  $D = r_C - r_W$  for prefix consistency (larger  $D$  is better).** Macro-averaged over problems with at least one correct and one wrong initial sample.  $r_C \geq r_W$  holds on every (model, benchmark) cell, and a larger  $D$  predicts a larger PC-WMV advantage over Standard MV (Theorem 1).

Benchmark	GPT-OSS-120B			GPT-OSS-20B			Nemotron3-30B			Nemotron2-9B			Ministral3-14B		
	$r_C$	$r_W$	$D$	$r_C$	$r_W$	$D$	$r_C$	$r_W$	$D$	$r_C$	$r_W$	$D$	$r_C$	$r_W$	$D$
FrontierScience-Olympiad	66.0	22.3	43.7	55.4	14.0	41.4	50.9	24.7	26.2	45.0	37.5	7.4	56.4	26.0	30.4
HMMT Feb 2026	87.8	48.1	39.7	78.3	29.7	48.6	80.0	40.4	39.6	79.3	49.6	29.7	74.5	32.0	42.4
AIME 2025	95.5	61.7	33.7	87.8	42.6	45.2	74.7	38.2	36.5	69.5	43.2	26.3	77.3	26.1	51.1
Brumo 2025	83.8	56.7	27.1	82.8	39.0	43.7	75.6	15.3	60.3	81.2	54.7	26.6	76.2	24.4	51.8

Table 2: **AUROC for correctness discrimination (higher is better).** Macro-averaged AUROC per (model, benchmark), with the best per column in bold.

Signal	GPT-OSS-120B				GPT-OSS-20B				Nemotron3-30B				Nemotron2-9B				Ministral3-14B			
	FSci	HMMT	AIME	Brumo	FSci	HMMT	AIME	Brumo	FSci	HMMT	AIME	Brumo	FSci	HMMT	AIME	Brumo	FSci	HMMT	AIME	Brumo
Prefix consistency	<b>.719</b>	.698	.669	<b>.636</b>	<b>.707</b>	<b>.743</b>	<b>.726</b>	<b>.719</b>	<b>.631</b>	<b>.698</b>	<b>.682</b>	<b>.801</b>	.537	<b>.648</b>	.631	.633	<b>.652</b>	<b>.712</b>	<b>.756</b>	<b>.759</b>
Self-certainty	.570	.664	.641	.549	.545	.570	.560	.484	.496	.414	.520	.655	.458	.605	.537	.580	.318	.359	.408	.342
DeepConf bottom-10%	.525	.640	.601	.486	.525	.580	.565	.481	.474	.413	.514	.607	.434	.515	.529	.515	.342	.331	.395	.347
DeepConf tail	.565	<b>.728</b>	<b>.703</b>	.606	.583	.659	.645	.557	.508	.588	.465	.755	.494	.628	.665	.641	.349	.404	.421	.358
Verbal 0-100	.516	.552	.505	.436	.516	.574	.561	.511	.524	.489	.606	.532	.571	.563	.584	.548	.505	.525	.525	.450
P(True)	.568	.550	.551	.527	.587	.667	.592	.583	.493	.532	.578	.564	<b>.620</b>	.635	<b>.724</b>	<b>.708</b>	.469	.454	.441	.477

Abbreviations: FSci = FrontierScience-Olympiad, HMMT = HMMT Feb 2026, AIME = AIME 2025, Brumo = Brumo 2025.

AUROC pooled across problems conflates within-problem discrimination with cross-problem score-difficulty correlation, and only the former predicts whether confidence-weighted self-consistency improves over Standard MV. They also report that calibration metrics such as Expected Calibration Error (ECE) and Brier score are similarly unsuitable. In their data, the best-calibrated source (verbalized binary) gave the smallest improvement while the strongest method (P(True) therein) was only moderately calibrated. At vote time, every WMV method (including PC-WMV and all baselines) compares scores only among samples from the same problem, and thus we consider  $\overline{\text{AUROC}}$  to better measure discriminative ability between correct traces and wrong traces.

Table 1 reports the discrimination gap  $D = r_C - r_W$  for prefix consistency:  $D > 0$  on every (model, benchmark) cell, confirming the asymmetry  $r_C > r_W$ . Table 2 reports  $\overline{\text{AUROC}}$  for prefix consistency against the WMV baselines. Prefix consistency has the highest  $\overline{\text{AUROC}}$  on 15 of 20 cells (typically around 0.7), separating correct from wrong traces more clearly than the baselines. Baselines’  $\overline{\text{AUROC}}$  often hovers near 0.5 (= random<sup>1</sup>) on harder cells, where their scores differ little between correct and wrong samples, reaching  $\sim 0.7$  only on some easier cells.

## 4.2 Weighted Majority Voting Results

We compare PC-WMV against existing WMV methods under the same computational cost.

**Weighting variants.** We use the power family  $w^{(n)}(c) = c^n$  for  $n \in \{1, 2, 3\}$ , denoted PC-linear, PC-quadratic, and PC-cubic, where the “PC” prefix abbreviates prefix consistency. Under  $K = 1$ ,  $c_i(a) \in \{0, 1/2, 1\}$ . Thus, a candidate that is reproduced under regeneration ( $c = 1$ ) receives weight 1, while a candidate that appears in only one of the two traces ( $c = 1/2$ ) receives weight  $1/2^n$ . The weight ratio between a reproduced candidate and a single-trace one is therefore  $2^n : 1$ , that is, 2 : 1 for linear, 4 : 1 for quadratic, and 8 : 1 for cubic. The larger  $n$  is, the more pronounced the relative weight given to reproduced answers.

**Cost-equivalent evaluation.** We measure inference cost by the total number of generated tokens, treating each generated token as equally expensive, and log-probability access as free. For each model and benchmark, we first generate  $N=128$  initial samples per problem ( $N=64$  for Ministral3-14B), from which all methods sample with replacement under a common token budget  $B$ . See Appendix G for the pool construction, trial design, and confidence-interval definition.

<sup>1</sup> $\overline{\text{AUROC}} = 0.5$  is the value attained by a random signal that is uninformative about correctness.

Table 3: **Weighted majority voting accuracy at fixed token budget  $B$  (higher is better)**. Each method’s accuracy at  $B \in \{250k, 1M, 5M\}$  tokens sampled from the shared pool, with the best per (model,  $B$ ) column in bold.

Benchmark	Method	GPT-OSS-120B			Nemotron3-30B			Ministral3-14B		
		$B=250k$	$B=1M$	$B=5M$	$B=250k$	$B=1M$	$B=5M$	$B=250k$	$B=1M$	$B=5M$
FrontierScience-Olympiad	Standard MV	.493±.001	.495±.001	.499±.001	.404±.002	.468±.002	.490±.001	.137±.001	.141±.001	.142±.001
	Self-certainty	.494±.001	.495±.001	.497±.001	.402±.002	.468±.002	.491±.001	.130±.001	.135±.001	.137±.001
	DeepConf tail	.493±.001	.495±.001	.497±.001	.405±.002	.470±.002	.494±.001	.130±.001	.134±.001	.137±.001
	P(True)	.493±.001	.500±.001	.500±.000	.394±.003	.465±.002	.492±.002	.137±.001	.143±.001	.146±.001
	PC-linear	.495±.001	.496±.001	.496±.001	.429±.002	.481±.002	.494±.001	.149±.002	.160±.001	.162±.001
	PC-quadratic	.502±.001	.504±.001	.503±.001	<b>.433±.002</b>	<b>.486±.002</b>	<b>.504±.002</b>	.156±.002	.170±.001	.173±.001
	PC-cubic	<b>.506±.001</b>	<b>.508±.001</b>	<b>.507±.001</b>	<b>.433±.002</b>	<b>.486±.002</b>	.503±.001	<b>.158±.002</b>	<b>.174±.001</b>	<b>.181±.001</b>
HMMT Feb 2026	Standard MV	.708±.003	.745±.003	.763±.001	.736±.004	.777±.003	.802±.002	.413±.004	<b>.440±.003</b>	.458±.002
	Self-certainty	.713±.003	.749±.003	.768±.002	.734±.004	.779±.003	<b>.804±.002</b>	.409±.004	.429±.003	.438±.002
	DeepConf tail	.720±.003	.758±.003	.783±.002	.740±.004	.779±.003	.801±.002	.408±.004	.427±.003	.436±.002
	P(True)	.706±.003	.743±.003	.784±.002	.736±.004	.779±.003	<b>.804±.002</b>	.404±.003	.429±.003	.433±.002
	PC-linear	.717±.003	.751±.002	.764±.001	<b>.742±.004</b>	.785±.003	.802±.002	<b>.418±.004</b>	<b>.440±.003</b>	.444±.002
	PC-quadratic	.725±.003	.764±.002	.782±.001	<b>.742±.004</b>	<b>.787±.003</b>	.803±.002	.415±.004	<b>.440±.003</b>	.447±.002
	PC-cubic	<b>.727±.003</b>	<b>.771±.002</b>	<b>.786±.001</b>	<b>.742±.004</b>	<b>.787±.003</b>	<b>.804±.002</b>	.414±.004	<b>.440±.003</b>	<b>.461±.002</b>
AIME 2025	Standard MV	.901±.002	.901±.001	.900±.000	.935±.002	<b>.966±.000</b>	<b>.967±.000</b>	.508±.003	.535±.003	.569±.002
	Self-certainty	.904±.002	.903±.001	.900±.000	.935±.002	<b>.966±.000</b>	<b>.967±.000</b>	.503±.003	.533±.003	.565±.002
	DeepConf tail	.906±.002	.905±.001	.900±.000	<b>.937±.002</b>	<b>.966±.000</b>	<b>.967±.000</b>	.506±.003	.533±.003	.565±.002
	P(True)	.902±.002	.909±.001	.906±.001	.930±.003	.964±.001	<b>.967±.000</b>	.495±.003	.523±.003	.542±.002
	PC-linear	.906±.002	.913±.002	.909±.001	.932±.003	.964±.001	<b>.967±.000</b>	.556±.003	.583±.003	.600±.002
	PC-quadratic	.912±.002	.922±.002	.930±.002	.932±.003	.963±.001	<b>.967±.000</b>	<b>.565±.003</b>	.595±.003	.616±.002
	PC-cubic	<b>.913±.002</b>	<b>.926±.002</b>	<b>.941±.002</b>	.932±.003	.963±.001	<b>.967±.000</b>	.564±.003	<b>.597±.003</b>	<b>.621±.002</b>
Bruno 2025	Standard MV	.801±.003	.821±.002	.833±.000	.896±.003	.928±.002	.931±.001	.669±.004	.691±.003	.699±.003
	Self-certainty	.805±.003	.826±.002	.833±.000	.918±.003	.954±.002	.963±.001	.659±.004	.682±.003	.686±.002
	DeepConf tail	.810±.003	.831±.001	.833±.000	.920±.003	.955±.002	.965±.001	.659±.004	.681±.003	.683±.002
	P(True)	.794±.003	.821±.003	.844±.002	.886±.003	.917±.002	.929±.001	.632±.004	.658±.003	.661±.003
	PC-linear	.810±.003	.830±.002	.833±.000	<b>.933±.003</b>	<b>.961±.002</b>	<b>.968±.001</b>	.675±.004	.705±.003	.723±.002
	PC-quadratic	.815±.003	.837±.002	.842±.001	.932±.003	.959±.002	<b>.968±.001</b>	.684±.004	.719±.003	.740±.002
	PC-cubic	<b>.818±.003</b>	<b>.842±.002</b>	<b>.857±.001</b>	.929±.003	.953±.002	.964±.001	<b>.686±.004</b>	<b>.727±.003</b>	<b>.759±.003</b>

Table 3 reports accuracy under fixed token budgets (250k, 1M, and 5M tokens) across the three models and four benchmarks. At 1M tokens, prefix consistency matches or exceeds all baselines on the more difficult benchmarks (FrontierScience-Olympiad, HMMT Feb 2026), while the advantage is smaller on AIME 2025 where Standard MV already achieves high accuracy. The improvements are consistent across weighting functions (PC-linear, PC-quadratic, and PC-cubic). PC-cubic provides the greatest improvement for the most difficult problems. Per-model tables with the full set of baselines (DeepConf variants, Response probability, verbalized confidence, P(True)) for all five models, including the two not shown above (GPT-OSS-20B, Nemotron2-9B), are reported in Appendix D.3.

### 4.3 Token Efficiency

Section 4.2 reported accuracy under fixed budget constraints. We next compare how many tokens each method needs to reach the same target accuracy.

Table 4 shows the token-efficiency ratio  $B_{\text{method}}/B_{\text{MV}}$ , where  $B_X$  is the budget method  $X$  needs to reach the target accuracy  $\text{Pass}@1 + \alpha \times (\text{Standard MV plateau} - \text{Pass}@1)$  for  $\alpha \in \{75\%, 90\%, 99\%\}$ . The Standard MV plateau is Standard MV’s bootstrap-saturated accuracy on the  $N$ -sample pool (Appendix G.3), so  $\alpha$  interpolates between  $\text{Pass}@1$  ( $\alpha=0$ ) and this plateau ( $\alpha=1$ ). A ratio  $< 1$  means  $X$  is more cost-efficient than Standard MV at the target; e.g.,  $0.05 \times$  corresponds to the  $21 \times$  saving in Figure 1. The headline numbers in this paper (median  $4.6 \times$ , up to  $21 \times$  vs. Standard MV, up to  $10 \times$  vs. AC sweep) are computed at  $\alpha=99\%$  across all 20 (model, benchmark) cells: Table 4 together with Table 12 (GPT-OSS-20B) and Table 14 (Nemotron2-9B) in Appendix D.3.

PC-cubic is more cost-efficient than Standard MV on 11 out of 12 model and benchmark settings at  $\alpha=99\%$ . The strongest savings are  $0.05 \times$  on both FrontierScience-Olympiad with GPT-OSS-120B and AIME 2025 with Ministral3-14B, and  $0.08 \times$  on FrontierScience-Olympiad with Ministral3-14B. All three correspond to cells with large  $D$  (Table 1).

The savings track the discrimination gap  $D$  (Table 1): pairs with the largest  $D$  yield the largest reductions. PC-cubic offers little advantage over Standard MV on two cells (it underperforms on Nemotron3-30B AIME 2025 and only marginally beats Standard MV on Nemotron3-30B HMMT Feb 2026), both of which have a small  $\text{Pass}@1$ -to-plateau gap of at most .11 (.902  $\rightarrow$  .967 and .708  $\rightarrow$  .810), leaving little room above  $\text{Pass}@1$  for any reweighting irrespective of  $D$ . The practical penalty in this regime, where  $\text{Pass}@1$  is close to Standard MV plateau, is correspondingly small.

Table 4: **Token efficiency ratio  $B_{\text{method}}/B_{\text{MV}}$  at target accuracy  $\alpha$  between Pass@1 and the Standard MV plateau (smaller is better).**  $B_X$  is the budget method  $X$  needs to reach Pass@1 +  $\alpha \times$  (Standard MV plateau – Pass@1) for  $\alpha \in \{75\%, 90\%, 99\%\}$ . Cells  $<1$  indicate more cost-efficient than Standard MV. “N/A” indicates the method’s plateau is below the target. Best method per column in bold.

Benchmark	Method	GPT-OSS-120B			Nemotron3-30B			Ministral3-14B		
		$\alpha=75\%$	$\alpha=90\%$	$\alpha=99\%$	$\alpha=75\%$	$\alpha=90\%$	$\alpha=99\%$	$\alpha=75\%$	$\alpha=90\%$	$\alpha=99\%$
FrontierScience-Olympiad	Pass@1 / Standard MV plateau	.338 / .500			.295 / .493			.091 / .142		
	Standard MV budget ( $B_{\text{MV}}$ )	45k	107k	2.5M	486k	1.3M	6.0M	118k	249k	924k
	Self-certainty	$0.89 \pm 0.04 \times$	$0.87 \pm 0.06 \times$	N/A	$1.04 \pm 0.06 \times$	$1.01 \pm 0.11 \times$	$0.85 \pm 0.19 \times$	$1.62 \pm 0.20 \times$	$>10 \times$	N/A
	DeepConf tail	$0.91 \pm 0.05 \times$	$0.91 \pm 0.07 \times$	N/A	$0.97 \pm 0.06 \times$	$0.88 \pm 0.08 \times$	$0.56 \pm 0.14 \times$	$1.54 \pm 0.18 \times$	$>10 \times$	N/A
	P(True)	$1.23 \pm 0.05 \times$	$1.20 \pm 0.10 \times$	$0.23 \pm 0.09 \times$	$1.14 \pm 0.06 \times$	$1.10 \pm 0.11 \times$	$0.75 \pm 0.18 \times$	$1.10 \pm 0.12 \times$	$1.01 \pm 0.27 \times$	$0.48 \pm 0.30 \times$
	AC sweep	$1.93 \pm 0.09 \times$	$1.54 \pm 0.12 \times$	$0.29 \pm 0.15 \times$	$1.24 \pm 0.07 \times$	$0.87 \pm 0.09 \times$	$0.49 \pm 0.13 \times$	$2.48 \pm 0.40 \times$	$4.28 \pm 1.45 \times$	N/A
	ESC sweep	$2.74 \pm 0.08 \times$	$5.59 \pm 0.70 \times$	$0.94 \pm 0.53 \times$	$2.06 \pm 0.26 \times$	$3.62 \pm 0.41 \times$	$2.23 \pm 0.58 \times$	$4.53 \pm 1.55 \times$	$>10 \times$	$>10 \times$
	PC-linear	$0.70 \pm 0.03 \times$	$0.63 \pm 0.05 \times$	$3.88 \pm 0.37 \times$	$0.67 \pm 0.04 \times$	$0.54 \pm 0.05 \times$	$0.40 \pm 0.09 \times$	<b><math>0.38 \pm 0.04 \times</math></b>	$0.26 \pm 0.07 \times$	$0.10 \pm 0.07 \times$
	PC-quadratic	<b><math>0.65 \pm 0.03 \times</math></b>	<b><math>0.52 \pm 0.04 \times</math></b>	$0.06 \pm 0.02 \times$	<b><math>0.61 \pm 0.03 \times</math></b>	<b><math>0.48 \pm 0.04 \times</math></b>	$0.24 \pm 0.06 \times$	<b><math>0.38 \pm 0.04 \times</math></b>	<b><math>0.24 \pm 0.06 \times</math></b>	<b><math>0.08 \pm 0.05 \times</math></b>
	PC-cubic	<b><math>0.65 \pm 0.03 \times</math></b>	<b><math>0.52 \pm 0.04 \times</math></b>	<b><math>0.05 \pm 0.02 \times</math></b>	<b><math>0.61 \pm 0.03 \times</math></b>	<b><math>0.48 \pm 0.04 \times</math></b>	<b><math>0.22 \pm 0.05 \times</math></b>	<b><math>0.38 \pm 0.04 \times</math></b>	<b><math>0.24 \pm 0.06 \times</math></b>	<b><math>0.08 \pm 0.05 \times</math></b>
HMMT Feb 2026	Pass@1 / Standard MV plateau	.589 / .760			.708 / .810			.270 / .463		
	Standard MV budget ( $B_{\text{MV}}$ )	364k	858k	1.8M	1.6M	4.2M	8.5M	258k	1.2M	7.4M
	Self-certainty	$0.74 \pm 0.07 \times$	$0.85 \pm 0.07 \times$	$0.87 \pm 0.11 \times$	$0.85 \pm 0.15 \times$	$0.89 \pm 0.14 \times$	$0.93 \pm 0.12 \times$	$1.29 \pm 0.17 \times$	N/A	N/A
	DeepConf tail	$0.63 \pm 0.09 \times$	$0.72 \pm 0.08 \times$	$0.57 \pm 0.07 \times$	$0.82 \pm 0.15 \times$	$0.97 \pm 0.19 \times$	N/A	$1.29 \pm 0.17 \times$	N/A	N/A
	P(True)	$1.05 \pm 0.14 \times$	$1.17 \pm 0.14 \times$	$0.94 \pm 0.09 \times$	$0.86 \pm 0.15 \times$	$0.90 \pm 0.12 \times$	$0.82 \pm 0.10 \times$	$1.33 \pm 0.14 \times$	N/A	N/A
	AC sweep	<b><math>0.42 \pm 0.05 \times</math></b>	$0.63 \pm 0.10 \times$	N/A	<b><math>0.51 \pm 0.09 \times</math></b>	<b><math>0.34 \pm 0.05 \times</math></b>	<b><math>0.24 \pm 0.03 \times</math></b>	$1.52 \pm 0.28 \times$	$1.21 \pm 0.28 \times$	<b><math>0.60 \pm 0.20 \times</math></b>
	ESC sweep	$1.96 \pm 0.33 \times$	$6.66 \pm 1.29 \times$	N/A	$4.33 \pm 1.24 \times$	$3.12 \pm 0.46 \times$	$1.88 \pm 0.26 \times$	$8.79 \pm 1.33 \times$	$4.75 \pm 1.03 \times$	$2.05 \pm 0.75 \times$
	PC-linear	$0.70 \pm 0.08 \times$	$0.79 \pm 0.08 \times$	$0.88 \pm 0.11 \times$	$0.62 \pm 0.11 \times$	$0.86 \pm 0.16 \times$	N/A	<b><math>0.85 \pm 0.11 \times</math></b>	$1.11 \pm 0.28 \times$	N/A
	PC-quadratic	$0.52 \pm 0.05 \times$	$0.49 \pm 0.04 \times$	$0.41 \pm 0.04 \times$	$0.56 \pm 0.10 \times$	$0.80 \pm 0.15 \times$	$1.10 \pm 0.15 \times$	$0.91 \pm 0.11 \times$	$1.01 \pm 0.26 \times$	N/A
	PC-cubic	$0.52 \pm 0.05 \times$	<b><math>0.46 \pm 0.04 \times</math></b>	<b><math>0.35 \pm 0.04 \times</math></b>	$0.59 \pm 0.10 \times$	$0.79 \pm 0.13 \times$	$0.95 \pm 0.14 \times$	$1.03 \pm 0.12 \times$	$0.98 \pm 0.20 \times$	$0.67 \pm 0.20 \times$
AIME 2025	Pass@1 / Standard MV plateau	.789 / .900			.902 / .967			.345 / .576		
	Standard MV budget ( $B_{\text{MV}}$ )	56k	99k	189k	396k	589k	1.2M	371k	2.0M	6.9M
	Self-certainty	$0.81 \pm 0.06 \times$	$0.81 \pm 0.07 \times$	$0.66 \pm 0.11 \times$	$0.97 \pm 0.06 \times$	$0.96 \pm 0.06 \times$	$0.84 \pm 0.12 \times$	$1.21 \pm 0.15 \times$	$1.20 \pm 0.12 \times$	N/A
	DeepConf tail	<b><math>0.68 \pm 0.04 \times</math></b>	<b><math>0.70 \pm 0.06 \times</math></b>	$0.56 \pm 0.09 \times$	$0.95 \pm 0.06 \times$	$0.95 \pm 0.06 \times$	$0.89 \pm 0.13 \times$	$1.22 \pm 0.15 \times$	$1.20 \pm 0.12 \times$	$1.43 \pm 0.26 \times$
	P(True)	$1.14 \pm 0.08 \times$	$1.13 \pm 0.09 \times$	$1.01 \pm 0.16 \times$	$1.12 \pm 0.07 \times$	$1.15 \pm 0.07 \times$	$1.20 \pm 0.20 \times$	$1.93 \pm 0.22 \times$	N/A	N/A
	AC sweep	$1.03 \pm 0.12 \times$	$1.06 \pm 0.26 \times$	$2.98 \pm 0.82 \times$	<b><math>0.21 \pm 0.01 \times</math></b>	<b><math>0.18 \pm 0.01 \times</math></b>	<b><math>0.21 \pm 0.05 \times</math></b>	$0.91 \pm 0.11 \times$	$0.54 \pm 0.06 \times$	$0.49 \pm 0.10 \times$
	ESC sweep	$0.96 \pm 0.06 \times$	$1.38 \pm 0.57 \times$	$>10 \times$	$0.28 \pm 0.01 \times$	$0.24 \pm 0.05 \times$	$0.59 \pm 0.18 \times$	$4.44 \pm 0.83 \times$	$2.41 \pm 0.22 \times$	$1.38 \pm 0.26 \times$
	PC-linear	$0.87 \pm 0.05 \times$	$0.73 \pm 0.06 \times$	$0.58 \pm 0.10 \times$	$1.13 \pm 0.08 \times$	$1.21 \pm 0.08 \times$	$1.29 \pm 0.24 \times$	<b><math>0.25 \pm 0.03 \times</math></b>	$1.11 \pm 0.01 \times$	$0.07 \pm 0.01 \times$
	PC-quadratic	$0.86 \pm 0.05 \times$	<b><math>0.70 \pm 0.06 \times</math></b>	<b><math>0.53 \pm 0.08 \times</math></b>	$1.22 \pm 0.09 \times$	$1.33 \pm 0.10 \times$	$1.44 \pm 0.24 \times$	$0.26 \pm 0.03 \times$	<b><math>0.09 \pm 0.01 \times</math></b>	<b><math>0.05 \pm 0.01 \times</math></b>
	PC-cubic	$0.86 \pm 0.05 \times$	$0.71 \pm 0.06 \times$	<b><math>0.53 \pm 0.08 \times</math></b>	$1.23 \pm 0.08 \times$	$1.39 \pm 0.10 \times$	$1.67 \pm 0.26 \times$	$0.27 \pm 0.03 \times$	<b><math>0.09 \pm 0.01 \times</math></b>	<b><math>0.05 \pm 0.01 \times</math></b>
Bromo 2025	Pass@1 / Standard MV plateau	.713 / .833			.816 / .932			.421 / .698		
	Standard MV budget ( $B_{\text{MV}}$ )	274k	934k	3.3M	342k	651k	2.5M	92k	265k	1.8M
	Self-certainty	$0.73 \pm 0.18 \times$	$0.76 \pm 0.10 \times$	$0.59 \pm 0.09 \times$	$0.45 \pm 0.05 \times$	$0.41 \pm 0.05 \times$	$0.14 \pm 0.07 \times$	$1.35 \pm 0.11 \times$	$1.47 \pm 0.22 \times$	N/A
	DeepConf tail	$0.50 \pm 0.12 \times$	$0.47 \pm 0.06 \times$	$0.35 \pm 0.06 \times$	$0.40 \pm 0.05 \times$	$0.39 \pm 0.07 \times$	$0.14 \pm 0.07 \times$	$1.35 \pm 0.11 \times$	$1.56 \pm 0.23 \times$	N/A
	P(True)	$1.46 \pm 0.36 \times$	$1.07 \pm 0.11 \times$	$0.60 \pm 0.11 \times$	$1.40 \pm 0.14 \times$	$2.05 \pm 0.31 \times$	$3.39 \pm 1.62 \times$	$2.33 \pm 0.22 \times$	N/A	N/A
	AC sweep	<b><math>0.32 \pm 0.09 \times</math></b>	<b><math>0.26 \pm 0.03 \times</math></b>	$0.20 \pm 0.04 \times$	<b><math>0.27 \pm 0.03 \times</math></b>	<b><math>0.18 \pm 0.03 \times</math></b>	$0.12 \pm 0.07 \times$	$1.42 \pm 0.14 \times$	$1.85 \pm 0.32 \times$	$1.20 \pm 0.75 \times$
	ESC sweep	$3.19 \pm 1.47 \times$	$6.11 \pm 0.65 \times$	N/A	$0.30 \pm 0.03 \times$	$0.34 \pm 0.06 \times$	$0.25 \pm 0.21 \times$	$2.39 \pm 0.38 \times$	$7.42 \pm 2.14 \times$	$7.95 \pm 4.31 \times$
	PC-linear	$0.56 \pm 0.15 \times$	$0.51 \pm 0.07 \times$	$0.39 \pm 0.06 \times$	$0.34 \pm 0.04 \times$	$0.28 \pm 0.04 \times$	<b><math>0.09 \pm 0.05 \times</math></b>	$0.93 \pm 0.07 \times$	$0.80 \pm 0.12 \times$	$0.32 \pm 0.19 \times$
	PC-quadratic	$0.44 \pm 0.11 \times$	$0.37 \pm 0.04 \times$	$0.19 \pm 0.03 \times$	$0.33 \pm 0.03 \times$	$0.28 \pm 0.04 \times$	$0.10 \pm 0.05 \times$	<b><math>0.86 \pm 0.06 \times</math></b>	<b><math>0.61 \pm 0.09 \times</math></b>	$0.20 \pm 0.12 \times$
	PC-cubic	$0.44 \pm 0.11 \times$	$0.32 \pm 0.04 \times$	<b><math>0.16 \pm 0.02 \times</math></b>	$0.35 \pm 0.04 \times$	$0.30 \pm 0.04 \times$	$0.11 \pm 0.06 \times$	<b><math>0.86 \pm 0.06 \times</math></b>	$0.62 \pm 0.09 \times$	<b><math>0.18 \pm 0.11 \times</math></b>

**Comparison with adaptive-stopping baselines.** PC-cubic is competitive with or better than AC sweep on most cells and outperforms ESC sweep at  $\alpha=99\%$  on every (model, benchmark) cell except Nemotron3-30B on AIME 2025, despite being a non-adaptive reweighting of the same initial pool that AC and ESC consume sequentially. The advantage is most pronounced on large- $D$  cells (FrontierScience-Olympiad on every model, and most Ministral3-14B benchmarks), e.g. PC-cubic at  $0.05 \times$  vs. AC sweep at  $0.29 \times$  at  $\alpha=99\%$  on GPT-OSS-120B FrontierScience-Olympiad.

AC substantially outperforms PC only on the two cells noted above where Pass@1 is close to Standard MV plateau (Nemotron3-30B on AIME 2025 and HMMT Feb 2026), since the aggregated vote on wrong answers is small and AC’s early stop alone bounds the cost. However, on 2 out of 12 (model, benchmark) cells at  $\alpha=99\%$  (marked “N/A” in Table 4) AC’s accuracy never reaches Standard MV plateau, because its early-stop rule terminates generation before the running accuracy reaches the  $\alpha=99\%$  target. PC-cubic reaches the target on all 12.

ESC stops at the first fixed-size window of samples that all share the same answer, which is too strict on benchmarks where wrong answers are diverse, so ESC either stops well after AC or fails to stop within the budget. PC and adaptive stopping act on orthogonal axes: PC reweights votes while AC and ESC decide when to stop sampling. A hybrid that votes by PC weights and stops by the AC rule would combine AC’s cost bound on easy cells with PC’s accuracy on difficult ones (left to future work).

**Remark on the cost accounting.** Treating log-probability access as free is implementation-dependent but holds for our vLLM setup. This favors baselines that read log-probabilities of the initial trace without generating extra tokens (Self-certainty, DeepConf, Response probability), while prefix consistency spends budget on the regeneration tokens. Even so, the PC-WMV has significant advantage. Imposing any cost for log-probability retrieval only widens the margin.

Additional results on token-efficiency ratios are reported per model in Appendix D.3.

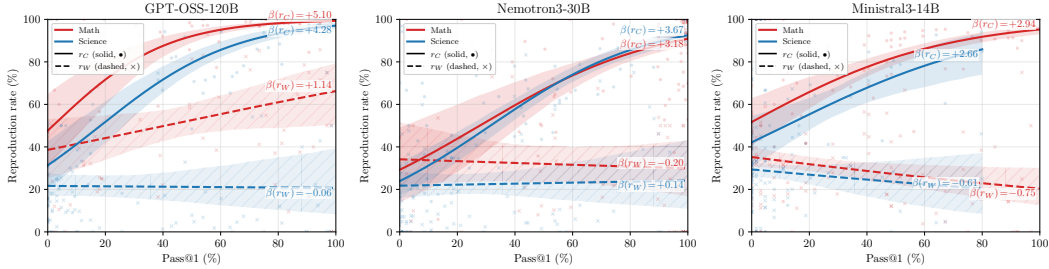


Figure 3: **Per-problem reproduction rates vs. Pass@1.** One panel per model. Solid (●):  $r_C$ . Dashed (×):  $r_W$ . Both are per-category logistic-regression fits with shaded  $2\sigma$  cluster-bootstrap CIs over problems and per-problem scatter overlays; curves are labeled with the GLM slope  $\beta$ .  $r_C > r_W$  holds across the full Pass@1 range, including below 50%. Science: FrontierScience-Olympiad. Math: HMMT Feb 2026  $\cup$  AIME 2025  $\cup$  Brumo 2025.

#### 4.4 How Problem Difficulty Affects the Discrimination Gap $D$

The discrimination gap  $D$  determines where prefix consistency improves WMV (Theorem 1), so we now study how  $D$  varies with problem difficulty, indexed by Pass@1.

Figure 3 plots per-problem  $r_C$  and  $r_W$  as a function of Pass@1 for three of the five models (the remaining two are in Appendix D.7.1), stratified by category. Across all five models,  $r_C$  rises with problem easiness,  $r_W$  depends on the model and category but only weakly on Pass@1, and  $D = r_C - r_W$  inherits both. We discuss  $r_C$  and  $r_W$  in turn below.

First,  $r_C$  (solid lines) increases with Pass@1 for both categories. Pass@1 here indexes problem easiness within a fixed model, and on easier problems, the correct answer is more reliably reproduced under regeneration. Logistic generalized linear model (GLM) slopes  $\beta(r_C)$  on  $\text{logit}(r) = \beta_0 + \beta \cdot \text{Pass@1}$  range from +2.7 to +5.1 across the six (model, category) pairs shown in Figure 3, all significantly positive (cluster-bootstrap  $p < 0.005$ , see Appendix D.7.1).

Second,  $r_W$  (dashed lines) depends more weakly on Pass@1 than  $r_C$ :  $|\beta(r_W)| \leq 1.14$  across the six pairs, and among four out of six curves, we cannot statistically reject  $\beta = 0$  at a  $2\sigma$  confidence level. For the remaining two non-zero slopes,  $\beta$  is +1.14 (GPT-OSS-120B Math) and  $-0.75$  (Ministral3-14B Math), with opposite signs, both smaller in magnitude than the smallest  $r_C$  slope. The level of  $r_W$  varies by category, sitting at  $\sim 15$ – $40\%$  on Science and  $\sim 25$ – $60\%$  on Math. Math errors may reflect internally consistent miscalculations and science errors may reflect more diffuse knowledge gaps, but this is a hypothesis: our results establish  $r_C > r_W$  as a behavioral regularity, and a mechanistic verification (e.g., calculation-heavy vs. concept-heavy subsets) is left to future work.

The finding that  $D$  widens on easier cells may appear to conflict with the “savings track  $D$ ” claim of Section 4.3, since easier cells also have a smaller gap between Pass@1 and Standard MV plateau. The two reconcile by noting that PC-WMV’s advantage over Standard MV depends on both  $D$  and the gap above Pass@1: a large  $D$  pays off only when there is room to reweight votes, which is why the two cells where PC-cubic offers little advantage over Standard MV are precisely the cells with Pass@1 concentrated within  $\sim .10$  of Standard MV plateau (Nemotron3-30B on AIME 2025 and HMMT Feb 2026).

## 5 Conclusion

We introduced prefix consistency, a reliability signal for weighted majority voting that truncates each CoT and checks whether answers reproduce under regeneration. Across benchmarks, prefix consistency is a stronger correctness predictor than existing baselines, and PC-WMV improves upon existing weighted majority voting methods under cost-equivalent comparison, especially on more difficult benchmarks. Our analysis highlights the discrimination gap  $D = r_C - r_W$  as the key quantity governing when the method helps: PC-WMV is most effective when  $D > 0$  and Pass@1 leaves a meaningful gap below Standard MV plateau. Regeneration stability is thus a practically useful test-time signal for aggregating votes, not merely a descriptive property of Chain-of-Thought.

## References

- Pranjal Aggarwal, Aman Madaan, Yiming Yang, and Mausam. Let’s Sample Step by Step: Adaptive-Consistency for Efficient Reasoning and Coding with LLMs. In Houda Bouamor, Juan Pino, and Kalika Bali, editors, *Proceedings of the 2023 Conference on Empirical Methods in Natural Language Processing*, pages 12375–12396, Singapore, December 2023. Association for Computational Linguistics. doi: 10.18653/v1/2023.emnlp-main.761. URL <https://aclanthology.org/2023.emnlp-main.761/>.
- Pranjal Aggarwal, Seungone Kim, Jack Lanchantin, Sean Welleck, Jason Weston, Ilia Kulikov, and Swarnadeep Saha. OptimalThinkingBench: Evaluating Over and Underthinking in LLMs. In *The Fourteenth International Conference on Learning Representations*, 2026. URL <https://openreview.net/forum?id=N5kWa3sRJt>.
- Anthropic. Claude Sonnet 4.6 System Card, 2026. URL <https://www-cdn.anthropic.com/bbd8ef16d70b7a1665f14f306ee88b53f686aa75.pdf>.
- Mislav Balunović, Jasper Dekoninck, Ivo Petrov, Nikola Jovanović, and Martin Vechev. Math-Arena: Evaluating LLMs on Uncontaminated Math Competitions. In *Thirty-ninth Conference on Neural Information Processing Systems Datasets and Benchmarks Track*, 2025. URL <https://openreview.net/forum?id=y0zL9IZxZ7>.
- Maciej Besta, Nils Blach, Ales Kubicek, Robert Gerstenberger, Michal Podstawski, Lukas Gianinazzi, Joanna Gajda, Tomasz Lehmann, Hubert Niewiadomski, Piotr Nyczyk, and Torsten Hoefler. Graph of Thoughts: Solving Elaborate Problems with Large Language Models. *Proceedings of the AAAI Conference on Artificial Intelligence*, 38(16):17682–17690, Mar. 2024. doi: 10.1609/aaai.v38i16.29720. URL <https://ojs.aaai.org/index.php/AAAI/article/view/29720>.
- Siddharth Boppana, Annabel Ma, Max Loeffler, Raphael Sarfati, Eric Bigelow, Atticus Geiger, Owen Lewis, and Jack Merullo. Reasoning Theater: Disentangling Model Beliefs from Chain-of-Thought. *arXiv preprint arXiv:2603.05488*, 2026. URL <https://arxiv.org/abs/2603.05488>.
- Xingyu Chen, Jiahao Xu, Tian Liang, Zhiwei He, Jianhui Pang, Dian Yu, Linfeng Song, Qiuzhi Liu, Mengfei Zhou, Zhuosheng Zhang, Rui Wang, Zhaopeng Tu, Haitao Mi, and Dong Yu. Do NOT Think That Much for  $2+3=?$ : On the Overthinking of Long Reasoning Models. In *Proceedings of the 42nd International Conference on Machine Learning*, volume 267 of *Proceedings of Machine Learning Research*, pages 9487–9499. PMLR, 2025. URL <https://proceedings.mlr.press/v267/chen25bx.html>.
- Ekaterina Fadeeva, Aleksandr Rubashevskii, Artem Shelmanov, Sergey Petrakov, Haonan Li, Hamdy Mubarak, Evgenii Tsymbalov, Gleb Kuzmin, Alexander Panchenko, Timothy Baldwin, Preslav Nakov, and Maxim Panov. Fact-checking the output of large language models via token-level uncertainty quantification. In Lun-Wei Ku, Andre Martins, and Vivek Srikumar, editors, *Findings of the Association for Computational Linguistics: ACL 2024*, pages 9367–9385, Bangkok, Thailand, August 2024. Association for Computational Linguistics. doi: 10.18653/v1/2024.findings-acl.558. URL <https://aclanthology.org/2024.findings-acl.558/>.
- Gonçalo Faria and Noah A. Smith. Sample, Don’t Search: Rethinking Test-Time Alignment for Language Models. *arXiv preprint arXiv:2504.03790*, 2025. URL <https://arxiv.org/abs/2504.03790>.
- Gonçalo R. A. Faria, Sweta Agrawal, António Farinhas, Ricardo Rei, José G. C. de Souza, and André F. T. Martins. QUEST: Quality-Aware Metropolis-Hastings Sampling for Machine Translation. In *Advances in Neural Information Processing Systems*, volume 37, 2024. URL <https://openreview.net/forum?id=dLnduWGTB4>.
- Yunzhen Feng, Julia Kempe, Cheng Zhang, Parag Jain, and Anthony Hartshorn. What Characterizes Effective Reasoning? Revisiting Length, Review, and Structure of CoT. In *NeurIPS 2025 Workshop on Efficient Reasoning*, 2025. URL <https://openreview.net/forum?id=8VNIId3aihj>. Spotlight.
- Yao Fu, Hao Peng, Ashish Sabharwal, Peter Clark, and Tushar Khot. Complexity-Based Prompting for Multi-step Reasoning. In *The Eleventh International Conference on Learning Representations*, 2023. URL <https://openreview.net/forum?id=yf1icZHC-19>.

- Yichao Fu, Xuewei Wang, Hao Zhang, Yuandong Tian, and Jiawei Zhao. Deep Think with Confidence. In *The Fourteenth International Conference on Learning Representations*, 2026. URL <https://openreview.net/forum?id=8LqHsOKIM7>.
- Zeyu Gan, Yun Liao, and Yong Liu. Rethinking External Slow-Thinking: From Snowball Errors to Probability of Correct Reasoning. In *Forty-second International Conference on Machine Learning*, 2025. URL <https://openreview.net/forum?id=1Aj22UxZy>.
- Hasan Abed Al Kader Hammoud, Hani Itani, and Bernard Ghanem. Beyond the Last Answer: Your Reasoning Trace Uncovers More than You Think. *arXiv preprint arXiv:2504.20708*, 2025. URL <https://arxiv.org/abs/2504.20708>.
- Enyi Jiang, Changming Xu, Nischay Singh, Tian Qiu, and Gagandeep Singh. Robust Answers, Fragile Logic: Probing the Decoupling Hypothesis in LLM Reasoning. *arXiv preprint arXiv:2505.17406*, 2025. URL <https://arxiv.org/abs/2505.17406>.
- Ishan Jindal, Sai Prashanth Akuthota, Jayant Taneja, and SACHIN DEV SHARMA. THE PATH OF LEAST RESISTANCE: GUIDING LLM REASONING TRAJECTORIES WITH PREFIX CONSENSUS. In *The Fourteenth International Conference on Learning Representations*, 2026. URL <https://openreview.net/forum?id=hrnSqERgPn>.
- Saurav Kadavath, Tom Conerly, Amanda Askell, Tom Henighan, Dawn Drain, Ethan Perez, Nicholas Schiefer, Zac Hatfield-Dodds, Nova DasSarma, Eli Tran-Kemp, Scott Johnston, Sheer El-Showk, Andy Jones, Nelson Elhage, Tristan Hume, Anna Chen, Yuntao Bai, Sam Bowman, Stanislav Fort, Deep Ganguli, Danny Hernandez, Josh Jacobson, Jackson Kernion, Shauna Kravec, Liane Lovitt, Kamal Ndousse, Catherine Olsson, Sam Ringer, Dario Amodei, Tom Brown, Jack Clark, Nicholas Joseph, Ben Mann, Sam McCandlish, Chris Olah, and Jared Kaplan. Language Models (Mostly) Know What They Know. *arXiv preprint arXiv:2207.05221*, 2022. URL <https://arxiv.org/abs/2207.05221>.
- Zhewei Kang, Xuandong Zhao, and Dawn Song. Scalable Best-of-N Selection for Large Language Models via Self-Certainty. In *Advances in Neural Information Processing Systems*, 2025. URL <https://openreview.net/forum?id=29FRqmVQK8>.
- Juno Kim, Denny Wu, Jason D. Lee, and Taiji Suzuki. Metastable Dynamics of Chain-of-Thought Reasoning: Provable Benefits of Search, RL and Distillation. In *Forty-second International Conference on Machine Learning*, 2025. URL <https://openreview.net/forum?id=2HJcVtuovs>.
- Takeshi Kojima, Shixiang (Shane) Gu, Machel Reid, Yutaka Matsuo, and Yusuke Iwasawa. Large Language Models are Zero-Shot Reasoners. In *Advances in Neural Information Processing Systems*, volume 35, pages 22199–22213. Curran Associates, Inc., 2022. URL <https://openreview.net/forum?id=e2TBb5y0yFf>.
- Junpei Komiyama, Daisuke Oba, and Masafumi Oyamada. Best-of- $\infty$ : Asymptotic Performance of Test-Time LLM Ensembling. In *The Fourteenth International Conference on Learning Representations*, 2026. URL <https://openreview.net/forum?id=3qiCnLf3jf>.
- Tamera Lanham, Anna Chen, Ansh Radhakrishnan, Benoit Steiner, Carson Denison, Danny Hernandez, Dustin Li, Esin Durmus, Evan Hubinger, Jackson Kernion, Kamilė Lukošiuūtė, Karina Nguyen, Newton Cheng, Nicholas Joseph, Nicholas Schiefer, Oliver Rausch, Robin Larson, Sam McCandlish, Sandipan Kundu, Saurav Kadavath, Shannon Yang, Thomas Henighan, Timothy Maxwell, Timothy Telleen-Langton, Tristan Hume, Zac Hatfield-Dodds, Jared Kaplan, Jan Brauner, Samuel R. Bowman, and Ethan Perez. Measuring Faithfulness in Chain-of-Thought Reasoning. *arXiv preprint arXiv:2307.13702*, 2023. URL <https://arxiv.org/abs/2307.13702>.
- Yiwei Li, Peiwen Yuan, Shaoxiong Feng, Boyuan Pan, Xinglin Wang, Bin Sun, Heda Wang, and Kan Li. Escape Sky-high Cost: Early-stopping Self-Consistency for Multi-step Reasoning. In *The Twelfth International Conference on Learning Representations*, 2024. URL <https://openreview.net/forum?id=ndR8Ytrzhh>.
- Hunter Lightman, Vineet Kosaraju, Yuri Burda, Harrison Edwards, Bowen Baker, Teddy Lee, Jan Leike, John Schulman, Ilya Sutskever, and Karl Cobbe. Let’s Verify Step by Step. In *The Twelfth International Conference on Learning Representations*, 2024. URL <https://openreview.net/forum?id=v8L0pN6EOi>.

- Stephanie Lin, Jacob Hilton, and Owain Evans. Teaching Models to Express Their Uncertainty in Words. *Transactions on Machine Learning Research*, 2022. ISSN 2835-8856. URL <https://openreview.net/forum?id=8s8K2UZGTZ>.
- Pan Lu, Swaroop Mishra, Tony Xia, Liang Qiu, Kai-Wei Chang, Song-Chun Zhu, Oyvind Tafjord, Peter Clark, and Ashwin Kalyan. Learn to Explain: Multimodal Reasoning via Thought Chains for Science Question Answering. In Alice H. Oh, Alekh Agarwal, Danielle Belgrave, and Kyunghyun Cho, editors, *Advances in Neural Information Processing Systems*, 2022. URL [https://openreview.net/forum?id=HjwK-Tc\\_Bc](https://openreview.net/forum?id=HjwK-Tc_Bc).
- Mistral AI. Mistral 3. *arXiv preprint arXiv:2601.08584*, 2026. URL <https://arxiv.org/abs/2601.08584>.
- Niklas Muennighoff, Zitong Yang, Weijia Shi, Xiang Lisa Li, Li Fei-Fei, Hannaneh Hajishirzi, Luke Zettlemoyer, Percy Liang, Emmanuel Candès, and Tatsunori Hashimoto. s1: Simple test-time scaling. In Christos Christodoulopoulos, Tanmoy Chakraborty, Carolyn Rose, and Violet Peng, editors, *Proceedings of the 2025 Conference on Empirical Methods in Natural Language Processing*, pages 20275–20321, Suzhou, China, November 2025. Association for Computational Linguistics. ISBN 979-8-89176-332-6. doi: 10.18653/v1/2025.emnlp-main.1025. URL <https://aclanthology.org/2025.emnlp-main.1025/>.
- NVIDIA. Nemotron 3 Nano: Open, Efficient Mixture-of-Experts Hybrid Mamba-Transformer Model for Agentic Reasoning. *arXiv preprint arXiv:2512.20848*, 2025a. URL <https://arxiv.org/abs/2512.20848>.
- NVIDIA. NVIDIA Nemotron Nano 2: An Accurate and Efficient Hybrid Mamba-Transformer Reasoning Model. *arXiv preprint arXiv:2508.14444*, 2025b. URL <https://arxiv.org/abs/2508.14444>.
- OpenAI. gpt-oss-120b & gpt-oss-20b Model Card. *arXiv preprint arXiv:2508.10925*, 2025. URL <https://arxiv.org/abs/2508.10925>.
- Shubham Parashar, Blake Olson, Sambhav Khurana, Eric Li, Hongyi Ling, James Caverlee, and Shuiwang Ji. Inference-Time Computations for LLM Reasoning and Planning: A Benchmark and Insights. *arXiv preprint arXiv:2502.12521*, 2025. URL <https://arxiv.org/abs/2502.12521>.
- Xiao Pu, Michael Saxon, Wenyue Hua, and William Yang Wang. ThoughtTerminator: Benchmarking, Calibrating, and Mitigating Overthinking in Reasoning Models. In *Second Conference on Language Modeling*, 2025. URL <https://openreview.net/forum?id=oHR862dpMC>.
- Daniel Scalena, Leonidas Zotos, Elisabetta Fersini, Malvina Nissim, and Ahmet Üstün. EA-GER: Entropy-Aware GENEration for Adaptive Inference-Time Scaling. *arXiv preprint arXiv:2510.11170*, 2025. URL <https://arxiv.org/abs/2510.11170>.
- Aman Sharma and Paras Chopra. The Sequential Edge: Inverse-Entropy Voting Beats Parallel Self-Consistency at Matched Compute. *arXiv preprint arXiv:2511.02309*, 2025. URL <https://arxiv.org/abs/2511.02309>.
- Amir Taubenfeld, Tom Sheffer, Eran Ofek, Amir Feder, Ariel Goldstein, Zorik Gekhman, and Gal Yona. Confidence Improves Self-Consistency in LLMs. In Wanxiang Che, Joyce Nabende, Ekaterina Shutova, and Mohammad Taher Pilehvar, editors, *Findings of the Association for Computational Linguistics: ACL 2025*, pages 20090–20111, Vienna, Austria, July 2025. Association for Computational Linguistics. ISBN 979-8-89176-256-5. doi: 10.18653/v1/2025.findings-acl.1030. URL <https://aclanthology.org/2025.findings-acl.1030/>.
- Harsh Trivedi, Niranjan Balasubramanian, Tushar Khot, and Ashish Sabharwal. Interleaving Retrieval with Chain-of-Thought Reasoning for Knowledge-Intensive Multi-Step Questions. In Anna Rogers, Jordan Boyd-Graber, and Naoaki Okazaki, editors, *Proceedings of the 61st Annual Meeting of the Association for Computational Linguistics (Volume 1: Long Papers)*, pages 10014–10037, Toronto, Canada, July 2023. Association for Computational Linguistics. doi: 10.18653/v1/2023.acl-long.557. URL <https://aclanthology.org/2023.acl-long.557/>.

- Alexander von Recum, Leander Girrbach, and Zeynep Akata. Are Reasoning LLMs Robust to Interventions on Their Chain-of-Thought? In *The Fourteenth International Conference on Learning Representations*, 2026. URL <https://openreview.net/forum?id=aQZIpELFwp>.
- Keheng Wang, Feiyu Duan, Sirui Wang, Peiguang Li, Yunsen Xian, Chuantao Yin, Wenge Rong, and Zhang Xiong. Knowledge-Driven CoT: Exploring Faithful Reasoning in LLMs for Knowledge-Intensive Question Answering. *arXiv preprint arXiv:2308.13259*, 2023a. URL <https://arxiv.org/abs/2308.13259>.
- Lei Wang, Yi Hu, Jiabang He, Xing Xu, Ning Liu, Hui Liu, and Heng Tao Shen. T-SciQ: Teaching multimodal chain-of-thought reasoning via large language model signals for science question answering. In *Proceedings of the AAAI Conference on Artificial Intelligence*, volume 38, pages 19162–19170, 2024. doi: 10.1609/aaai.v38i17.29884. URL <https://ojs.aaai.org/index.php/AAAI/article/view/29884>.
- Miles Wang, Robi Lin, Kat Hu, Joy Jiao, Neil Chowdhury, Ethan Chang, and Tejal Patwardhan. FrontierScience: Evaluating AI’s Ability to Perform Expert-Level Scientific Tasks. *arXiv preprint arXiv:2601.21165*, 2025. URL <https://arxiv.org/abs/2601.21165>.
- Xuezhi Wang, Jason Wei, Dale Schuurmans, Quoc V Le, Ed H. Chi, Sharan Narang, Aakanksha Chowdhery, and Denny Zhou. Self-Consistency Improves Chain of Thought Reasoning in Language Models. In *The Eleventh International Conference on Learning Representations*, 2023b. URL <https://openreview.net/forum?id=1PL1NIMMrw>.
- Jason Wei, Xuezhi Wang, Dale Schuurmans, Maarten Bosma, Brian Ichter, Fei Xia, Ed Chi, Quoc V Le, and Denny Zhou. Chain-of-Thought Prompting Elicits Reasoning in Large Language Models. In *Advances in Neural Information Processing Systems*, volume 35, pages 24824–24837. Curran Associates, Inc., 2022. URL [https://openreview.net/forum?id=\\_VjQlMeSB\\_J](https://openreview.net/forum?id=_VjQlMeSB_J).
- Xumeng Wen, Zihan Liu, Shun Zheng, Shengyu Ye, Zhirong Wu, Yang Wang, Zhijian Xu, Xiao Liang, Junjie Li, Ziming Miao, Jiang Bian, and Mao Yang. Reinforcement Learning with Verifiable Rewards Implicitly Incentivizes Correct Reasoning in Base LLMs. In *The Fourteenth International Conference on Learning Representations*, 2026. URL <https://openreview.net/forum?id=jGbrWwIidy>.
- Miao Xiong, Zhiyuan Hu, Xinyang Lu, Yifei Li, Jie Fu, Junxian He, and Bryan Hooi. Can LLMs Express Their Uncertainty? An Empirical Evaluation of Confidence Elicitation in LLMs. In *The Twelfth International Conference on Learning Representations*, 2024. URL <https://openreview.net/forum?id=gjeQKfXfpZ>.
- Shunyu Yao, Dian Yu, Jeffrey Zhao, Izhak Shafran, Thomas L. Griffiths, Yuan Cao, and Karthik Narasimhan. Tree of Thoughts: Deliberate Problem Solving with Large Language Models. In *Advances in Neural Information Processing Systems*, volume 36, 2023. URL <https://openreview.net/forum?id=5Xc1ecx01h>.
- Tong Yu, Yongcheng Jing, Xikun Zhang, Wentao Jiang, Wenjie Wu, Yingjie Wang, Wenbin Hu, Bo Du, and Dacheng Tao. Benchmarking Reasoning Robustness in Large Language Models. *arXiv preprint arXiv:2503.04550*, 2025. URL <https://arxiv.org/abs/2503.04550>.
- Anqi Zhang, Yulin Chen, Jane Pan, Chen Zhao, Aurojit Panda, Jinyang Li, and He He. Reasoning Models Know When They’re Right: Probing Hidden States for Self-Verification. In *Second Conference on Language Modeling*, 2025. URL <https://openreview.net/forum?id=06IOAv7683>.
- Denny Zhou, Nathanael Schärli, Le Hou, Jason Wei, Nathan Scales, Xuezhi Wang, Dale Schuurmans, Claire Cui, Olivier Bousquet, Quoc V Le, and Ed H. Chi. Least-to-Most Prompting Enables Complex Reasoning in Large Language Models. In *The Eleventh International Conference on Learning Representations*, 2023. URL <https://openreview.net/forum?id=WZH7099tgfM>.
- Jiace Zhu, Yuanzhe Huang, Yingtao Shen, Jie Zhao, and An Zou. Path-Consistency with Prefix Enhancement for Efficient Inference in LLMs. *arXiv preprint arXiv:2409.01281*, 2024. URL <https://arxiv.org/abs/2409.01281>.

<b>A</b>	<b>Related Work</b>	<b>15</b>
A.1	Test-Time Scaling . . . . .	15
A.2	Chain-of-Thought . . . . .	16
<b>B</b>	<b>Limitations and Future Work</b>	<b>16</b>
<b>C</b>	<b>Asymptotic Analysis</b>	<b>17</b>
C.1	Notation and Useful Tools . . . . .	17
C.2	Asymptotic Convergence of PC-WMV . . . . .	19
C.3	Proof of Theorem 1 . . . . .	20
C.4	Empirical Verification of Assumptions . . . . .	21
<b>D</b>	<b>Additional Experiments</b>	<b>22</b>
D.1	ROC Curves for Correctness Predictors . . . . .	22
D.2	Cost–Accuracy Curves . . . . .	23
D.3	Full Baseline Comparison . . . . .	23
D.4	Pool Coverage vs. Reweighting . . . . .	28
D.5	Sensitivity to $\tau$ and $K$ . . . . .	30
D.6	Robustness to Judge Choice . . . . .	32
D.7	Reliability Signals vs. Pass@1 . . . . .	34
<b>E</b>	<b>Baseline Implementation Details</b>	<b>38</b>
<b>F</b>	<b>Examples of Prefix Consistency</b>	<b>41</b>
<b>G</b>	<b>Evaluation Protocol</b>	<b>42</b>
G.1	Setup . . . . .	42
G.2	$\overline{\text{AUROC}}$ for the Correctness-Predictor Evaluation (Section 4.1) . . . . .	43
G.3	Cost-Accuracy Evaluation (Sections 4.2 and 4.3) . . . . .	43
G.4	Reproduction-Rate GLM (Section 4.4) . . . . .	44
<b>H</b>	<b>Answer Extraction and Equivalence Judging</b>	<b>44</b>
H.1	Answer Extraction . . . . .	45
H.2	Equivalence Judging . . . . .	46
<b>I</b>	<b>Reproducibility Statement</b>	<b>47</b>

## A Related Work

### A.1 Test-Time Scaling

**Sequential and parallel scaling.** Test-time compute scaling comes in two paradigms. Sequential scaling extends a single reasoning chain, for example by appending continuation tokens to lengthen CoT [Muennighoff et al., 2025]. Parallel scaling generates multiple independent solutions and aggregates them: self-consistency is the canonical instance, while tree search [Yao et al., 2023] branches over candidate steps and process-reward verifiers rerank parallel samples [Lightman et al., 2024]. Parashar et al. [2025] benchmarked a range of inference-time techniques across reasoning and planning tasks and reported that no single method is consistently best. Our method sits between the two: it uses parallel samples but introduces a structured perturbation (truncation + regeneration) that probes the robustness of each sample’s reasoning. Beyond aggregation, the same perturbation could serve as a quality estimate for partial reasoning states inside richer search procedures such as Graph-of-Thoughts [Besta et al., 2024], which extends Tree-of-Thoughts to a directed graph with refinement and aggregation operations.

**Majority voting.** Wang et al. [2023b] introduced self-consistency for CoT reasoning: sample multiple reasoning traces and take the majority vote over extracted answers. A line of work targets the cost of self-consistency by stopping early. Aggarwal et al. [2023] introduced Adaptive Consistency, which evaluates a Beta-binomial posterior over the running top-1 and top-2 answer counts and stops once the posterior margin of the top answer crosses a threshold. Li et al. [2024] introduced Early-Stopping Self-Consistency, which inspects fixed-size windows of samples for unanimity and stops at the first unanimous window. Sharma and Chopra [2025] showed that sequential, entropy-aware voting can outperform parallel self-consistency at matched compute, highlighting the importance of cost-equivalent comparisons. Komiyama et al. [2026] analyzed the asymptotic behavior of majority voting (best-of- $\infty$ ) and proposed a Bayesian nonparametric stopping rule. Our work is complementary: we assess the quality of each vote through regeneration weighting, which is compatible with the adaptive stopping rules above.

**Confidence-based weighting.** Kang et al. [2025] proposed *self-certainty*, a trace-level quality score defined as the mean KL divergence of the per-token output distribution from uniform, and used it to rerank best-of- $N$  candidates. Fu et al. [2026] then extended self-certainty. In addition to the global trace mean (equivalent to self-certainty), they introduced a sliding-window group confidence and proposed the use of their bottom 10% (bottom-10% group confidence) and the mean over the final tokens of a trace (tail confidence) as alternative trace-level scores for confidence-weighted majority voting. Taubenfeld et al. [2025] demonstrated that combining self-assessed confidence (most effectively via  $P(\text{True})$ , the model’s own probability that its answer is correct) with self-consistency improves accuracy, though this still relies on the model’s introspective calibration. Xiong et al. [2024] studied whether LLMs can express uncertainty and found that verbalized confidence is often poorly calibrated. Scalena et al. [2025] used per-token entropy to allocate compute adaptively during generation, a token-level compute-allocation complement to our sample-level reliability estimation. All of these signals rely on the model’s own log-probabilities or verbalized self-assessment. We show that such confidence signals are unreliable on difficult problems and propose an alternative based on prefix self-reproduction that requires neither.

**Prefix continuation as a per-sample signal.** Several recent methods regenerated from a truncated reasoning prefix or extracted a structural signal from a CoT and used it to select or weight samples. Hammoud et al. [2025] proposed SubthoughtReasoner, which segments a single greedy trace into sequential subthoughts at linguistic cues and takes the mode over per-subthought regenerations as the final answer (single-trace refinement, +13pp on AIME 2024 vs. the same trace’s last answer). Faria and Smith [2025] also regenerated from intermediate states, but for test-time alignment via Metropolis-Hastings (building on quality-aware machine-translation sampling [Faria et al., 2024]) rather than answer aggregation. Zhu et al. [2024] iteratively promoted a high-confidence prefix among  $N$  initial partial answers via Beta-gated agreement on the extracted-answer distribution and resampled subsequent branches conditioned on it (up to 40.5% latency reduction at matched accuracy). Jindal et al. [2026] clustered the first 256 tokens of  $N$  initial samples and expanded only the dominant cluster (up to 60% token reduction at matched accuracy). Feng et al. [2025] scored each of  $N=64$  traces by its Failed-Step Fraction (the proportion of abandoned reasoning branches) and selected the

lowest-FSF trace, yielding 5% to 13% improvements over random selection on AIME 2025. The latter three collapsed  $N$  samples onto a subset (a single best prefix, the dominant cluster, or one selected trace) and therefore inherited the failure mode of Standard MV when the subset misses the correct answer: Jindal et al. [2026] reported a 10pp drop on AIME 2025 (76.7% to 66.7%) where the largest prefix cluster need not contain the correct answer. PC-WMV moves in the converse direction: it keeps all  $N$  samples and *reweights* the vote by each sample’s prefix self-reproduction, so a minority sample whose prefix continuation reproduces its own answer is upweighted rather than discarded. The two directions are complementary, since prefix-cluster pruning could feed PC-WMV reweighting on the surviving traces. Under cost-equivalent comparison, SubthoughtReasoner does not consistently improve over Standard MV in our experiments, filling the comparison left open by Hammoud et al. [2025].

## A.2 Chain-of-Thought

**Internal answer determination.** Several lines of evidence suggest that LLMs determine their answer internally before the visible CoT concludes. Lanham et al. [2023] found that truncating a CoT mid-reasoning and forcing an early answer often does not change the prediction, especially for larger models. Boppana et al. [2026] confirmed this with attention probes: on easy problems, the internal answer is determined well before the visible reasoning ends. Zhang et al. [2025] showed that linear probes on hidden states can classify the correctness of the future final answer at intermediate CoT stages. These observations are consistent with the  $r_C > r_W$  asymmetry we measure.

**Error propagation.** In CoT reasoning, errors compound across steps: once an error is introduced, subsequent reasoning builds on it [Gan et al., 2025]. Kim et al. [2025] modeled CoT as a metastable Markov process on a reasoning graph, where dense intra-cluster (easy) and sparse inter-cluster (difficult) steps induce timescale separation. Our  $r_C$  and  $r_W$  are analogous in spirit to within-cluster persistence rates, although we measure them at the answer level under regeneration rather than at the reasoning-step level along a single trace.

**Reasoning robustness.** Several works have studied the robustness of LLM reasoning. Yu et al. [2025] found that reasoning models can be brittle to minor perturbations in the input. von Recum et al. [2026] systematically evaluated seven intervention types on open-weight reasoning LLMs and found that robustness degrades more when interventions occur early in the CoT. Jiang et al. [2025] showed that correct answers persist even when reasoning logic is perturbed, suggesting a decoupling between answer stability and reasoning faithfulness. Our work uses this asymmetry between correct and wrong reasoning traces as a practical signal for answer aggregation.

**Overthinking and length scaling.** Reasoning models tend to allocate compute disproportionately to problem difficulty, which limits the improvements from extending a single CoT. Chen et al. [2025] reported that o1-like models generate up to 1953% more tokens than non-thinking models on trivial arithmetic, and reach the correct answer in the first generated solution in over 92% of cases while later solutions still account for roughly 40% of tokens. Pu et al. [2025] introduced DUMB500 to quantify overthinking on easy problems and proposed ThoughtTerminator, a training-free decoding-time termination scheme that reduces overthinking tokens by 76% to 98% with minimal accuracy loss. Aggarwal et al. [2026] formalized the trade-off as a joint over- and underthinking benchmark and found that no current model balances the two: even o3 reaches only 71.1% on their unified score. These results motivate aggregating multiple short samples rather than extending a single long trace, which is the setting our method targets.

## B Limitations and Future Work

The effectiveness of prefix consistency depends on the discrimination gap  $D = r_C - r_W$ . When incorrect answers are themselves stable under regeneration,  $r_W$  remains high, and the advantage of PC-WMV over Standard MV becomes small (e.g., on very difficult problems). Likewise, when the correct answer is reproduced only weakly from the chosen prefix,  $r_C$  remains low, and the signal becomes less informative. In this sense, the method is most effective in regimes where regeneration behavior meaningfully separates correct from incorrect traces.

The practical advantage of PC-WMV also depends on the available room above Pass@1. When Pass@1 is already close to Standard MV plateau, the aggregated vote on wrong answers is small, so even a strong reliability signal yields only limited accuracy improvements. This explains the small-gap settings in our experiments where PC-WMV does not outperform Standard MV (or simple verbalized-confidence baselines) by a large margin (Appendix D.3).

Although prefix consistency does not require token log-probabilities, it is not without cost: it incurs additional inference cost through prefix truncation and regeneration. This trade-off may be less favorable in deployments where log-probability access is readily available and inexpensive. Relatedly, the method introduces hyperparameters such as the truncation fraction  $\tau$ , the number of regenerations  $K$ , and the weighting function  $w$ , and in this work, we use fixed defaults rather than selecting them adaptively for each model or task.

A further practical limitation is that our method assumes access to an explicit Chain-of-Thought trace that can be truncated and continued from a prefix. This assumption does not hold for many frontier closed models and commercial APIs, including systems where the full internal reasoning trace is hidden or only summarized. In such settings, prefix consistency cannot be applied directly, even if the model can generate correct final answers. Extending the method to settings without visible CoT, for example by using intermediate summaries, structured scratchpads, or other externally exposed reasoning states, is an important direction for future work.

More broadly, our results establish prefix consistency as a useful behavioral signal, but not as a mechanistic explanation of why correct traces are more reproducible than incorrect ones. Understanding the origin of the observed asymmetry  $r_C > r_W$  remains future work. Finally, our evaluation is limited to reasoning-oriented models and math/science-style benchmarks, so the extent to which the same phenomenon holds for other domains, model families, or API settings remains to be established.

As shown in Section 4.4,  $r_C$  rises with problem easiness,  $r_W$  depends on the model and category but only weakly on Pass@1, and  $D = r_C - r_W$  inherits both. This pattern is consistent with reinforcement learning with verifiable rewards encouraging reasoning that survives verification [Wen et al., 2026]. State-of-the-art LLMs are designed to increase the mass of correct reasoning paths via widening the discrimination gap  $D$ . We do not test this connection directly, and whether the same pattern holds for non-RLVR-trained reasoners is left to future work.

## C Asymptotic Analysis

We analyze the asymptotic convergence of PC-WMV, prove Theorem 1 along the way, and verify the required assumptions empirically.

### C.1 Notation and Useful Tools

Fix  $\tau \in (0, 1)$  throughout, and omit it from subscripts: e.g., write  $\tilde{a}_i$  for  $\tilde{a}_i^{(\tau)}$  and  $c_i(a)$  for  $c_i^{(\tau)}(a)$ . The score takes values  $c_i(a) \in \{0, \frac{1}{2}, 1\}$ .

We define the transition probability as follows:

$$T(b \rightarrow a) := \Pr[\tilde{a}_i = a \mid a_i = b]. \quad (12)$$

The reproduction rates of Section 3.1 can be written in terms of  $T$ :

$$r_C = T(a^* \rightarrow a^*), \quad r_W = \mathbb{E}[T(a_i \rightarrow a_i) \mid a_i \neq a^*]. \quad (13)$$

Let  $\pi$  and  $\pi^{\rightarrow}$  be the marginal distributions of  $a_i$  and  $\tilde{a}_i$ , respectively. Here  $\pi(a^*)$  is the same per-problem Pass@1 introduced in Section 2 and used in Theorem 1. We keep the  $\pi$  notation in this appendix so the population-level expressions in Eq. (14) below align with the proof.

$$\pi(a) := \Pr[a_i = a], \quad \pi^{\rightarrow}(a) := \Pr[\tilde{a}_i = a] = \sum_{b \in \mathcal{A}} \pi(b) T(b \rightarrow a). \quad (14)$$

All quantities above ( $T$ ,  $r_C$ ,  $r_W$ ,  $\pi$ ,  $\pi^{\rightarrow}$ ) are defined per problem. The results in this section are statements about a fixed problem  $q$ , and the i.i.d. assumption across  $i$  refers to independent samples within  $q$ .

For completeness, we restate the definitions of the MV and PC-WMV votes. Let  $w: [0, 1] \rightarrow \mathbb{R}_{\geq 0}$  satisfy  $w(0) = 0$ . For each  $a \in \mathcal{A}$ , define the aggregated PC-WMV score over  $N$  groups by

$$V_N^{(w)}(a) := \sum_{i=1}^N w(c_i(a)),$$

where each term is the per-group PC-WMV vote given in Eq. (8). We then define the PC-WMV estimator and MV voting methods by

$$\hat{a}_N^{\text{PC}} := \arg \max_{a \in \mathcal{A}} V_N^{(w)}(a), \quad \hat{a}_N^{\text{MV}} := \arg \max_{a \in \mathcal{A}} \frac{1}{N} \sum_{i=1}^N \mathbf{1}\{a_i = a\}. \quad (15)$$

We next identify the population objective associated with the PC-WMV estimator.

**Proposition 1** (Population objective). *Assume that the pairs  $(a_i, \tilde{a}_i)$  are i.i.d. across  $i$ , and that, conditional on  $a_i$ , the variable  $\tilde{a}_i$  is drawn from  $T(a_i, \cdot)$ . Then, for every  $a \in \mathcal{A}$ ,*

$$\frac{1}{N} V_N^{(w)}(a) \xrightarrow{\text{a.s.}} \Phi_w(a) := \sum_{b \in \mathcal{A}} \pi(b) \mathbb{E}_{Z \sim \text{Bern}(T(b \rightarrow a))} \left[ w \left( \frac{\mathbf{1}\{a = b\} + Z}{2} \right) \right]. \quad (16)$$

Moreover, if  $\Phi_w$  has a unique maximizer, then  $\hat{a}_N^{\text{PC}}$  converges to that maximizer almost surely.

*Proof.* For each fixed  $a \in \mathcal{A}$ , the random variables  $\{w(c_i(a))\}_{i=1}^N$  are i.i.d., so the strong law of large numbers yields

$$\frac{1}{N} V_N^{(w)}(a) \xrightarrow{\text{a.s.}} \mathbb{E}[w(c_i(a))].$$

Conditional on  $a_i = b$ , we have  $\mathbf{1}\{\tilde{a}_i = a\} \sim \text{Bern}(T(b \rightarrow a))$ , and

$$2c_i(a) = \mathbf{1}\{a = b\} + \mathbf{1}\{\tilde{a}_i = a\}.$$

Hence,

$$\mathbb{E}[w(c_i(a)) \mid a_i = b] = \mathbb{E}_{Z \sim \text{Bern}(T(b \rightarrow a))} \left[ w \left( \frac{\mathbf{1}\{a = b\} + Z}{2} \right) \right].$$

Taking expectation with respect to  $b \sim \pi$  gives Eq. (16). For the final claim,  $\frac{1}{N} V_N^{(w)}(a) \rightarrow \Phi_w(a)$  a.s. for each  $a$  in the finite set  $\mathcal{A}$ , so when  $\Phi_w$  has a unique maximizer  $a^*$ , eventually  $\hat{a}_N^{\text{PC}} = \arg \max_a V_N^{(w)}(a) = a^*$  almost surely.  $\square$

We next derive an explicit decomposition of  $\Phi_w$  that exposes its dependence on the marginal  $\pi(a)$  and the self-transition  $T(a \rightarrow a)$ .

**Proposition 2** (Exact decomposition of  $\Phi_w$ ). *For every  $a \in \mathcal{A}$ ,*

$$\Phi_w(a) = w\left(\frac{1}{2}\right) [\pi(a) + \pi^\rightarrow(a)] + \lambda_w \pi(a) T(a \rightarrow a), \quad \lambda_w := w(1) - 2w\left(\frac{1}{2}\right). \quad (17)$$

*Proof.* Fix  $a \in \mathcal{A}$ . Since  $c_i(a)$  is the average of the two indicators

$$\mathbf{1}\{a_i = a\} \quad \text{and} \quad \mathbf{1}\{\tilde{a}_i = a\},$$

it takes only the three values  $0$ ,  $\frac{1}{2}$ , and  $1$ .

More precisely,  $c_i(a) = 1$  if and only if both  $a_i = a$  and  $\tilde{a}_i = a$  hold. Thus,

$$\Pr(c_i(a) = 1) = \pi(a) T(a \rightarrow a).$$

Next,  $c_i(a) = \frac{1}{2}$  if and only if exactly one of the two events  $\{a_i = a\}$  and  $\{\tilde{a}_i = a\}$  occurs. Therefore,

$$\Pr(c_i(a) = \frac{1}{2}) = \Pr(a_i = a, \tilde{a}_i \neq a) + \Pr(a_i \neq a, \tilde{a}_i = a).$$

The first term is

$$\Pr(a_i = a, \tilde{a}_i \neq a) = \pi(a)(1 - T(a \rightarrow a)).$$

For the second term, recall that  $\pi^\rightarrow(a) = \Pr(\tilde{a}_i = a)$ , so

$$\Pr(a_i \neq a, \tilde{a}_i = a) = \Pr(\tilde{a}_i = a) - \Pr(a_i = a, \tilde{a}_i = a) = \pi^\rightarrow(a) - \pi(a)T(a \rightarrow a).$$

Combining the two expressions yields

$$\Pr(c_i(a) = \frac{1}{2}) = \pi(a) + \pi^\rightarrow(a) - 2\pi(a)T(a \rightarrow a).$$

Finally, since  $w(0) = 0$  and  $c_i(a) \in \{0, \frac{1}{2}, 1\}$ ,

$$\Phi_w(a) = \mathbb{E}[w(c_i(a))] = w(1)\Pr(c_i(a) = 1) + w(\frac{1}{2})\Pr(c_i(a) = \frac{1}{2}).$$

Substituting the above probabilities, we obtain

$$\Phi_w(a) = w(1)\pi(a)T(a \rightarrow a) + w(\frac{1}{2})[\pi(a) + \pi^\rightarrow(a) - 2\pi(a)T(a \rightarrow a)].$$

Rearranging terms gives

$$\Phi_w(a) = w(\frac{1}{2})[\pi(a) + \pi^\rightarrow(a)] + (w(1) - 2w(\frac{1}{2}))\pi(a)T(a \rightarrow a),$$

which is exactly Eq. (17).  $\square$

## C.2 Asymptotic Convergence of PC-WMV

Throughout this subsection we assume the i.i.d. setup of Proposition 1.

By Proposition 2, applied to  $a^*$  and to any wrong  $a$  and subtracting,

$$\begin{aligned} \Phi_w(a^*) - \Phi_w(a) &= \underbrace{w(\frac{1}{2}) [\pi(a^*) + \pi^\rightarrow(a^*)] - (\pi(a) + \pi^\rightarrow(a))}_{\text{pooled-mass term}} \\ &\quad + \underbrace{\lambda_w [\pi(a^*)T(a^* \rightarrow a^*) - \pi(a)T(a \rightarrow a)]}_{\text{self-reproduction term}}. \end{aligned} \tag{18}$$

By Proposition 1, identifying  $a^*$  as the population maximizer requires this difference to be positive for every wrong  $a$ . The two assumptions below control the two terms separately.

**Assumption 1** (Self-reproduction dominance). *For every  $a \neq a^*$ ,*

$$\pi(a^*)T(a^* \rightarrow a^*) > \pi(a)T(a \rightarrow a). \tag{19}$$

**Interpretation.**  $\pi(a^*)T(a^* \rightarrow a^*)$  is the population mass of groups whose initial answer is correct and is reproduced correctly, and  $\pi(a)T(a \rightarrow a)$  is the corresponding mass for the wrong answer  $a$  that is reproduced as itself. Assumption 1 requires that correct self-reproduction dominate every individual wrong self-reproduction. Equivalently, it makes the self-reproduction term in the decomposition strictly positive whenever  $\lambda_w > 0$ .

**Assumption 2** (Pooled-mass dominance). *For every  $a \neq a^*$ ,*

$$\pi(a^*) + \pi^\rightarrow(a^*) > \pi(a) + \pi^\rightarrow(a). \tag{20}$$

**Interpretation.**  $\pi(a) + \pi^\rightarrow(a)$  is the total population mass on candidate  $a$ , combining initial occurrences and regeneration arrivals. Assumption 2 requires that  $a^*$  have the largest such total. By the same decomposition, it makes the pooled-mass term strictly positive whenever  $w(\frac{1}{2}) > 0$ .

**Theorem 2** (Asymptotic convergence of PC-WMV). *Let  $w$  satisfy  $w(0) = 0$ ,  $w(1) > 0$ , and  $\lambda_w := w(1) - 2w(\frac{1}{2}) \geq 0$ . Then:*

- (a) *If Assumptions 1 and 2 hold, then  $\hat{a}_N^{\text{PC}} \rightarrow a^*$  almost surely.*
- (b) *If  $w(\frac{1}{2}) = 0$ , then Assumption 2 is unnecessary: Assumption 1 alone implies  $\hat{a}_N^{\text{PC}} \rightarrow a^*$  almost surely.*

*Proof.* Fix any wrong  $a \neq a^*$ . By Assumption 1, the self-reproduction bracket of Eq. (18) is strictly positive, so the self-reproduction term is nonnegative and is strictly positive whenever  $\lambda_w > 0$ .

For part (a), Assumption 2 makes the pooled-mass bracket of Eq. (18) strictly positive, so the pooled-mass term is nonnegative and is strictly positive whenever  $w(\frac{1}{2}) > 0$ . Since  $w(1) = \lambda_w + 2w(\frac{1}{2}) > 0$ , at least one of  $\lambda_w$  and  $w(\frac{1}{2})$  is strictly positive, so  $\Phi_w(a^*) > \Phi_w(a)$  for every wrong  $a$ . Hence  $a^*$  is the unique maximizer of  $\Phi_w$ , and Proposition 1 yields  $\hat{a}_N^{\text{PC}} \rightarrow a^*$  almost surely.

For part (b), if  $w(\frac{1}{2}) = 0$  the pooled-mass term vanishes identically and  $\lambda_w = w(1) > 0$ , so the strict positivity of the self-reproduction term suffices to give  $\Phi_w(a^*) > \Phi_w(a)$  for every wrong  $a$ . Thus  $\hat{a}_N^{\text{PC}} \rightarrow a^*$  almost surely without Assumption 2.  $\square$

### C.3 Proof of Theorem 1

Theorem 1 follows from Theorem 2 by specializing to the binary case  $\mathcal{A} = \{a^*, a'\}$ , where  $a^*$  is the correct answer and  $a'$  is the only wrong answer (so  $\pi(a') = 1 - \pi(a^*)$ ). In this case, the two assumptions of Theorem 2 reduce to the same condition and the exact margin takes a one-bracket form, from which the asymptotic boundary  $\pi(a^*) > r_W/(r_C + r_W)$  follows.

**The two assumptions coincide.** With the only wrong answer being  $a'$  and  $\pi(a') = 1 - \pi(a^*)$ , Assumption 1 becomes the binary boundary

$$\pi(a^*) T(a^* \rightarrow a^*) > (1 - \pi(a^*)) T(a' \rightarrow a'). \quad (21)$$

For Assumption 2, expand  $\pi^\rightarrow$  via Eq. (14), using  $T(a^* \rightarrow a') = 1 - T(a^* \rightarrow a^*)$  and  $T(a' \rightarrow a^*) = 1 - T(a' \rightarrow a')$  (each row of  $T$  sums to one):

$$\begin{aligned} \pi^\rightarrow(a^*) &= \pi(a^*) T(a^* \rightarrow a^*) + (1 - \pi(a^*)) (1 - T(a' \rightarrow a')), \\ \pi^\rightarrow(a') &= \pi(a^*) (1 - T(a^* \rightarrow a^*)) + (1 - \pi(a^*)) T(a' \rightarrow a'). \end{aligned}$$

Adding  $\pi(a^*)$  and  $\pi(a') = 1 - \pi(a^*)$  and simplifying,

$$\begin{aligned} \pi(a^*) + \pi^\rightarrow(a^*) &= 1 + [\pi(a^*) T(a^* \rightarrow a^*) - (1 - \pi(a^*)) T(a' \rightarrow a')], \\ \pi(a') + \pi^\rightarrow(a') &= 1 - [\pi(a^*) T(a^* \rightarrow a^*) - (1 - \pi(a^*)) T(a' \rightarrow a')]. \end{aligned}$$

Subtracting,

$$[\pi(a^*) + \pi^\rightarrow(a^*)] - [\pi(a') + \pi^\rightarrow(a')] = 2 [\pi(a^*) T(a^* \rightarrow a^*) - (1 - \pi(a^*)) T(a' \rightarrow a')].$$

Hence Assumptions 1 and 2 reduce to the same condition Eq. (21), and Theorem 2 (a) gives  $\hat{a}_N^{\text{PC}} \rightarrow a^*$  a.s. whenever Eq. (21) holds.

**The exact margin.** Applying Eq. (18) with  $a = a'$ , the self-reproduction term contributes  $\lambda_w$  times the quantity  $\pi(a^*) T(a^* \rightarrow a^*) - (1 - \pi(a^*)) T(a' \rightarrow a')$ . By the identity above, the pooled-mass term contributes  $2w(\frac{1}{2})$  times the same bracket. Their sum is  $w(1) = \lambda_w + 2w(\frac{1}{2})$  times the bracket:

$$\Phi_w(a^*) - \Phi_w(a') = w(1) [\pi(a^*) T(a^* \rightarrow a^*) - (1 - \pi(a^*)) T(a' \rightarrow a')]. \quad (22)$$

The choice of  $w$  thus enters only through  $w(1)$ .

*Proof.* By Eq. (22) and  $w(1) > 0$ ,  $\Phi_w(a^*) > \Phi_w(a')$  if and only if

$$\pi(a^*) T(a^* \rightarrow a^*) > (1 - \pi(a^*)) T(a' \rightarrow a').$$

By Proposition 1, this is equivalent to  $\hat{a}_N^{\text{PC}} \rightarrow a^*$  almost surely. Identifying  $r_C := T(a^* \rightarrow a^*)$  and  $r_W := T(a' \rightarrow a')$  via Eq. (13) rewrites the threshold as

$$\pi(a^*) > \frac{r_W}{r_C + r_W}.$$

Standard MV's vote count  $\frac{1}{N} \sum_{i=1}^N \mathbf{1}\{a_i = a\}$  converges to  $\pi(a)$  a.s. by the strong law of large numbers, so Standard MV converges to  $a^*$  if and only if  $\pi(a^*) > \frac{1}{2}$ . Hence PC-WMV converges where Standard MV does not on the interval  $r_W/(r_C + r_W) < \pi(a^*) \leq \frac{1}{2}$ , which has positive length if and only if  $r_C > r_W$ .  $\square$

#### C.4 Empirical Verification of Assumptions

Table 5 verifies that Assumption 1 (A1) and Assumption 2 (A2) hold empirically on  $\mathcal{Q}' := \{q \in \mathcal{Q} : 0 < \pi_q(a_q^*) < 1\}$ , the subset of problems on which the verification is non-degenerate. At  $\pi_q(a_q^*) = 1$  no wrong answer carries population mass, so A1 and A2 hold vacuously and would only inflate the reported probabilities. At  $\pi_q(a_q^*) = 0$  the per-problem rate  $r_{C,q} = T(a_q^* \rightarrow a_q^*)$  is undefined and  $a_q^*$  is not a population maximizer, so the framework does not apply.  $\mathcal{Q}'$  also matches the subset used in the  $\overline{\text{AUROC}}$  analysis (Section 4.1, Appendix G.2). The table further reports the per-problem indicator  $\Delta_{w^{(n)}} := \min_{a \neq a^*} [\Phi_{w^{(n)}}(a^*) - \Phi_{w^{(n)}}(a)]$  for  $w^{(n)}(c) = c^n$ ,  $n \in \{1, 2, 3\}$  ( $\Delta_{w^{(n)}} > 0$  is equivalent to  $a^*$  being the unique maximizer of  $\Phi_{w^{(n)}}$ ).

$\Pr[\text{A1}]$  is non-negligible across a wide range of benchmarks and models, so A1 is not a rare or pathological event in practice. Conditional on A1,  $\Pr[\text{A2} \mid \text{A1}]$  is at least 87.5% on every cell and reaches 100% on 40% of them, so the joint occurrence of A1 and A2 is common. The last three columns ( $\Pr[\Delta_{w^{(n)}} > 0 \mid \text{A1}]$ ) further show that the positive gap predicted by Theorem 2 occurs with overwhelmingly high probability for  $w^{(n)}(c) = c^n$ ,  $n \in \{1, 2, 3\}$ , even under the weaker condition that does not require A2. These findings indicate that the assumptions are not artificially imposed but rather reflect patterns that arise naturally and frequently in real experimental data.

Table 5: **Empirical verification of Theorem 2’s assumptions** on  $\mathcal{Q}'$ , checking A1 and A2 for every wrong  $a$ . All probabilities are macro-averaged: each problem in  $\mathcal{Q}'$  contributes one indicator per event. Theorem 2 predicts  $\Pr[\Delta_{w^{(n)}} > 0 \mid \text{A1} \cap \text{A2}] = 1$  for every convex  $w$ . The last three columns report the weaker  $\Pr[\Delta_{w^{(n)}} > 0 \mid \text{A1}]$  for  $w^{(n)}(c) = c^n$ ,  $n \in \{1, 2, 3\}$ .

Benchmark	Model	$\mathcal{Q}'$	$\Pr[\text{A1}]$	$\Pr[\text{A2} \mid \text{A1}]$	$\Pr[\Delta_{w^{(n)}} > 0 \mid \text{A1}]$		
					$n=1$	$n=2$	$n=3$
FrontierScience-Olympiad	GPT-OSS-120B	73	64.4	93.6	93.6	97.9	97.9
	GPT-OSS-20B	74	70.3	96.2	96.2	98.1	100.0
	Nemotron3-30B	80	61.3	93.9	93.9	98.0	100.0
	Nemotron2-9B	59	35.6	90.5	90.5	90.5	100.0
	Ministral3-14B	47	36.2	94.1	94.1	100.0	100.0
HMMT Feb 2026	GPT-OSS-120B	24	79.2	94.7	94.7	100.0	100.0
	GPT-OSS-20B	24	83.3	100.0	100.0	100.0	100.0
	Nemotron3-30B	20	80.0	100.0	100.0	100.0	100.0
	Nemotron2-9B	23	56.5	100.0	100.0	100.0	100.0
	Ministral3-14B	23	69.6	87.5	87.5	93.8	100.0
AIME 2025	GPT-OSS-120B	23	100.0	91.3	91.3	95.7	100.0
	GPT-OSS-20B	26	92.3	100.0	100.0	100.0	100.0
	Nemotron3-30B	17	100.0	100.0	100.0	100.0	100.0
	Nemotron2-9B	23	73.9	100.0	100.0	100.0	100.0
	Ministral3-14B	23	73.9	94.1	94.1	100.0	100.0
Brumo 2025	GPT-OSS-120B	21	81.0	94.1	94.1	94.1	100.0
	GPT-OSS-20B	23	95.7	95.5	95.5	95.5	100.0
	Nemotron3-30B	20	95.0	100.0	100.0	100.0	100.0
	Nemotron2-9B	20	70.0	100.0	100.0	100.0	100.0
	Ministral3-14B	26	88.5	91.3	91.3	95.7	100.0

## D Additional Experiments

### D.1 ROC Curves for Correctness Predictors

Tables 1 and 2 report  $\overline{\text{AUROC}}$  as a single number per (model, benchmark, signal). Figure 4 visualizes the underlying ROC curves on the same 5 model  $\times$  4 benchmark grid, overlaying prefix consistency and the WMV baselines per panel. Curves are macro-averaged: each problem’s ROC is interpolated onto a common false-positive-rate grid and then averaged over the same problem subset  $\mathcal{Q}'$  used in  $\overline{\text{AUROC}}$  (problems with at least one correct and one wrong initial sample, Appendix G.2).

The visual pattern matches the  $\overline{\text{AUROC}}$  numbers: prefix consistency’s curve sits at or above the baselines on FrontierScience-Olympiad and HMMT Feb 2026 in 8 of the 10 (model, benchmark) settings across the five models, while on AIME 2025 and Brumo 2025 the gap shrinks as the baselines’ curves move closer to PC. The two cells where PC is not visibly above are Nemotron2-9B FrontierScience-Olympiad (where P(True) leads, consistent with PC’s smallest discrimination gap  $D$  in Table 1) and GPT-OSS-120B HMMT Feb 2026 (where DeepConf tail edges PC by .03 in AUROC).

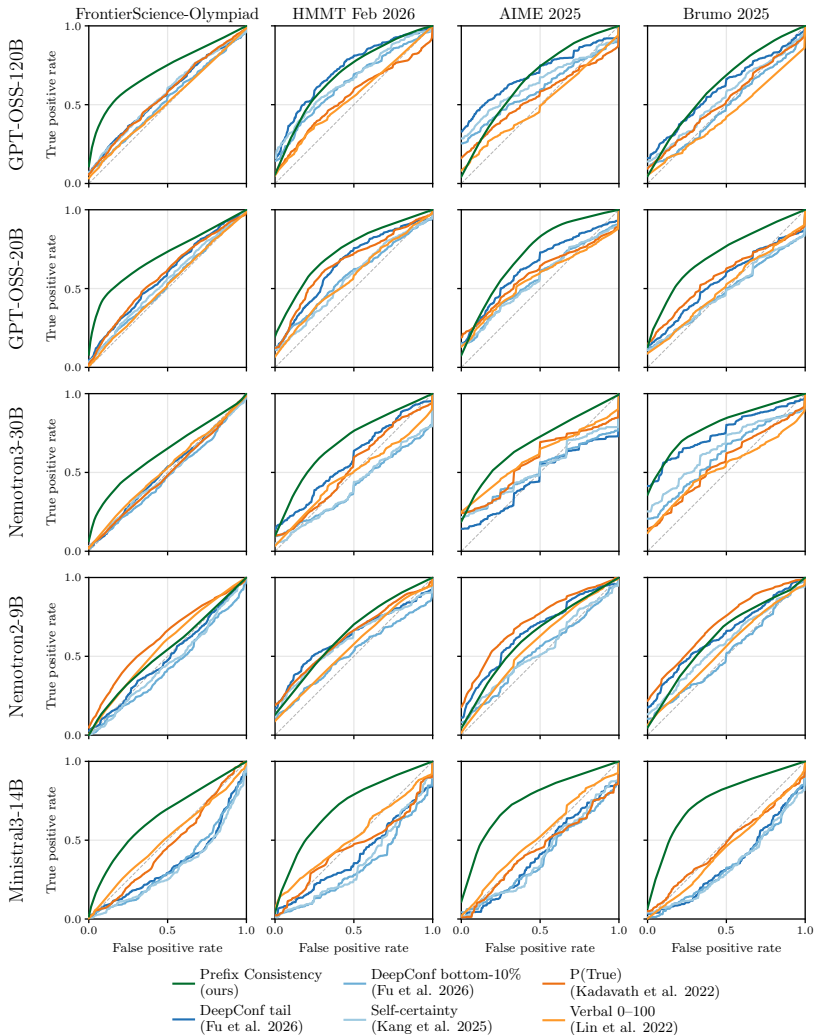


Figure 4: **Macro ROC curves for prefix consistency and the WMV baselines, all 20 (model, benchmark) cells.** Rows are models, columns are benchmarks. Each curve is the per-problem ROC averaged on a common false-positive-rate grid, restricted to problems with at least one correct and one wrong initial sample. The dashed diagonal is the random-classifier baseline.

## D.2 Cost–Accuracy Curves

Figure 5 extends the cost–accuracy analysis of Figure 1 to all 20 (model, benchmark) cells, complementing the fixed-budget tables in Appendix D.3. Across nearly all 20 cells PC-cubic (green) sits above the other baselines once the budget exceeds the per-problem regeneration cost, and reaches Standard MV plateau at a noticeably smaller budget. The discrimination gap is largest on FrontierScience-Olympiad and shrinks as Standard MV plateau approaches its peak (AIME 2025, Brumo 2025).

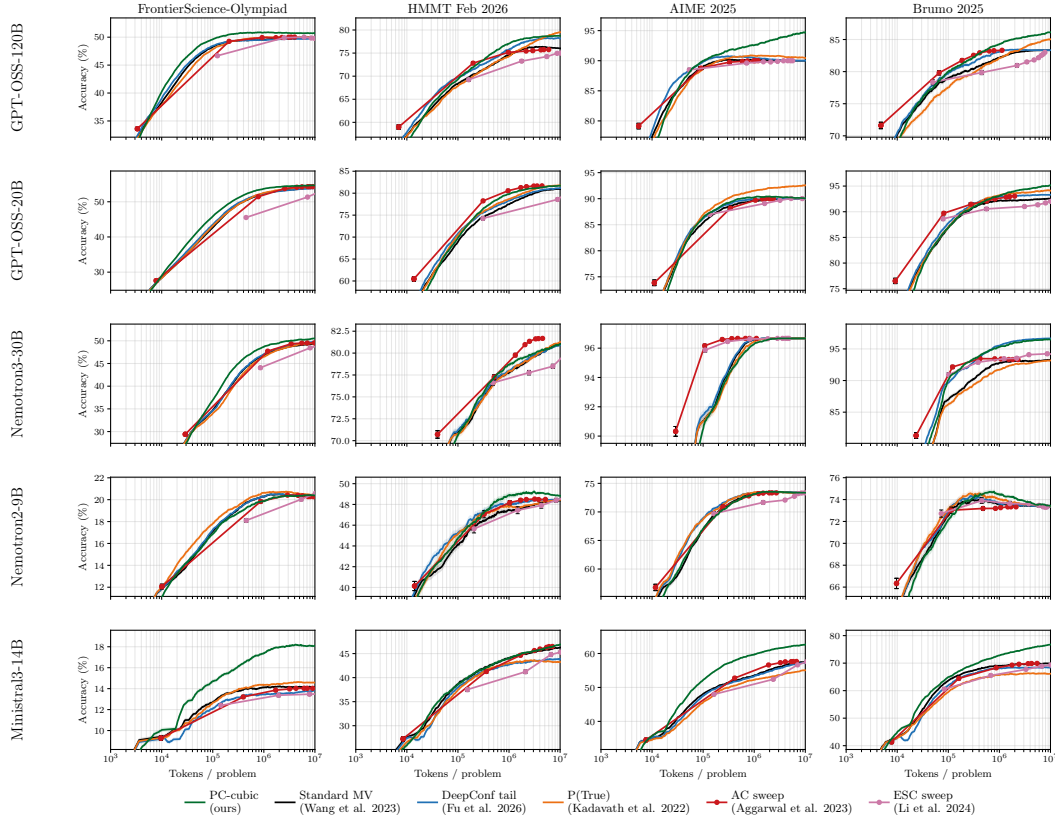


Figure 5: **Cost–accuracy curves for all 20 (model, benchmark) cells.** Rows are models, columns are benchmarks. Y-axes are auto-zoomed to the Pass@1–plateau range. Shaded bands are  $\pm 2\sigma$  confidence intervals on accuracy; AC and ESC operating points carry vertical (accuracy) and horizontal (cost)  $\pm 2\sigma$  error bars.

## D.3 Full Baseline Comparison

Figure 6 extends Figure 5 to the full baseline set plus the oracle upper bounds. The three PC variants form a tight green band near the plateau across nearly every cell, while the DeepConf variants and especially their filtered variants spread out widely.

Tables 6, 7, 8, 9, and 10 report fixed-budget accuracy at  $B \in \{250k, 1M, 5M\}$  tokens for every evaluated baseline (Standard MV, all five DeepConf aggregation strategies [Fu et al., 2026] and their filtered variants, Response probability, verbalized confidence and P(True) [Taubenfeld et al., 2025, Kadavath et al., 2022], and PC-linear/quadratic/cubic), one table per model. See Appendix E for baseline definitions. Tables 11, 12, 13, 14, and 15 report the corresponding token-efficiency ratios at  $\alpha \in \{75\%, 90\%, 99\%\}$ .

Two patterns emerge. First, on the more difficult science benchmark (FrontierScience-Olympiad) PC-cubic is the best non-oracle method at  $B=250k$  and  $B=1M$  for the four models with non-trivial discrimination gap (GPT-OSS-120B, GPT-OSS-20B, Nemotron3-30B, Ministral3-14B): at  $B=1M$  it reaches .508, .537, .486, and .174 respectively, against the strongest non-PC baseline at .503, .525,

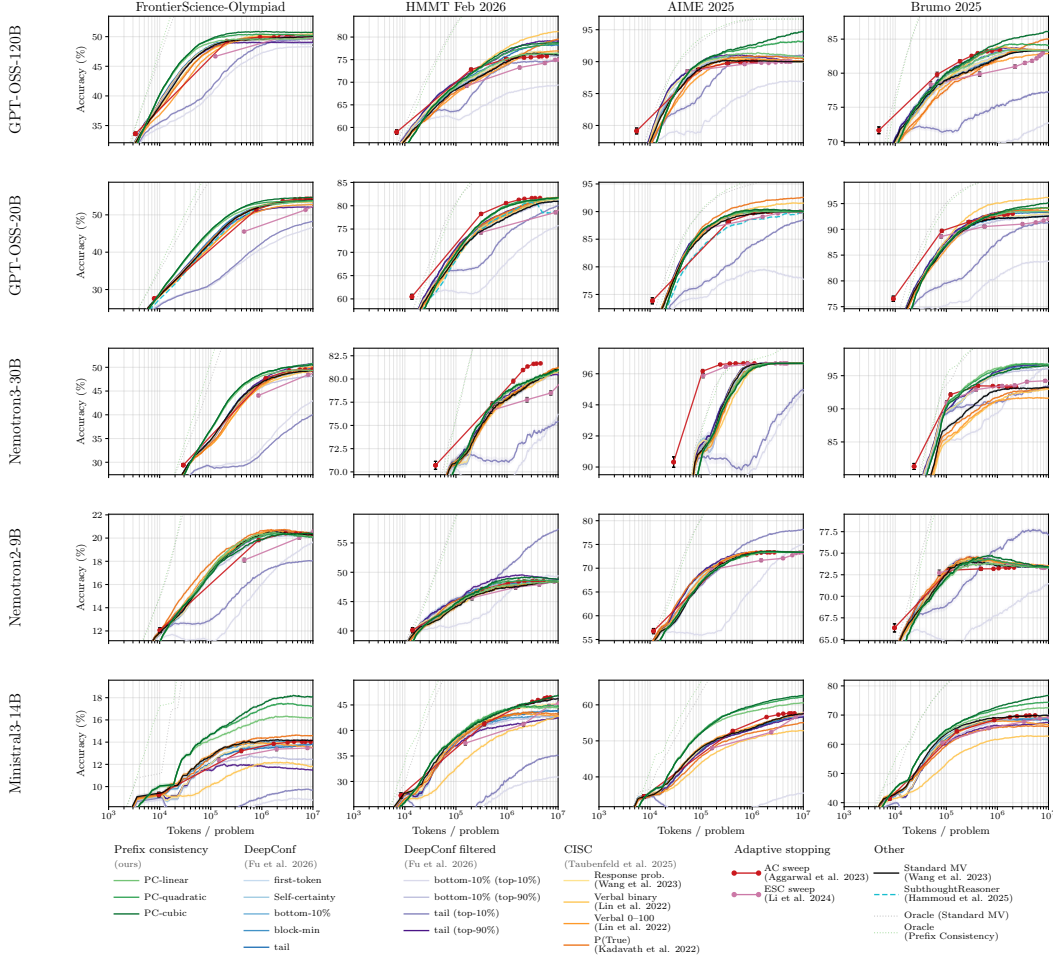


Figure 6: **Cost–accuracy curves with the full baseline set.** Same layout as Figure 5, but additionally includes the oracle upper bounds alongside all evaluated baselines. Methods are colored by family: greens for PC, blues for DeepConf, purples for filtered DeepConf, browns/oranges for CISC, red for AC, mauve for ESC, cyan for SubthoughtReasoner, gray for Standard MV. Oracles are dotted. Shaded bands are  $\pm 2\sigma$  confidence intervals on accuracy; AC and ESC operating points carry vertical (accuracy) and horizontal (cost)  $\pm 2\sigma$  error bars.

.472, and .143. At  $B=5M$  PC-cubic remains best on three of these four, with PC-quadratic narrowly ahead on Nemotron3-30B (.504 vs. .503, within  $2\sigma$ ). The PC-linear  $\leq$  PC-quadratic  $\leq$  PC-cubic ordering holds in 11 of the 12 (model, budget) FrontierScience-Olympiad cells over these four models, with the Nemotron3-30B 5M cell as the only inversion, consistent with the convex-weight analysis: in Eq. (17), the coefficient  $\lambda_w := w(1) - 2w(\frac{1}{2})$  on the self-reproduction term  $\pi(a)T(a \rightarrow a)$  (the joint probability that  $a$  is both the initial and the regenerated answer) takes values  $0, \frac{1}{2}, \frac{3}{4}$  for PC-linear, PC-quadratic, PC-cubic respectively, so larger  $n$  upweights self-reproducing candidates more strongly. The exception is Nemotron2-9B, whose FrontierScience-Olympiad discrimination gap is the smallest in our suite ( $D = 7.4\%$ , Table 1). PC-WMV there roughly matches Standard MV (PC-cubic .199 vs. Standard MV .203 at  $B=1M$ ), consistent with Theorem 1 predicting no advantage when  $D$  is small.

Second, on the easier benchmarks (AIME 2025, Brumo 2025) where Standard MV plateau already sits close to its peak, verbalized confidence (Verbal binary, P(True)) and DeepConf tail (top-90%) become competitive or take the lead in a few cells (e.g. Verbal binary on GPT-OSS-20B Brumo reaches .951 at  $B=1M$  vs. .931 for PC-cubic). This matches the cost–quality trade-off discussed in

Section 4, where PC’s larger per-group cost is no longer amortized once Standard MV is near its plateau.

SubthoughtReasoner [Hammoud et al., 2025] appears only in the GPT-OSS-20B tables, the only model for which it has been re-evaluated under the unified incremental path. SubthoughtReasoner does not consistently improve over Standard MV (vs. Standard MV at  $B=1M$ : .778 vs. .775 on HMMT, .518 vs. .523 on FrontierScience-Olympiad, .886 vs. .896 on AIME 2025), and the GPT-OSS-20B Brumo cell and other-model cells are not evaluated.

Table 6: All baselines, GPT-OSS-120B (higher accuracy is better). Bold marks the best non-oracle per column. Subscripts are  $\pm 2\sigma$  CI.

Method	FrontierScience-Olympiad			HMMT Feb 2026			AIME 2025			Brumo 2025		
	$B=250k$	$B=1M$	$B=5M$	$B=250k$	$B=1M$	$B=5M$	$B=250k$	$B=1M$	$B=5M$	$B=250k$	$B=1M$	$B=5M$
<i>Baseline</i>												
Standard MV	.493 $\pm$ .001	.495 $\pm$ .001	.499 $\pm$ .001	.708 $\pm$ .003	.745 $\pm$ .003	.763 $\pm$ .001	.901 $\pm$ .002	.901 $\pm$ .001	.900 $\pm$ .000	.801 $\pm$ .003	.821 $\pm$ .002	.833 $\pm$ .000
<i>DeepConf</i>												
DeepConf first-token	.493 $\pm$ .001	.495 $\pm$ .001	.499 $\pm$ .001	.708 $\pm$ .003	.745 $\pm$ .003	.763 $\pm$ .001	.901 $\pm$ .002	.901 $\pm$ .001	.900 $\pm$ .000	.801 $\pm$ .003	.821 $\pm$ .002	.833 $\pm$ .000
Self-certainty	.494 $\pm$ .001	.495 $\pm$ .001	.497 $\pm$ .001	.713 $\pm$ .003	.749 $\pm$ .003	.768 $\pm$ .002	.904 $\pm$ .002	.903 $\pm$ .001	.900 $\pm$ .000	.805 $\pm$ .003	.826 $\pm$ .002	.833 $\pm$ .000
DeepConf bottom-10%	.493 $\pm$ .001	.495 $\pm$ .001	.496 $\pm$ .001	.710 $\pm$ .003	.747 $\pm$ .003	.764 $\pm$ .001	.902 $\pm$ .002	.902 $\pm$ .001	.900 $\pm$ .000	.802 $\pm$ .003	.823 $\pm$ .002	.833 $\pm$ .000
DeepConf block-min	.494 $\pm$ .001	.495 $\pm$ .001	.497 $\pm$ .001	.708 $\pm$ .003	.747 $\pm$ .003	.764 $\pm$ .001	.902 $\pm$ .002	.902 $\pm$ .001	.900 $\pm$ .000	.802 $\pm$ .003	.824 $\pm$ .002	.833 $\pm$ .000
DeepConf tail	.493 $\pm$ .001	.495 $\pm$ .001	.497 $\pm$ .001	.720 $\pm$ .003	.758 $\pm$ .003	.783 $\pm$ .002	.906 $\pm$ .002	.905 $\pm$ .001	.900 $\pm$ .000	.810 $\pm$ .003	.831 $\pm$ .001	.833 $\pm$ .000
<i>DeepConf (filtered)</i>												
DeepConf bottom-10% (top-10%)	.440 $\pm$ .002	.472 $\pm$ .001	.483 $\pm$ .001	.638 $\pm$ .004	.675 $\pm$ .003	.690 $\pm$ .002	.823 $\pm$ .003	.856 $\pm$ .002	.869 $\pm$ .001	.683 $\pm$ .004	.697 $\pm$ .003	.716 $\pm$ .002
DeepConf bottom-10% (top-90%)	.490 $\pm$ .001	.490 $\pm$ .001	.489 $\pm$ .001	.713 $\pm$ .003	.746 $\pm$ .002	.759 $\pm$ .001	.903 $\pm$ .002	.903 $\pm$ .001	.900 $\pm$ .000	.803 $\pm$ .003	.825 $\pm$ .002	.833 $\pm$ .000
DeepConf tail (top-10%)	.450 $\pm$ .002	.485 $\pm$ .001	.495 $\pm$ .001	.681 $\pm$ .004	.739 $\pm$ .003	.745 $\pm$ .002	.884 $\pm$ .003	.907 $\pm$ .002	.909 $\pm$ .002	.731 $\pm$ .004	.753 $\pm$ .004	.770 $\pm$ .002
DeepConf tail (top-90%)	.489 $\pm$ .001	.489 $\pm$ .001	.490 $\pm$ .001	.728 $\pm$ .003	.766 $\pm$ .003	.791 $\pm$ .002	.909 $\pm$ .002	.909 $\pm$ .001	.902 $\pm$ .001	.816 $\pm$ .003	.835 $\pm$ .001	.835 $\pm$ .001
<i>CISC</i>												
Response probability	.493 $\pm$ .001	.495 $\pm$ .001	.497 $\pm$ .001	.714 $\pm$ .003	.750 $\pm$ .003	.768 $\pm$ .002	.905 $\pm$ .002	.902 $\pm$ .001	.900 $\pm$ .000	.804 $\pm$ .003	.825 $\pm$ .002	.833 $\pm$ .000
Verbal binary	.492 $\pm$ .001	.503 $\pm$ .001	.504 $\pm$ .001	.729 $\pm$ .003	.777 $\pm$ .002	.807 $\pm$ .001	.902 $\pm$ .002	.904 $\pm$ .001	.901 $\pm$ .000	.813 $\pm$ .003	.839 $\pm$ .002	.835 $\pm$ .001
Verbal 0-100	.490 $\pm$ .001	.499 $\pm$ .001	.500 $\pm$ .001	.702 $\pm$ .003	.739 $\pm$ .003	.766 $\pm$ .002	.896 $\pm$ .002	.904 $\pm$ .001	.902 $\pm$ .001	.802 $\pm$ .003	.818 $\pm$ .002	.827 $\pm$ .001
P(True)	.493 $\pm$ .001	.500 $\pm$ .001	.500 $\pm$ .000	.706 $\pm$ .003	.743 $\pm$ .003	.784 $\pm$ .002	.902 $\pm$ .002	.909 $\pm$ .001	.906 $\pm$ .001	.794 $\pm$ .003	.821 $\pm$ .003	.844 $\pm$ .002
<i>Prefix consistency</i>												
PC-linear	.495 $\pm$ .001	.496 $\pm$ .001	.496 $\pm$ .001	.717 $\pm$ .003	.751 $\pm$ .002	.764 $\pm$ .001	.906 $\pm$ .002	.913 $\pm$ .002	.909 $\pm$ .001	.810 $\pm$ .003	.830 $\pm$ .002	.833 $\pm$ .000
PC-quadratic	.502 $\pm$ .001	.504 $\pm$ .001	.503 $\pm$ .001	.725 $\pm$ .003	.764 $\pm$ .002	.782 $\pm$ .001	.912 $\pm$ .002	.922 $\pm$ .002	.930 $\pm$ .002	.815 $\pm$ .003	.837 $\pm$ .002	.842 $\pm$ .001
PC-cubic	.506 $\pm$ .001	.508 $\pm$ .001	.507 $\pm$ .001	.727 $\pm$ .003	.771 $\pm$ .002	.786 $\pm$ .001	.913 $\pm$ .002	.926 $\pm$ .002	.941 $\pm$ .002	.818 $\pm$ .003	.842 $\pm$ .002	.857 $\pm$ .001

Table 7: All baselines, GPT-OSS-20B (higher accuracy is better). Bold marks the best non-oracle per column. Subscripts are  $\pm 2\sigma$  CI.

Method	FrontierScience-Olympiad			HMMT Feb 2026			AIME 2025			Brumo 2025		
	$B=250k$	$B=1M$	$B=5M$	$B=250k$	$B=1M$	$B=5M$	$B=250k$	$B=1M$	$B=5M$	$B=250k$	$B=1M$	$B=5M$
<i>Baseline</i>												
Standard MV	.482 $\pm$ .002	.523 $\pm$ .001	.537 $\pm$ .001	.736 $\pm$ .003	.775 $\pm$ .002	.807 $\pm$ .001	.881 $\pm$ .002	.896 $\pm$ .001	.900 $\pm$ .000	.901 $\pm$ .003	.922 $\pm$ .002	.924 $\pm$ .001
<i>DeepConf</i>												
DeepConf first-token	.482 $\pm$ .002	.523 $\pm$ .001	.537 $\pm$ .001	.736 $\pm$ .003	.775 $\pm$ .002	.807 $\pm$ .001	.881 $\pm$ .002	.896 $\pm$ .001	.900 $\pm$ .000	.901 $\pm$ .003	.922 $\pm$ .002	.924 $\pm$ .001
Self-certainty	.482 $\pm$ .002	.522 $\pm$ .001	.535 $\pm$ .001	.738 $\pm$ .003	.778 $\pm$ .003	.808 $\pm$ .001	.885 $\pm$ .002	.898 $\pm$ .001	.900 $\pm$ .000	.903 $\pm$ .003	.924 $\pm$ .002	.927 $\pm$ .001
DeepConf bottom-10%	.483 $\pm$ .002	.521 $\pm$ .001	.536 $\pm$ .001	.737 $\pm$ .003	.777 $\pm$ .002	.808 $\pm$ .001	.882 $\pm$ .002	.896 $\pm$ .001	.900 $\pm$ .000	.900 $\pm$ .003	.921 $\pm$ .002	.924 $\pm$ .001
DeepConf block-min	.483 $\pm$ .002	.523 $\pm$ .001	.536 $\pm$ .001	.739 $\pm$ .003	.776 $\pm$ .003	.807 $\pm$ .001	.883 $\pm$ .002	.896 $\pm$ .001	.900 $\pm$ .000	.900 $\pm$ .003	.921 $\pm$ .002	.925 $\pm$ .001
DeepConf tail	.486 $\pm$ .002	.524 $\pm$ .001	.536 $\pm$ .001	.746 $\pm$ .003	.783 $\pm$ .002	.809 $\pm$ .001	.886 $\pm$ .002	.899 $\pm$ .001	.900 $\pm$ .000	.908 $\pm$ .003	.930 $\pm$ .002	.933 $\pm$ .001
<i>DeepConf (filtered)</i>												
DeepConf bottom-10% (top-10%)	.351 $\pm$ .002	.410 $\pm$ .002	.453 $\pm$ .001	.614 $\pm$ .004	.678 $\pm$ .004	.741 $\pm$ .003	.769 $\pm$ .004	.792 $\pm$ .003	.785 $\pm$ .003	.760 $\pm$ .004	.808 $\pm$ .004	.837 $\pm$ .002
DeepConf bottom-10% (top-90%)	.472 $\pm$ .002	.512 $\pm$ .001	.526 $\pm$ .001	.737 $\pm$ .003	.777 $\pm$ .002	.805 $\pm$ .002	.883 $\pm$ .002	.896 $\pm$ .001	.900 $\pm$ .000	.896 $\pm$ .003	.917 $\pm$ .002	.926 $\pm$ .001
DeepConf tail (top-10%)	.356 $\pm$ .002	.425 $\pm$ .002	.472 $\pm$ .001	.667 $\pm$ .005	.740 $\pm$ .003	.786 $\pm$ .002	.794 $\pm$ .004	.840 $\pm$ .003	.876 $\pm$ .002	.813 $\pm$ .005	.876 $\pm$ .004	.909 $\pm$ .003
DeepConf tail (top-90%)	.476 $\pm$ .002	.513 $\pm$ .002	.521 $\pm$ .001	.749 $\pm$ .003	.788 $\pm$ .002	.811 $\pm$ .001	.887 $\pm$ .002	.901 $\pm$ .002	.900 $\pm$ .000	.909 $\pm$ .003	.933 $\pm$ .002	.936 $\pm$ .001
<i>CISC</i>												
Response probability	.482 $\pm$ .002	.522 $\pm$ .001	.534 $\pm$ .001	.739 $\pm$ .003	.778 $\pm$ .003	.809 $\pm$ .001	.882 $\pm$ .002	.897 $\pm$ .001	.900 $\pm$ .000	.903 $\pm$ .003	.924 $\pm$ .002	.928 $\pm$ .001
Verbal binary	.465 $\pm$ .002	.518 $\pm$ .001	.534 $\pm$ .001	.742 $\pm$ .003	.783 $\pm$ .002	.811 $\pm$ .001	.885 $\pm$ .002	.905 $\pm$ .002	.915 $\pm$ .002	.922 $\pm$ .003	.951 $\pm$ .002	.959 $\pm$ .001
Verbal 0-100	.465 $\pm$ .002	.511 $\pm$ .001	.527 $\pm$ .001	.741 $\pm$ .003	.780 $\pm$ .002	.813 $\pm$ .001	.887 $\pm$ .002	.899 $\pm$ .002	.900 $\pm$ .001	.903 $\pm$ .003	.930 $\pm$ .002	.936 $\pm$ .001
P(True)	.480 $\pm$ .002	.525 $\pm$ .001	.540 $\pm$ .001	.750 $\pm$ .003	.787 $\pm$ .002	.815 $\pm$ .001	.895 $\pm$ .002	.916 $\pm$ .002	.924 $\pm$ .001	.906 $\pm$ .003	.932 $\pm$ .002	.940 $\pm$ .002
<i>SubthoughtReasoner</i>												
SubthoughtReasoner	.464 $\pm$ .002	.518 $\pm$ .001	.536 $\pm$ .001	.732 $\pm$ .004	.778 $\pm$ .003	.790 $\pm$ .003	.860 $\pm$ .003	.886 $\pm$ .002	.897 $\pm$ .002	—	—	—
<i>Prefix consistency</i>												
PC-linear	.495 $\pm$ .002	.524 $\pm$ .001	.535 $\pm$ .001	.751 $\pm$ .003	.797 $\pm$ .002	.812 $\pm$ .001	.887 $\pm$ .002	.899 $\pm$ .001	.900 $\pm$ .000	.903 $\pm$ .003	.928 $\pm$ .002	.934 $\pm$ .001
PC-quadratic	.502 $\pm$ .002	.532 $\pm$ .001	.537 $\pm$ .001	.752 $\pm$ .003	.800 $\pm$ .002	.814 $\pm$ .001	.888 $\pm$ .002	.901 $\pm$ .002	.901 $\pm$ .001	.904 $\pm$ .003	.930 $\pm$ .002	.940 $\pm$ .001
PC-cubic	.502 $\pm$ .002	.537 $\pm$ .001	.545 $\pm$ .001	.753 $\pm$ .004	.797 $\pm$ .002	.814 $\pm$ .001	.888 $\pm$ .002	.902 $\pm$ .002	.902 $\pm$ .001	.903 $\pm$ .003	.931 $\pm$ .002	.947 $\pm$ .002

Table 8: All baselines, Nemotron3-30B (higher accuracy is better). Bold marks the best non-oracle per column. Subscripts are  $\pm 2\sigma$  CI.

Method	FrontierScience-Olympiad			HMMT Feb 2026			AIME 2025			Brumo 2025		
	B=250k	B=1M	B=5M	B=250k	B=1M	B=5M	B=250k	B=1M	B=5M	B=250k	B=1M	B=5M
<i>Baseline</i>												
Standard MV	.404 $\pm$ .002	.468 $\pm$ .002	.490 $\pm$ .001	.736 $\pm$ .004	.777 $\pm$ .003	.802 $\pm$ .002	.935 $\pm$ .002	<b>.966</b> $\pm$ .000	<b>.967</b> $\pm$ .000	.896 $\pm$ .003	.928 $\pm$ .002	.931 $\pm$ .001
<i>DeepConf</i>												
DeepConf first-token	.403 $\pm$ .002	.467 $\pm$ .002	.490 $\pm$ .001	.736 $\pm$ .004	.777 $\pm$ .003	.802 $\pm$ .002	.934 $\pm$ .002	<b>.966</b> $\pm$ .001	<b>.967</b> $\pm$ .000	.895 $\pm$ .003	.927 $\pm$ .002	.931 $\pm$ .001
Self-certainty	.402 $\pm$ .002	.468 $\pm$ .002	.491 $\pm$ .001	.734 $\pm$ .004	.779 $\pm$ .003	<b>.804</b> $\pm$ .002	.935 $\pm$ .002	<b>.966</b> $\pm$ .000	<b>.967</b> $\pm$ .000	.918 $\pm$ .003	.954 $\pm$ .002	.963 $\pm$ .001
DeepConf bottom-10%	.401 $\pm$ .002	.466 $\pm$ .002	.489 $\pm$ .001	.732 $\pm$ .004	.779 $\pm$ .003	.802 $\pm$ .002	.930 $\pm$ .003	<b>.966</b> $\pm$ .000	<b>.967</b> $\pm$ .000	.918 $\pm$ .003	.953 $\pm$ .002	.963 $\pm$ .001
DeepConf block-min	.400 $\pm$ .002	.467 $\pm$ .002	.491 $\pm$ .001	.735 $\pm$ .004	.778 $\pm$ .003	.802 $\pm$ .002	.933 $\pm$ .003	<b>.966</b> $\pm$ .001	<b>.967</b> $\pm$ .000	.919 $\pm$ .003	.954 $\pm$ .002	.962 $\pm$ .001
DeepConf tail	.405 $\pm$ .002	.470 $\pm$ .002	.494 $\pm$ .001	.740 $\pm$ .004	.779 $\pm$ .003	.801 $\pm$ .002	<b>.937</b> $\pm$ .002	<b>.966</b> $\pm$ .000	<b>.967</b> $\pm$ .000	.920 $\pm$ .003	.955 $\pm$ .002	.965 $\pm$ .001
<i>DeepConf (filtered)</i>												
DeepConf bottom-10% (top-10%)	.297 $\pm$ .003	.329 $\pm$ .003	.406 $\pm$ .002	.688 $\pm$ .004	.688 $\pm$ .004	.738 $\pm$ .004	.889 $\pm$ .003	.898 $\pm$ .003	.935 $\pm$ .002	.860 $\pm$ .004	.893 $\pm$ .004	.947 $\pm$ .003
DeepConf bottom-10% (top-90%)	.398 $\pm$ .002	.458 $\pm$ .002	.479 $\pm$ .002	.732 $\pm$ .004	.778 $\pm$ .003	.799 $\pm$ .002	.930 $\pm$ .003	.965 $\pm$ .001	<b>.967</b> $\pm$ .000	.918 $\pm$ .003	.950 $\pm$ .002	.959 $\pm$ .001
DeepConf tail (top-10%)	.290 $\pm$ .003	.319 $\pm$ .002	.381 $\pm$ .002	.718 $\pm$ .004	.712 $\pm$ .004	.746 $\pm$ .003	.906 $\pm$ .003	.905 $\pm$ .003	.938 $\pm$ .002	.905 $\pm$ .003	.910 $\pm$ .003	.928 $\pm$ .002
DeepConf tail (top-90%)	.404 $\pm$ .003	.472 $\pm$ .002	.503 $\pm$ .002	.740 $\pm$ .004	.782 $\pm$ .003	.801 $\pm$ .002	<b>.937</b> $\pm$ .002	<b>.966</b> $\pm$ .000	<b>.967</b> $\pm$ .000	.920 $\pm$ .003	.955 $\pm$ .002	.966 $\pm$ .000
<i>CISC</i>												
Response probability	.401 $\pm$ .002	.468 $\pm$ .002	.491 $\pm$ .001	.734 $\pm$ .004	.779 $\pm$ .003	.803 $\pm$ .002	.934 $\pm$ .002	<b>.966</b> $\pm$ .000	<b>.967</b> $\pm$ .000	.918 $\pm$ .003	.954 $\pm$ .002	.963 $\pm$ .001
Verbal binary	.386 $\pm$ .003	.459 $\pm$ .002	.487 $\pm$ .002	.734 $\pm$ .004	.777 $\pm$ .003	.800 $\pm$ .002	.925 $\pm$ .003	.962 $\pm$ .001	<b>.967</b> $\pm$ .000	.875 $\pm$ .003	.912 $\pm$ .002	.927 $\pm$ .001
Verbal 0-100	.387 $\pm$ .003	.462 $\pm$ .002	.497 $\pm$ .002	.732 $\pm$ .004	.779 $\pm$ .003	<b>.804</b> $\pm$ .002	.928 $\pm$ .003	.963 $\pm$ .001	<b>.967</b> $\pm$ .000	.878 $\pm$ .003	.912 $\pm$ .002	.916 $\pm$ .001
P(True)	.394 $\pm$ .003	.465 $\pm$ .002	.492 $\pm$ .002	.736 $\pm$ .004	.779 $\pm$ .003	<b>.804</b> $\pm$ .002	.930 $\pm$ .003	.964 $\pm$ .001	<b>.967</b> $\pm$ .000	.886 $\pm$ .003	.917 $\pm$ .002	.929 $\pm$ .001
<i>Prefix consistency</i>												
PC-linear	.429 $\pm$ .002	.481 $\pm$ .002	.494 $\pm$ .001	<b>.742</b> $\pm$ .004	.785 $\pm$ .003	.802 $\pm$ .002	.932 $\pm$ .003	.964 $\pm$ .001	<b>.967</b> $\pm$ .000	<b>.933</b> $\pm$ .003	<b>.961</b> $\pm$ .002	<b>.968</b> $\pm$ .001
PC-quadratic	<b>.433</b> $\pm$ .002	<b>.486</b> $\pm$ .002	<b>.504</b> $\pm$ .002	<b>.742</b> $\pm$ .004	<b>.787</b> $\pm$ .003	.803 $\pm$ .002	.932 $\pm$ .003	.963 $\pm$ .001	<b>.967</b> $\pm$ .000	.932 $\pm$ .003	.959 $\pm$ .002	<b>.968</b> $\pm$ .001
PC-cubic	<b>.433</b> $\pm$ .002	<b>.486</b> $\pm$ .002	.503 $\pm$ .001	<b>.742</b> $\pm$ .004	<b>.787</b> $\pm$ .003	<b>.804</b> $\pm$ .002	.932 $\pm$ .003	.963 $\pm$ .001	<b>.967</b> $\pm$ .000	.929 $\pm$ .003	.953 $\pm$ .002	.964 $\pm$ .001

Table 9: All baselines, Nemotron2-9B (higher accuracy is better). Bold marks the best non-oracle per column. Subscripts are  $\pm 2\sigma$  CI.

Method	FrontierScience-Olympiad			HMMT Feb 2026			AIME 2025			Brumo 2025		
	B=250k	B=1M	B=5M	B=250k	B=1M	B=5M	B=250k	B=1M	B=5M	B=250k	B=1M	B=5M
<i>Baseline</i>												
Standard MV	.187 $\pm$ .001	.203 $\pm$ .001	.203 $\pm$ .001	.461 $\pm$ .004	.475 $\pm$ .002	.482 $\pm$ .001	.708 $\pm$ .003	.731 $\pm$ .002	.734 $\pm$ .000	.737 $\pm$ .003	.736 $\pm$ .002	.734 $\pm$ .001
<i>DeepConf</i>												
DeepConf first-token	.187 $\pm$ .001	.203 $\pm$ .001	.203 $\pm$ .001	.460 $\pm$ .004	.475 $\pm$ .002	.482 $\pm$ .001	.706 $\pm$ .003	.730 $\pm$ .002	.734 $\pm$ .000	.738 $\pm$ .003	.736 $\pm$ .002	.734 $\pm$ .001
Self-certainty	.187 $\pm$ .001	.202 $\pm$ .001	.203 $\pm$ .001	.468 $\pm$ .004	.478 $\pm$ .002	.483 $\pm$ .001	.717 $\pm$ .003	.733 $\pm$ .002	.734 $\pm$ .001	.743 $\pm$ .003	.737 $\pm$ .002	.734 $\pm$ .001
DeepConf bottom-10%	.186 $\pm$ .001	.202 $\pm$ .001	.202 $\pm$ .001	.463 $\pm$ .004	.476 $\pm$ .002	.483 $\pm$ .001	.709 $\pm$ .003	.731 $\pm$ .002	.734 $\pm$ .001	.739 $\pm$ .003	.735 $\pm$ .002	.734 $\pm$ .001
DeepConf block-min	.188 $\pm$ .001	.204 $\pm$ .001	<b>.205</b> $\pm$ .001	.463 $\pm$ .004	.475 $\pm$ .002	.482 $\pm$ .001	.709 $\pm$ .003	.730 $\pm$ .002	.734 $\pm$ .001	.739 $\pm$ .003	.736 $\pm$ .002	.734 $\pm$ .001
DeepConf tail	.188 $\pm$ .001	.203 $\pm$ .001	.204 $\pm$ .001	.471 $\pm$ .004	.481 $\pm$ .002	.484 $\pm$ .000	.716 $\pm$ .003	.733 $\pm$ .002	.734 $\pm$ .001	.741 $\pm$ .003	.736 $\pm$ .002	.734 $\pm$ .001
<i>DeepConf (filtered)</i>												
DeepConf bottom-10% (top-10%)	.127 $\pm$ .002	.160 $\pm$ .001	.188 $\pm$ .001	.422 $\pm$ .004	.464 $\pm$ .003	.492 $\pm$ .003	.568 $\pm$ .005	.656 $\pm$ .004	.733 $\pm$ .003	.654 $\pm$ .004	.678 $\pm$ .003	.705 $\pm$ .003
DeepConf bottom-10% (top-90%)	.183 $\pm$ .001	.198 $\pm$ .001	.202 $\pm$ .001	.467 $\pm$ .004	.482 $\pm$ .003	.486 $\pm$ .001	.707 $\pm$ .003	.731 $\pm$ .002	.735 $\pm$ .001	.739 $\pm$ .003	.739 $\pm$ .002	.734 $\pm$ .001
DeepConf tail (top-10%)	.146 $\pm$ .002	.170 $\pm$ .001	.179 $\pm$ .001	.466 $\pm$ .004	<b>.506</b> $\pm$ .004	<b>.561</b> $\pm$ .003	.703 $\pm$ .004	<b>.757</b> $\pm$ .003	<b>.778</b> $\pm$ .002	.716 $\pm$ .004	<b>.755</b> $\pm$ .004	<b>.778</b> $\pm$ .003
DeepConf tail (top-90%)	.186 $\pm$ .001	.203 $\pm$ .001	<b>.205</b> $\pm$ .001	<b>.476</b> $\pm$ .004	.493 $\pm$ .003	.491 $\pm$ .001	.719 $\pm$ .003	.734 $\pm$ .002	.735 $\pm$ .001	.743 $\pm$ .003	.741 $\pm$ .003	.733 $\pm$ .003
<i>CISC</i>												
Response probability	.187 $\pm$ .001	.202 $\pm$ .001	.203 $\pm$ .001	.464 $\pm$ .004	.477 $\pm$ .002	.483 $\pm$ .001	.715 $\pm$ .003	.734 $\pm$ .002	.734 $\pm$ .001	.742 $\pm$ .003	.737 $\pm$ .002	.734 $\pm$ .001
Verbal binary	.189 $\pm$ .001	.204 $\pm$ .001	.203 $\pm$ .001	.461 $\pm$ .004	.475 $\pm$ .002	.482 $\pm$ .001	.707 $\pm$ .003	.732 $\pm$ .002	.733 $\pm$ .000	.743 $\pm$ .003	.740 $\pm$ .002	.735 $\pm$ .001
Verbal 0-100	.189 $\pm$ .001	.205 $\pm$ .001	<b>.205</b> $\pm$ .001	.460 $\pm$ .004	.474 $\pm$ .002	.483 $\pm$ .001	.713 $\pm$ .003	.735 $\pm$ .002	.734 $\pm$ .000	.741 $\pm$ .003	.739 $\pm$ .002	.737 $\pm$ .001
P(True)	<b>.192</b> $\pm$ .001	<b>.206</b> $\pm$ .001	<b>.205</b> $\pm$ .001	.468 $\pm$ .004	.478 $\pm$ .002	.482 $\pm$ .001	.713 $\pm$ .003	.735 $\pm$ .002	.734 $\pm$ .000	<b>.745</b> $\pm$ .003	.741 $\pm$ .002	.735 $\pm$ .001
<i>Prefix consistency</i>												
PC-linear	.191 $\pm$ .001	.203 $\pm$ .001	.203 $\pm$ .001	.463 $\pm$ .004	.478 $\pm$ .002	.483 $\pm$ .001	.705 $\pm$ .003	.729 $\pm$ .002	.733 $\pm$ .000	.735 $\pm$ .003	.737 $\pm$ .002	.734 $\pm$ .000
PC-quadratic	.188 $\pm$ .001	.201 $\pm$ .001	.202 $\pm$ .001	.466 $\pm$ .004	.484 $\pm$ .003	.486 $\pm$ .001	.705 $\pm$ .003	.730 $\pm$ .002	.734 $\pm$ .000	.738 $\pm$ .003	.741 $\pm$ .002	.734 $\pm$ .000
PC-cubic	.185 $\pm$ .001	.199 $\pm$ .001	.204 $\pm$ .001	.466 $\pm$ .004	.489 $\pm$ .003	.490 $\pm$ .001	.704 $\pm$ .003	.731 $\pm$ .002	.734 $\pm$ .001	.739 $\pm$ .003	.744 $\pm$ .002	.735 $\pm$ .001

Table 10: All baselines, Ministral3-14B (higher accuracy is better). Bold marks the best non-oracle per column. Subscripts are  $\pm 2\sigma$  CI.

Method	FrontierScience-Olympiad			HMMT Feb 2026			AIME 2025			Brumo 2025		
	B=250k	B=1M	B=5M	B=250k	B=1M	B=5M	B=250k	B=1M	B=5M	B=250k	B=1M	B=5M
<i>Baseline</i>												
Standard MV	.137 $\pm$ .001	.141 $\pm$ .001	.142 $\pm$ .001	.413 $\pm$ .004	<b>.440</b> $\pm$ .003	.458 $\pm$ .002	.508 $\pm$ .003	.535 $\pm$ .003	.569 $\pm$ .002	.669 $\pm$ .004	.691 $\pm$ .003	.699 $\pm$ .003
<i>DeepConf</i>												
DeepConf first-token	.135 $\pm$ .001	.140 $\pm$ .001	.142 $\pm$ .001	.411 $\pm$ .004	.438 $\pm$ .003	.458 $\pm$ .002	.505 $\pm$ .003	.532 $\pm$ .003	.569 $\pm$ .002	.668 $\pm$ .004	.690 $\pm$ .003	.698 $\pm$ .003
Self-certainty	.130 $\pm$ .001	.135 $\pm$ .001	.137 $\pm$ .001	.409 $\pm$ .004	.429 $\pm$ .003	.438 $\pm$ .002	.505 $\pm$ .003	.533 $\pm$ .003	.565 $\pm$ .002	.659 $\pm$ .004	.682 $\pm$ .003	.686 $\pm$ .002
DeepConf bottom-10%	.131 $\pm$ .001	.136 $\pm$ .001	.138 $\pm$ .001	.409 $\pm$ .004	.430 $\pm$ .003	.438 $\pm$ .002	.506 $\pm$ .003	.531 $\pm$ .003	.564 $\pm$ .002	.660 $\pm$ .004	.683 $\pm$ .003	.686 $\pm$ .002
DeepConf block-min	.135 $\pm$ .001	.140 $\pm$ .001	.141 $\pm$ .001	.404 $\pm$ .004	.423 $\pm$ .003	.428 $\pm$ .002	.509 $\pm$ .003	.534 $\pm$ .003	.566 $\pm$ .002	.662 $\pm$ .004	.683 $\pm$ .003	.691 $\pm$ .002
DeepConf tail	.130 $\pm$ .001	.134 $\pm$ .001	.137 $\pm$ .001	.408 $\pm$ .004	.427 $\pm$ .003	.436 $\pm$ .002	.506 $\pm$ .003	.533 $\pm$ .003	.563 $\pm$ .002	.659 $\pm$ .004	.681 $\pm$ .003	.683 $\pm$ .002
<i>DeepConf (filtered)</i>												
DeepConf bottom-10% (top-10%)	.075 $\pm$ .002	.084 $\pm$ .001	.089 $\pm$ .001	.240 $\pm$ .004	.284 $\pm$ .003	.304 $\pm$ .002	.301 $\pm$ .004	.316 $\pm$ .004	.347 $\pm$ .003	.289 $\pm$ .004	.285 $\pm$ .003	.262 $\pm$ .002
DeepConf bottom-10% (top-90%)	.124 $\pm$ .001	.126 $\pm$ .001	.125 $\pm$ .001	.401 $\pm$ .003	.420 $\pm$ .003	.428 $\pm$ .002	.505 $\pm$ .003					

Table 11: **Token efficiency, GPT-OSS-120B (smaller is better).** Cells <1 indicate more cost-efficient than Standard MV. “N/A” indicates target unreachable. Bold marks the best per column.

	FrontierScience-Olympiad			HMMT Feb 2026			AIME 2025			Brumo 2025										
	$\alpha=75\%$	$\alpha=90\%$	$\alpha=99\%$	$\alpha=75\%$	$\alpha=90\%$	$\alpha=99\%$	$\alpha=75\%$	$\alpha=90\%$	$\alpha=99\%$	$\alpha=75\%$	$\alpha=90\%$	$\alpha=99\%$								
Pass@1 / Standard MV plateau	.338 / 500	107k	2.5M	.589 / 760	858k	1.8M	.789 / 900	99k	189k	.713 / 833	934k	3.3M								
Standard MV budget ( $E_{MV}$ )	45k			364k			56k			274k										
<i>DeepConf</i>																				
DeepConf first-token	1.00±0.03 × 1.00±0.08 × 1.00±0.34	1.00±0.11 × 1.00±0.08 × 1.00±0.10	1.00±0.05 × 1.00±0.09 × 1.00±0.19	1.00±0.30 × 1.00±0.12 × 1.00±0.18	0.89±0.04 × 0.87±0.06 × N/A	0.74±0.07 × 0.85±0.07 × 0.87±0.11	0.81±0.06 × 0.81±0.07 × 0.66±0.11	0.73±0.18 × 0.76±0.10 × 0.59±0.09	0.97±0.04 × 0.97±0.08 × N/A	0.86±0.10 × 0.93±0.08 × 0.93±0.09	0.97±0.06 × 0.90±0.08 × 0.79±0.13	0.95±0.25 × 0.90±0.10 × 0.88±0.21	0.89±0.04 × 0.90±0.07 × N/A	0.93±0.11 × 0.96±0.08 × 0.92±0.09	0.98±0.06 × 0.95±0.08 × 0.86±0.14	0.95±0.23 × 0.88±0.10 × 0.96±0.21	0.91±0.05 × 0.91±0.07 × N/A	0.63±0.09 × 0.72±0.08 × 0.57±0.07	<b>0.68</b> ±0.04 × 0.70±0.06 × 0.56±0.09	0.50±0.12 × 0.47±0.06 × 0.35±0.06
DeepConf bottom-10%	>10 × N/A	N/A	N/A	N/A	N/A	N/A	N/A	N/A	N/A	N/A	N/A	N/A								
DeepConf bottom-10% (top-10%)	1.01±0.03 × 1.12±0.09 × N/A	0.81±0.09 × 0.98±0.09 × 1.19±0.18	0.98±0.06 × 0.95±0.09 × 0.80±0.15	0.84±0.22 × 0.79±0.09 × 0.64±0.11	7.10±0.31 × 8.20±0.76 × N/A	1.29±0.13 × 1.41±0.18 × N/A	3.14±0.21 × 2.87±0.27 × 2.12±0.34	N/A	N/A	N/A	N/A	N/A								
DeepConf bottom-10% (top-90%)	0.98±0.04 × 1.14±0.10 × N/A	0.45±0.04 × 0.52±0.05 × 0.42±0.04	0.69±0.04 × <b>0.69</b> ±0.06 × <b>0.53</b> ±0.08	0.45±0.11 × 0.36±0.04 × 0.21±0.04																
DeepConf tail (top-10%)																				
DeepConf tail (top-90%)																				
<i>CISC</i>																				
Response probability	0.95±0.05 × 0.96±0.08 × N/A	0.74±0.08 × 0.84±0.07 × 0.87±0.12	0.78±0.06 × 0.78±0.07 × 0.65±0.11	0.73±0.18 × 0.79±0.09 × 0.65±0.10	1.20±0.05 × 1.39±0.13 × 0.18±0.08	0.52±0.06 × <b>0.42</b> ±0.03 × <b>0.31</b> ±0.03	1.05±0.06 × 1.05±0.09 × 0.99±0.18	1.05±0.06 × 0.99±0.18 × 0.62±0.15	0.37±0.04 × 0.19±0.03	1.60±0.09 × 1.66±0.12 × 0.27±0.12	1.18±0.14 × 1.36±0.13 × 1.18±0.14	1.45±0.10 × 1.54±0.14 × 2.02±0.45	1.14±0.32 × 1.77±0.24 × N/A							
Verbal binary	1.23±0.05 × 1.20±0.10 × 0.23±0.09	1.05±0.10 × 1.17±0.14 × 0.94±0.09	1.14±0.08 × 1.13±0.09 × 1.01±0.16	1.46±0.36 × 1.07±0.11 × 0.60±0.11																
Verbal 0-100																				
P(True)																				
<i>Adaptive stopping</i>																				
AC sweep	1.93±0.09 × 1.54±0.12 × 0.29±0.15	<b>0.42</b> ±0.05 × 0.63±0.10 × N/A	1.03±0.12 × 1.06±0.26 × 2.98±0.82	<b>0.32</b> ±0.09 × <b>0.26</b> ±0.03 × 0.20±0.04	2.74±0.08 × 5.59±0.70 × 0.94±0.53	1.96±0.33 × 6.66±1.29 × N/A	0.96±0.06 × 1.38±0.57 × >10 ×	3.19±1.47 × 6.11±0.65 × N/A												
ESC sweep																				
<i>Prefix consistency</i>																				
PC-linear	0.70±0.03 × 0.63±0.05 × 3.88±2.37	0.70±0.08 × 0.79±0.08 × 0.88±0.11	0.87±0.05 × 0.73±0.06 × 0.58±0.10	0.56±0.15 × 0.51±0.07 × 0.39±0.06	0.65±0.03 × <b>0.52</b> ±0.04 × 0.06±0.02	0.52±0.05 × 0.49±0.04 × 0.41±0.04	0.86±0.05 × 0.70±0.06 × <b>0.53</b> ±0.08	0.44±0.11 × 0.37±0.04 × 0.19±0.03	0.65±0.03 × <b>0.52</b> ±0.04 × <b>0.05</b> ±0.02	0.52±0.05 × 0.46±0.04 × 0.35±0.04	0.86±0.05 × 0.71±0.06 × <b>0.53</b> ±0.08	0.44±0.11 × 0.32±0.04 × <b>0.16</b> ±0.02								
PC-quadratic																				
PC-cubic																				

Table 12: **Token efficiency, GPT-OSS-20B (smaller is better).** Cells <1 indicate more cost-efficient than Standard MV. “N/A” indicates target unreachable. Bold marks the best per column.

	FrontierScience-Olympiad			HMMT Feb 2026			AIME 2025			Brumo 2025										
	$\alpha=75\%$	$\alpha=90\%$	$\alpha=99\%$	$\alpha=75\%$	$\alpha=90\%$	$\alpha=99\%$	$\alpha=75\%$	$\alpha=90\%$	$\alpha=99\%$	$\alpha=75\%$	$\alpha=90\%$	$\alpha=99\%$								
Pass@1 / Standard MV plateau	.276 / 540	640k	5.0M	.601 / 809	517k	1.8M	5.3M	.742 / 900	312k	2.1M	.766 / 926	348k	5.3M							
Standard MV budget ( $E_{MV}$ )	215k							128k			150k									
<i>DeepConf</i>																				
DeepConf first-token	1.00±0.03 × 1.00±0.07 × 1.00±0.15	1.00±0.11 × 1.00±0.09 × 1.00±0.18	1.00±0.09 × 1.00±0.14 × 1.00±0.09	1.00±0.16 × 1.00±0.24 × 1.00±0.06	0.97±0.03 × 0.99±0.07 × N/A	0.85±0.10 × 0.93±0.08 × 0.87±0.14	0.93±0.07 × 0.78±0.11 × 0.72±0.18	0.95±0.06 × 0.87±0.10 × 0.18±0.43	1.00±0.04 × 1.07±0.07 × 1.42±0.29	0.88±0.10 × 0.96±0.08 × 0.89±0.15	0.92±0.07 × 0.91±0.12 × 0.86±0.24	1.03±0.06 × 1.07±0.15 × 0.91±1.27	0.97±0.03 × 1.00±0.07 × 1.42±0.33	0.91±0.10 × 0.95±0.08 × 0.93±0.16	0.96±0.07 × 0.94±0.15 × 0.99±0.26	1.06±0.08 × 1.08±0.17 × 0.85±1.00	0.90±0.04 × 0.89±0.06 × 1.38±0.28	0.68±0.08 × 0.71±0.06 × 0.81±0.14	0.81±0.06 × 0.76±0.10 × 0.57±0.10	0.84±0.06 × 0.76±0.10 × 0.10±0.26
DeepConf bottom-10%	>10 × N/A	N/A	N/A	N/A	N/A	N/A	N/A	N/A	N/A	N/A	N/A	N/A								
DeepConf bottom-10% (top-10%)	1.20±0.04 × 1.73±0.15 × N/A	0.84±0.09 × 1.14±0.13 × 1.17±0.20	0.93±0.07 × 0.93±0.14 × 0.90±0.27	1.10±0.09 × 1.49±0.24 × 0.83±1.50	>10 × N/A	3.24±0.33 × 3.22±0.33 × N/A	>10 × >10 × >10 ×	N/A	N/A	N/A	N/A	N/A								
DeepConf bottom-10% (top-90%)	1.11±0.04 × 1.65±0.16 × N/A	0.58±0.06 × 0.57±0.06 × 0.57±0.10	0.83±0.07 × 0.71±0.09 × 0.25±0.05	0.86±0.06 × 0.74±0.09 × 0.09±0.25																
DeepConf tail (top-10%)																				
DeepConf tail (top-90%)																				
<i>CISC</i>																				
Response probability	0.99±0.03 × 1.05±0.08 × 2.01±0.30	0.82±0.09 × 0.90±0.08 × 0.84±0.14	1.00±0.09 × 0.92±0.13 × 0.84±0.26	0.96±0.06 × 0.86±0.10 × 0.19±0.43	1.40±0.06 × 1.25±0.08 × N/A	0.69±0.07 × 0.79±0.09 × 0.74±0.12	0.86±0.07 × 0.78±0.10 × 0.24±0.05	0.79±0.05 × <b>0.54</b> ±0.06 × <b>0.05</b> ±0.14	1.37±0.06 × 1.76±0.13 × N/A	0.80±0.08 × 0.79±0.07 × 0.59±0.10	0.89±0.07 × 0.72±0.10 × 0.33±0.08	1.14±0.08 × 0.91±0.11 × 0.13±0.32								
Verbal binary	1.00±0.04 × 0.94±0.05 × 0.56±0.08	0.61±0.07 × 0.63±0.07 × 0.53±0.09	<b>0.73</b> ±0.05 × <b>0.54</b> ±0.07 × <b>0.13</b> ±0.03	0.97±0.07 × 0.79±0.09 × 0.10±0.26																
Verbal 0-100																				
P(True)																				
<i>SubthoughtReasoner</i>																				
SubthoughtReasoner	1.34±0.05 × 1.28±0.08 × 1.37±0.24	0.91±0.10 × 0.85±0.08 × 0.61±0.10	2.04±0.18 × 3.00±0.41 × N/A	— — —																
<i>Adaptive stopping</i>																				
AC sweep	1.65±0.07 × 1.19±0.09 × 0.51±0.08	<b>0.39</b> ±0.04 × <b>0.24</b> ±0.03 × <b>0.21</b> ±0.04	1.61±0.19 × 1.31±0.29 × 0.60±0.14	<b>0.45</b> ±0.04 × 0.57±0.10 × 0.15±0.38	5.04±0.41 × >10 × 3.43±0.48	1.86±0.41 × 5.47±0.60 × 3.15±0.61	1.06±0.08 × 2.38±0.58 × 1.90±0.48	0.53±0.09 × 7.49±4.48 × 2.50±0.93												
ESC sweep																				
<i>Prefix consistency</i>																				
PC-linear	0.71±0.02 × 0.74±0.05 × N/A	0.56±0.05 × 0.37±0.03 × 0.42±0.07	0.81±0.06 × 0.74±0.10 × 0.34±0.08	0.98±0.07 × 0.91±0.11 × 0.13±0.32	0.64±0.03 × <b>0.53</b> ±0.03 × 0.89±0.38	0.55±0.05 × 0.36±0.03 × 0.28±0.05	0.81±0.06 × 0.72±0.10 × 0.26±0.06	0.96±0.06 × 0.89±0.10 × 0.12±0.29	0.65±0.03 × 0.54±0.03 × <b>0.21</b> ±0.03	0.55±0.06 × 0.38±0.03 × 0.36±0.06	0.81±0.06 × 0.72±0.10 × 0.22±0.05	0.98±0.06 × 0.92±0.12 × 0.12±0.31								
PC-quadratic																				
PC-cubic																				

Table 13: **Token efficiency, Nemotron3-30B (smaller is better).** Cells <1 indicate more cost-efficient than Standard MV. “N/A” indicates target unreachable. Bold marks the best per column.

	FrontierScience-Olympiad			HMMT Feb 2026			AIME 2025			Brumo 2025										
	$\alpha=75\%$	$\alpha=90\%$	$\alpha=99\%$	$\alpha=75\%$	$\alpha=90\%$	$\alpha=99\%$	$\alpha=75\%$	$\alpha=90\%$	$\alpha=99\%$	$\alpha=75\%$	$\alpha=90\%$	$\alpha=99\%$								
Pass@1 / Standard MV plateau	.295 / 493	1.3M	6.0M	.708 / 810	4.2M	8.5M	.902 / 967	589k	1.2M	.816 / 932	651k	2.5M								
Standard MV budget ( $E_{MV}$ )	486k			1.6M			396k			342k										
<i>DeepConf</i>																				
DeepConf first-token	1.03±0.06 × 1.00±0.10 × 0.92±0.22	1.02±0.20 × 1.00±0.14 × 0.96±0.12	1.03±0.06 × 1.06±0.08 × 0.94±0.15	1.03±0.13 × 1.00±0.16 × 0.71±0.39	1.04±0.06 × 1.01±0.11 × 0.85±0.19	0.85±0.15 × 0.89±0.14 × 0.93±0.12	0.97±0.06 × 0.96±0.06 × 0.84±0.12	0.45±0.05 × 0.41±0.05 × 0.14±0.07	1.07±0.05 × 1.11±0.11 × 1.36±0.34	0.93±0.18 × 1.00±0.15 × 0.97±0.13	1.01±0.06 × 1.00±0.06 × 0.90±0.15	0.50±0.06 × 0.41±0.05 × 0.15±0.08	1.05±0.05 × 1.01±0.11 × 0.85±0.20	0.91±0.18 × 0.98±0.15 × 1.00±0.13	0.97±0.05 × 1.00±0.07 × 0.90±0.15	0.40±0.05 × 0.40±0.05 × 0.15±0.08	0.97±0.06 × 0.88±0.08 × 0.56±0.14	0.82±0.15 × 0.97±0.19 × N/A	0.95±0.06 × 0.95±0.06 × 0.89±0.13	0.40±0.05 × 0.39±0.07 × 0.14±0.07
DeepConf bottom-10%	>10 × N/A	N/A	N/A	N/A	N/A	N/A	N/A	N/A	N/A	N/A	N/A	N/A								
DeepConf bottom-10% (top-10%)	1.29±0.08 × 2.07±0.24 × N/A	1.00±0.21 × 1.28±0.23 × N/A	1.02±0.06 × 1.03±0.07 × 1.05±0.17	0.50±0.06 × 0.42±0.06 × 0.16±0.08	N/A	N/A	N/A	N/A	N/A	N/A	N/A	N/A								
DeepConf bottom-10% (top-90%)	0.99±0.06 × 0.83±0.08 × 0.36±0.09	0.74±0.14 × 0.97±0.20 × N/A	0.95±0.06 × 0.94±0.06 × 0.84±0.13	0.40±0.04 × 0.40±0.07 × 0.14±0.07																
DeepConf tail (top-10%)																				
DeepConf tail (top-90%)																				
<i>CISC</i>																				
Response probability	1.04±0.06 × 1.01±0.11 × 0.86±0.21	0.83±0.15 × 0.90±0.15 × 0.94±0.12	0.97±0.05 × 0.96±0.06 × 0.84±0.13	0.45±0.06 × 0.41±0.05 × 0.15±0.08	1.36±0.08 × 1.46±0.14 × 1.54±0.40	1.00±0.19 × 1.20±0.18 × N/A	1.42±0.10 × 1.48±0.10 × 1.66±0.28	1.88±0.21 × 2.66±0.37 × N/A	1.34±0.08 × 1.18±0.11 × 0.59±0.15	0.89±0.16 × 0.89±0.13 × 0.86±0.11	1.15±0.07 × 1.25±0.11 × 1.15±0.18	1.86±0.24 × N/A	N/A							
Verbal binary	1.14±0.06 × 1.10±0.11 × 0.75±0.18	0.86±0.15 × 0.90±0.12 × 0.82±0.10	1.12±0.07 × 1.15±0.07 × 1.20±0.20	1.40±0.14 × 2.05±0.31 × 3.39±1.62																
Verbal 0-100																				
P(True)																				
<i>Adaptive stopping</i>																				
AC sweep	1.24±0.07 × 0.87±0.09 × 0.49±0.13	<b>0.51</b> ±0.09 × <b>0.34</b> ±0.05 × <b>0.24</b> ±0.03	<b>0.21</b> ±0.01 × <b>0.18</b> ±0.01 × <b>0.21</b> ±0.05	<b>0.27</b> ±0.03 × <b>0.18</b> ±0.03 × 0.12±0.07	2.06±0.26 × 3.62±0.41 × 2.23±0.58	4.33±1.24 × 3.12±0.46 × 1.88														

Table 14: **Token efficiency, Nemotron2-9B (smaller is better).** Cells <1 indicate more cost-efficient than Standard MV. “N/A” indicates target unreachable. Bold marks the best per column.

	FrontierScience-Olympiad			HMMT Feb 2026			AIME 2025			Brumo 2025		
	$\alpha=75\%$	$\alpha=90\%$	$\alpha=99\%$	$\alpha=75\%$	$\alpha=90\%$	$\alpha=99\%$	$\alpha=75\%$	$\alpha=90\%$	$\alpha=99\%$	$\alpha=75\%$	$\alpha=90\%$	$\alpha=99\%$
Pass@1 / Standard MV plateau	.120 / .203			.401 / .484			.569 / .733			.660 / .733		
Standard MV budget ( $B_{MV}$ )	181k	383k	841k	274k	1.5M	6.1M	163k	374k	1.1M	77k	109k	126k
<i>DeepConf</i>												
DeepConf first-token	0.99 $\pm$ 0.10 $\times$	1.01 $\pm$ 0.08 $\times$	1.02 $\pm$ 0.17 $\times$	1.01 $\pm$ 0.20 $\times$	1.18 $\pm$ 0.74 $\times$	1.03 $\pm$ 0.25 $\times$	1.01 $\pm$ 0.08 $\times$	1.11 $\pm$ 0.13 $\times$	1.20 $\pm$ 0.31 $\times$	0.99 $\pm$ 0.08 $\times$	1.00 $\pm$ 0.13 $\times$	1.00 $\pm$ 0.09 $\times$
Self-certainty	1.03 $\pm$ 0.10 $\times$	1.04 $\pm$ 0.09 $\times$	1.02 $\pm$ 0.17 $\times$	0.61 $\pm$ 0.10 $\times$	0.38 $\pm$ 0.24 $\times$	0.60 $\pm$ 0.16 $\times$	0.77 $\pm$ 0.06 $\times$	0.69 $\pm$ 0.07 $\times$	0.58 $\pm$ 0.13 $\times$	0.94 $\pm$ 0.10 $\times$	0.85 $\pm$ 0.09 $\times$	<b>0.90</b> $\pm$ 0.08 $\times$
DeepConf bottom-10%	1.07 $\pm$ 0.11 $\times$	1.12 $\pm$ 0.10 $\times$	1.14 $\pm$ 0.18 $\times$	0.82 $\pm$ 0.14 $\times$	0.66 $\pm$ 0.37 $\times$	0.91 $\pm$ 0.22 $\times$	0.95 $\pm$ 0.07 $\times$	0.90 $\pm$ 0.10 $\times$	1.00 $\pm$ 0.26 $\times$	1.02 $\pm$ 0.08 $\times$	0.95 $\pm$ 0.11 $\times$	1.04 $\pm$ 0.11 $\times$
DeepConf block-min	0.95 $\pm$ 0.09 $\times$	1.01 $\pm$ 0.11 $\times$	0.94 $\pm$ 0.15 $\times$	0.86 $\pm$ 0.17 $\times$	0.87 $\pm$ 0.43 $\times$	1.31 $\pm$ 0.33 $\times$	0.95 $\pm$ 0.07 $\times$	1.00 $\pm$ 0.13 $\times$	1.33 $\pm$ 0.32 $\times$	1.05 $\pm$ 0.08 $\times$	0.98 $\pm$ 0.12 $\times$	1.05 $\pm$ 0.10 $\times$
DeepConf tail	0.96 $\pm$ 0.09 $\times$	1.00 $\pm$ 0.09 $\times$	1.00 $\pm$ 0.17 $\times$	0.60 $\pm$ 0.10 $\times$	0.28 $\pm$ 0.18 $\times$	0.41 $\pm$ 0.18 $\times$	0.72 $\pm$ 0.06 $\times$	0.70 $\pm$ 0.09 $\times$	0.65 $\pm$ 0.14 $\times$	0.99 $\pm$ 0.10 $\times$	0.86 $\pm$ 0.09 $\times$	0.92 $\pm$ 0.08 $\times$
<i>DeepConf (filtered)</i>												
DeepConf bottom-10% (top-10%)	>10 $\times$	>10 $\times$	N/A	3.60 $\pm$ 0.58 $\times$	0.99 $\pm$ 0.71 $\times$	0.33 $\pm$ 0.09 $\times$	>10 $\times$	8.32 $\pm$ 0.81 $\times$	4.28 $\pm$ 0.88 $\times$	N/A	N/A	N/A
DeepConf bottom-10% (top-90%)	1.35 $\pm$ 0.15 $\times$	1.53 $\pm$ 0.14 $\times$	2.37 $\pm$ 0.78 $\times$	0.76 $\pm$ 0.15 $\times$	0.30 $\pm$ 0.21 $\times$	0.20 $\pm$ 0.06 $\times$	0.96 $\pm$ 0.07 $\times$	0.91 $\pm$ 0.10 $\times$	0.97 $\pm$ 0.26 $\times$	1.02 $\pm$ 0.09 $\times$	0.95 $\pm$ 0.11 $\times$	1.09 $\pm$ 0.13 $\times$
DeepConf tail (top-10%)	N/A	N/A	N/A	0.61 $\pm$ 0.11 $\times$	0.29 $\pm$ 0.21 $\times$	0.08 $\pm$ 0.02 $\times$	1.23 $\pm$ 0.11 $\times$	0.87 $\pm$ 0.08 $\times$	<b>0.41</b> $\pm$ 0.08 $\times$	0.41 $\pm$ 0.08 $\times$	3.12 $\pm$ 0.31 $\times$	3.60 $\pm$ 0.45 $\times$
DeepConf tail (top-90%)	1.05 $\pm$ 0.10 $\times$	1.11 $\pm$ 0.11 $\times$	1.00 $\pm$ 0.15 $\times$	<b>0.58</b> $\pm$ 0.09 $\times$	<b>0.16</b> $\pm$ 0.11 $\times$	<b>0.07</b> $\pm$ 0.02 $\times$	<b>0.69</b> $\pm$ 0.06 $\times$	<b>0.65</b> $\pm$ 0.07 $\times$	<b>0.57</b> $\pm$ 0.13 $\times$	0.99 $\pm$ 0.10 $\times$	0.86 $\pm$ 0.09 $\times$	0.94 $\pm$ 0.09 $\times$
<i>CISC</i>												
Response probability	1.04 $\pm$ 0.10 $\times$	1.07 $\pm$ 0.10 $\times$	1.03 $\pm$ 0.17 $\times$	0.78 $\pm$ 0.17 $\times$	0.48 $\pm$ 0.30 $\times$	0.74 $\pm$ 0.18 $\times$	0.84 $\pm$ 0.06 $\times$	0.71 $\pm$ 0.08 $\times$	0.65 $\pm$ 0.14 $\times$	0.95 $\pm$ 0.09 $\times$	0.86 $\pm$ 0.09 $\times$	0.93 $\pm$ 0.09 $\times$
Verbal binary	0.90 $\pm$ 0.08 $\times$	1.01 $\pm$ 0.09 $\times$	0.87 $\pm$ 0.14 $\times$	1.07 $\pm$ 0.19 $\times$	0.56 $\pm$ 0.36 $\times$	1.00 $\pm$ 0.23 $\times$	1.04 $\pm$ 0.09 $\times$	1.00 $\pm$ 0.12 $\times$	0.90 $\pm$ 0.20 $\times$	0.98 $\pm$ 0.08 $\times$	1.01 $\pm$ 0.11 $\times$	1.14 $\pm$ 0.13 $\times$
Verbal 0-100	0.89 $\pm$ 0.09 $\times$	0.93 $\pm$ 0.08 $\times$	0.83 $\pm$ 0.13 $\times$	1.05 $\pm$ 0.27 $\times$	0.77 $\pm$ 0.49 $\times$	0.94 $\pm$ 0.23 $\times$	0.87 $\pm$ 0.07 $\times$	0.81 $\pm$ 0.09 $\times$	0.67 $\pm$ 0.18 $\times$	0.85 $\pm$ 0.08 $\times$	0.89 $\pm$ 0.11 $\times$	0.99 $\pm$ 0.11 $\times$
P(True)	<b>0.71</b> $\pm$ 0.07 $\times$	<b>0.83</b> $\pm$ 0.09 $\times$	<b>0.65</b> $\pm$ 0.10 $\times$	0.75 $\pm$ 0.15 $\times$	0.41 $\pm$ 0.28 $\times$	0.92 $\pm$ 0.21 $\times$	0.73 $\pm$ 0.06 $\times$	0.79 $\pm$ 0.09 $\times$	0.66 $\pm$ 0.14 $\times$	<b>0.82</b> $\pm$ 0.07 $\times$	0.82 $\pm$ 0.10 $\times$	<b>0.90</b> $\pm$ 0.09 $\times$
<i>Adaptive stopping</i>												
AC sweep	1.89 $\pm$ 0.19 $\times$	1.80 $\pm$ 0.19 $\times$	2.12 $\pm$ 0.49 $\times$	0.84 $\pm$ 0.19 $\times$	0.37 $\pm$ 0.30 $\times$	0.22 $\pm$ 0.08 $\times$	1.04 $\pm$ 0.10 $\times$	1.06 $\pm$ 0.17 $\times$	1.08 $\pm$ 0.25 $\times$	0.84 $\pm$ 0.10 $\times$	0.89 $\pm$ 0.14 $\times$	8.36 $\pm$ 5.34 $\times$
ESC sweep	2.86 $\pm$ 0.58 $\times$	6.58 $\pm$ 1.01 $\times$	7.64 $\pm$ 1.37 $\times$	1.54 $\pm$ 0.55 $\times$	1.27 $\pm$ 1.51 $\times$	1.17 $\pm$ 0.40 $\times$	1.00 $\pm$ 0.06 $\times$	4.32 $\pm$ 1.88 $\times$	6.59 $\pm$ 1.32 $\times$	0.94 $\pm$ 0.06 $\times$	<b>0.67</b> $\pm$ 0.13 $\times$	1.31 $\pm$ 0.46 $\times$
<i>Prefix consistency</i>												
PC-linear	0.84 $\pm$ 0.08 $\times$	0.86 $\pm$ 0.08 $\times$	0.83 $\pm$ 0.12 $\times$	0.90 $\pm$ 0.17 $\times$	0.41 $\pm$ 0.27 $\times$	0.94 $\pm$ 0.36 $\times$	1.08 $\pm$ 0.10 $\times$	1.03 $\pm$ 0.12 $\times$	1.23 $\pm$ 0.26 $\times$	1.19 $\pm$ 0.13 $\times$	1.37 $\pm$ 0.18 $\times$	1.47 $\pm$ 0.16 $\times$
PC-quadratic	0.96 $\pm$ 0.09 $\times$	1.10 $\pm$ 0.11 $\times$	1.30 $\pm$ 0.30 $\times$	0.80 $\pm$ 0.16 $\times$	0.30 $\pm$ 0.20 $\times$	0.10 $\pm$ 0.03 $\times$	1.10 $\pm$ 0.10 $\times$	1.07 $\pm$ 0.12 $\times$	1.04 $\pm$ 0.23 $\times$	1.17 $\pm$ 0.12 $\times$	1.16 $\pm$ 0.13 $\times$	1.35 $\pm$ 0.13 $\times$
PC-cubic	1.11 $\pm$ 0.11 $\times$	1.46 $\pm$ 0.17 $\times$	1.80 $\pm$ 0.31 $\times$	0.78 $\pm$ 0.14 $\times$	0.28 $\pm$ 0.19 $\times$	0.09 $\pm$ 0.02 $\times$	1.12 $\pm$ 0.09 $\times$	1.08 $\pm$ 0.12 $\times$	1.00 $\pm$ 0.20 $\times$	1.17 $\pm$ 0.12 $\times$	1.16 $\pm$ 0.14 $\times$	1.34 $\pm$ 0.13 $\times$

Table 15: **Token efficiency, Ministral3-14B (smaller is better).** Cells <1 indicate more cost-efficient than Standard MV. “N/A” indicates target unreachable. Bold marks the best per column.

	FrontierScience-Olympiad			HMMT Feb 2026			AIME 2025			Brumo 2025		
	$\alpha=75\%$	$\alpha=90\%$	$\alpha=99\%$	$\alpha=75\%$	$\alpha=90\%$	$\alpha=99\%$	$\alpha=75\%$	$\alpha=90\%$	$\alpha=99\%$	$\alpha=75\%$	$\alpha=90\%$	$\alpha=99\%$
Pass@1 / Standard MV plateau	.091 / .142			.270 / .463			.345 / .576			.421 / .698		
Standard MV budget ( $B_{MV}$ )	118k	249k	924k	258k	1.2M	7.4M	371k	2.0M	6.9M	92k	265k	1.8M
<i>DeepConf</i>												
DeepConf first-token	1.10 $\pm$ 0.10 $\times$	1.24 $\pm$ 0.37 $\times$	1.27 $\pm$ 1.04 $\times$	1.09 $\pm$ 0.13 $\times$	1.24 $\pm$ 0.28 $\times$	1.00 $\pm$ 0.30 $\times$	1.24 $\pm$ 0.15 $\times$	1.04 $\pm$ 0.11 $\times$	1.02 $\pm$ 0.20 $\times$	1.04 $\pm$ 0.08 $\times$	1.01 $\pm$ 0.16 $\times$	0.96 $\pm$ 0.48 $\times$
Self-certainty	1.62 $\pm$ 0.20 $\times$	>10 $\times$	N/A	1.29 $\pm$ 0.17 $\times$	N/A	N/A	1.21 $\pm$ 0.15 $\times$	1.20 $\pm$ 0.12 $\times$	N/A	1.35 $\pm$ 0.11 $\times$	1.47 $\pm$ 0.22 $\times$	N/A
DeepConf bottom-10%	1.49 $\pm$ 0.17 $\times$	2.25 $\pm$ 1.08 $\times$	N/A	1.23 $\pm$ 0.16 $\times$	N/A	N/A	1.20 $\pm$ 0.15 $\times$	1.24 $\pm$ 0.16 $\times$	N/A	1.29 $\pm$ 0.12 $\times$	1.42 $\pm$ 0.22 $\times$	N/A
DeepConf block-min	1.09 $\pm$ 0.11 $\times$	1.39 $\pm$ 0.39 $\times$	5.93 $\pm$ 2.20 $\times$	1.81 $\pm$ 0.31 $\times$	N/A	N/A	0.98 $\pm$ 0.12 $\times$	1.15 $\pm$ 0.13 $\times$	N/A	1.16 $\pm$ 0.09 $\times$	1.42 $\pm$ 0.24 $\times$	N/A
DeepConf tail	1.54 $\pm$ 0.18 $\times$	>10 $\times$	N/A	1.29 $\pm$ 0.17 $\times$	N/A	N/A	1.22 $\pm$ 0.15 $\times$	1.20 $\pm$ 0.12 $\times$	1.43 $\pm$ 0.26 $\times$	1.35 $\pm$ 0.11 $\times$	1.56 $\pm$ 0.23 $\times$	N/A
<i>DeepConf (filtered)</i>												
DeepConf bottom-10% (top-10%)	N/A	N/A	N/A	N/A	N/A	N/A	N/A	N/A	N/A	N/A	N/A	N/A
DeepConf bottom-10% (top-90%)	N/A	N/A	N/A	2.43 $\pm$ 0.56 $\times$	N/A	N/A	1.05 $\pm$ 0.12 $\times$	0.94 $\pm$ 0.10 $\times$	N/A	1.68 $\pm$ 0.13 $\times$	2.31 $\pm$ 0.37 $\times$	2.43 $\pm$ 1.15 $\times$
DeepConf tail (top-10%)	N/A	N/A	N/A	N/A	N/A	N/A	N/A	N/A	N/A	N/A	N/A	N/A
DeepConf tail (top-90%)	N/A	N/A	N/A	8.42 $\pm$ 2.58 $\times$	N/A	N/A	1.28 $\pm$ 0.19 $\times$	1.63 $\pm$ 0.25 $\times$	N/A	1.93 $\pm$ 0.19 $\times$	>10 $\times$	N/A
<i>CISC</i>												
Response probability	1.48 $\pm$ 0.15 $\times$	2.06 $\pm$ 0.58 $\times$	N/A	1.21 $\pm$ 0.15 $\times$	1.42 $\pm$ 0.32 $\times$	N/A	0.97 $\pm$ 0.11 $\times$	0.93 $\pm$ 0.10 $\times$	0.86 $\pm$ 0.15 $\times$	1.24 $\pm$ 0.10 $\times$	1.26 $\pm$ 0.20 $\times$	2.45 $\pm$ 1.64 $\times$
Verbal binary	N/A	N/A	N/A	>10 $\times$	N/A	N/A	5.25 $\pm$ 0.77 $\times$	N/A	N/A	>10 $\times$	N/A	N/A
Verbal 0-100	0.91 $\pm$ 0.10 $\times$	0.97 $\pm$ 0.27 $\times$	N/A	1.39 $\pm$ 0.19 $\times$	N/A	N/A	0.90 $\pm$ 0.13 $\times$	0.96 $\pm$ 0.11 $\times$	1.29 $\pm$ 0.22 $\times$	1.49 $\pm$ 0.12 $\times$	1.61 $\pm$ 0.24 $\times$	N/A
P(True)	1.10 $\pm$ 0.12 $\times$	1.01 $\pm$ 0.27 $\times$	0.48 $\pm$ 0.30 $\times$	1.33 $\pm$ 0.14 $\times$	N/A	N/A	1.93 $\pm$ 0.22 $\times$	N/A	N/A	2.33 $\pm$ 0.22 $\times$	N/A	N/A
<i>Adaptive stopping</i>												
AC sweep	2.48 $\pm$ 0.40 $\times$	4.28 $\pm$ 1.45 $\times$	N/A	1.52 $\pm$ 0.28 $\times$	1.21 $\pm$ 0.28 $\times$	<b>0.60</b> $\pm$ 0.20 $\times$	0.91 $\pm$ 0.11 $\times$	0.54 $\pm$ 0.06 $\times$	0.49 $\pm$ 0.10 $\times$	1.42 $\pm$ 0.14 $\times$	1.85 $\pm$ 0.32 $\times$	1.20 $\pm$ 0.75 $\times$
ESC sweep	4.53 $\pm$ 1.55 $\times$	>10 $\times$	>10 $\times$	8.79 $\pm$ 1.33 $\times$	4.75 $\pm$ 1.03 $\times$	2.05 $\pm$ 0.75 $\times$	4.44 $\pm$ 0.83 $\times$	2.41 $\pm$ 0.22 $\times$	1.38 $\pm$ 0.26 $\times$	2.39 $\pm$ 0.38 $\times$	7.42 $\pm$ 2.14 $\times$	7.95 $\pm$ 4.31 $\times$
<i>Prefix consistency</i>												
PC-linear	<b>0.38</b> $\pm$ 0.04 $\times$	0.26 $\pm$ 0.07 $\times$	0.10 $\pm$ 0.07 $\times$	<b>0.85</b> $\pm$ 0.11 $\times$	1.11 $\pm$ 0.28 $\times$	N/A	<b>0.25</b> $\pm$ 0.03 $\times$	0.11 $\pm$ 0.01 $\times$	0.07 $\pm$ 0.01 $\times$	0.93 $\pm$ 0.07 $\times$	0.80 $\pm$ 0.12 $\times$	0.32 $\pm$ 0.19 $\times$
PC-quadratic	<b>0.38</b> $\pm$ 0.04 $\times$	<b>0.24</b> $\pm$ 0.06 $\times$	<b>0.08</b> $\pm$ 0.05 $\times$	0.91 $\pm$ 0.11 $\times$	1.01 $\pm$ 0.26 $\times$	N/A	0.26 $\pm$ 0.03 $\times$	<b>0.09</b> $\pm$ 0.01 $\times$	<b>0.05</b> $\pm$ 0.01 $\times$	<b>0.86</b> $\pm$ 0.06 $\times$	<b>0.61</b> $\pm$ 0.09 $\times$	0.20 $\pm$ 0.12 $\times$
PC-cubic	<b></b>											

Oracle (Prefix Consistency) weakly above Oracle (Standard MV) at high  $B$  in a subset of cells. None of these effects involves the reweighting, so they cannot account for the PC-cubic vs. Standard MV gap in the same panels. PC-WMV’s advantage therefore comes from the weighting itself, with the prefix-consistency score  $c_i(a)$  acting as a per-candidate reliability signal (Section 3.1).

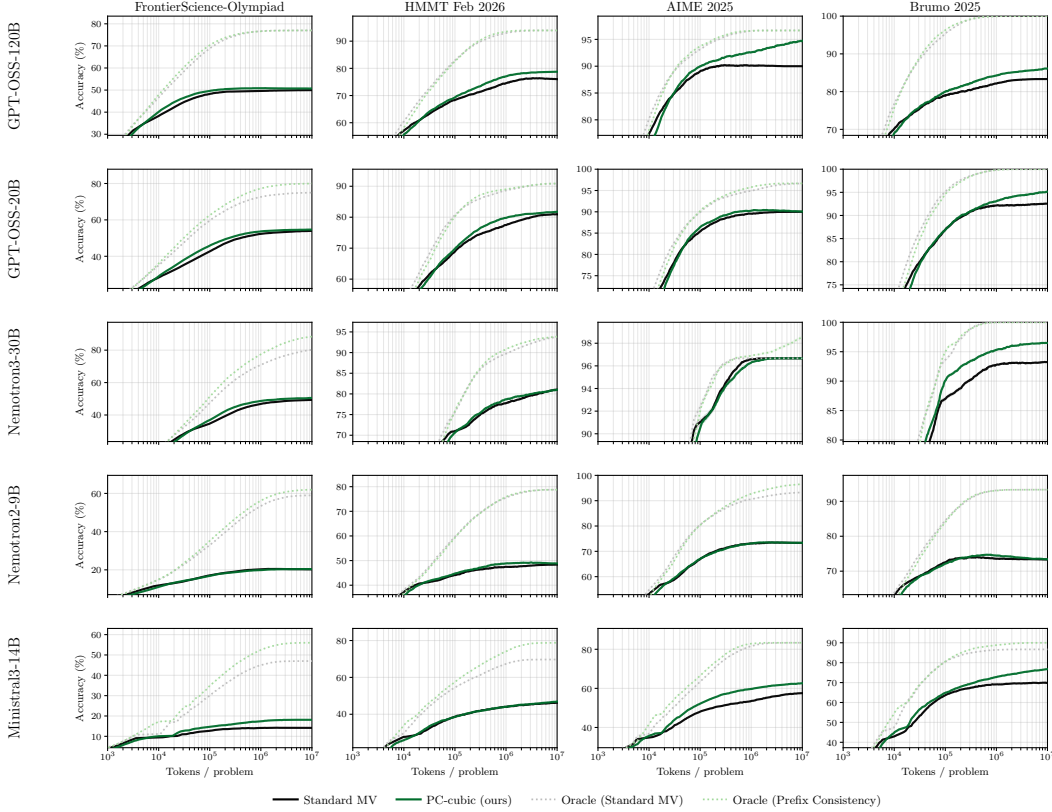


Figure 7: **Oracle decomposition: pool coverage vs. reweighting.** Same 5x4 layout as Figure 6, restricted to Standard MV, PC-cubic, and the two oracle upper bounds. Y-axes include the oracle range so the high-budget tails stay in view. The two oracles nearly coincide in every cell, indicating that PC-WMV’s advantage over the non-PC baselines does not come from regeneration adding new correct candidates to the pool. Shaded bands are  $\pm 2\sigma$  confidence intervals on accuracy.

**Per-problem marginal correctness.** Figure 8 gives a complementary per-problem view. Each point is the empirical estimate of the per-problem marginals  $\pi(a^*) = \Pr[a_i = a^*]$  over the initial answers and  $\pi^{\rightarrow}(a^*) = \Pr[\tilde{a}_i = a^*]$  over the regenerations (notation as defined in Appendix C.1, Eq. (14)). The plotted estimates  $\hat{\pi}(a^*)$  and  $\widehat{\pi^{\rightarrow}}(a^*)$  cluster tightly on the  $y = x$  diagonal in every cell, and their cell-level means agree within a few percentage points on most cells. The largest cell-mean difference is for Nemotron3-30B on AIME 2025, where the cell mean of  $\hat{\pi}(a^*)$  is 0.90 and that of  $\widehat{\pi^{\rightarrow}}(a^*)$  is 0.77, and across the 20 cells the differences run in both directions (e.g., Ministral3-14B has the cell mean of  $\widehat{\pi^{\rightarrow}}(a^*)$  above that of  $\hat{\pi}(a^*)$  on AIME 2025 and Brumo 2025). A paired Wilcoxon signed-rank test on the per-problem differences  $\hat{\pi}_q(a^*) - \widehat{\pi^{\rightarrow}}_q(a^*)$  rejects equality at the Bonferroni-corrected significance level  $\alpha_{\text{sig}} = 0.05/20$  on 5 of the 20 cells, with absolute cell-mean differences of at most 0.126 (the Nemotron3-30B AIME 2025 outlier, with the other four cells within 0.061). Among these 5 detected cells, 4 have the cell mean of  $\hat{\pi}(a^*)$  above the cell mean of  $\widehat{\pi^{\rightarrow}}(a^*)$ , that is, regenerated answers are statistically less correct on average than initial answers (the only exception is Ministral3-14B FrontierScience-Olympiad). Across all 20 cells the cell-mean difference is positive on 13 cells and negative on 7, indistinguishable from a 50/50 split (two-sided binomial sign test,  $p = 0.26$ ). The marginal correctness rate is therefore comparable for initial and regenerated answers, and the cell-mean differences do not systematically favor the regenerations. This is a stronger statement than mere equality of rates: PC-WMV’s advantage cannot come from

regeneration raising the per-answer correctness rate, because in the cells where the rate differs the regenerations have the lower marginal correctness.

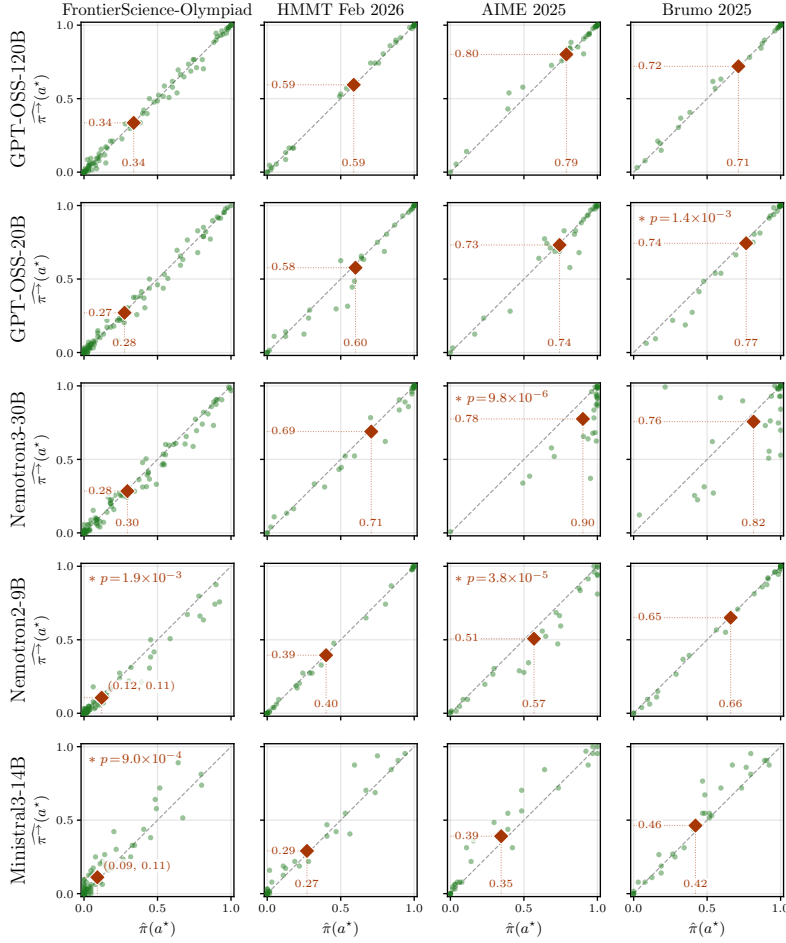


Figure 8: **Per-problem**  $\hat{\pi}(a^*)$  vs.  $\widehat{\pi}^{\rightarrow}(a^*)$ . Each point is one problem and the dashed line marks  $y = x$ . Red diamonds with dotted projection lines show each cell’s mean and its coordinates. \* flags cells where a paired Wilcoxon test rejects equality (Bonferroni-corrected significance level  $\alpha_{\text{sig}} = 0.05/20$ , not to be confused with the target-accuracy ratio  $\alpha$  of Section 4.3, with the panel-level  $p$ -value shown).

### D.5 Sensitivity to $\tau$ and $K$

Section 3.1 fixes  $K = 1$  to keep notation succinct. Here we extend it to the general- $K$  multiset of Eq. (4) and the corresponding score  $c_i^{(\tau, K)}(a) = |\{a' \in A_i^{(\tau, K)} : a' = a\}| / (K + 1)$ , sweeping  $K \in \{1, 2, 3\}$  and  $\tau \in \{0.25, 0.50, 0.75\}$ .

Table 16 sweeps the truncation fraction  $\tau \in \{0.25, 0.50, 0.75\}$  at  $K=1$  for GPT-OSS-20B. Both  $r_C$  and  $r_W$  decrease with deeper truncation, with  $r_W$  generally decreasing faster (e.g., on AIME 2025,  $r_C$  goes 87.8%  $\rightarrow$  73.0% and  $r_W$  goes 42.6%  $\rightarrow$  17.1% as  $\tau$  moves 0.75  $\rightarrow$  0.25). The discrimination gap  $D(\tau)$  varies by benchmark: it widens monotonically on AIME 2025 (45.2  $\rightarrow$  50.0  $\rightarrow$  55.9), peaks at  $\tau=0.50$  on HMMT and Brumo 2025, and narrows on FrontierScience-Olympiad (41.4  $\rightarrow$  39.5  $\rightarrow$  39.1). Deeper truncation also costs more per group, since regeneration covers a longer suffix. Cost-equivalent accuracy across  $(\tau, K)$  is reported in Table 17.

Table 17: **Sensitivity of PC-WMV accuracy to  $(\tau, K)$  on GPT-OSS-20B (higher is better).** Accuracy of PC-linear, PC-quadratic, PC-cubic at budgets 250k / 1M / 5M for every  $(\tau, K)$  in the sweep. Standard MV at the top for reference. Bold marks the best  $(\tau, K, \text{weight})$  per benchmark at each budget.

		GPT-OSS-20B												
$\tau$	$K$	Method	FrontierScience-Olympiad			HMMT Feb 2026			AIME 2025			Brumo 2025		
			$B=250k$	$B=1M$	$B=5M$	$B=250k$	$B=1M$	$B=5M$	$B=250k$	$B=1M$	$B=5M$	$B=250k$	$B=1M$	$B=5M$
		Standard MV	.482±.002	.523±.001	.537±.001	.736±.003	.775±.002	.807±.001	.881±.002	.896±.001	.900±.000	.901±.003	.922±.002	.924±.001
0.75	1	PC-linear	.495±.002	.524±.001	.535±.001	.751±.003	.797±.002	.812±.001	.887±.002	.899±.001	.900±.000	.903±.003	.928±.002	.934±.001
		PC-quadratic	.502±.002	.532±.001	.537±.001	.752±.003	<b>.800</b> ±.002	.814±.001	<b>.888</b> ±.002	.901±.002	.901±.001	.904±.003	.930±.002	.940±.001
		PC-cubic	.502±.002	.537±.001	.545±.001	<b>.753</b> ±.004	.797±.002	.814±.001	.888±.002	<b>.902</b> ±.002	.902±.001	.903±.003	.931±.002	<b>.947</b> ±.002
	2	PC-linear	.495±.002	.525±.001	.531±.001	.745±.004	.795±.002	.809±.001	.883±.002	.896±.002	.900±.001	.901±.003	.927±.002	.934±.001
		PC-quadratic	.500±.002	.532±.001	.537±.001	.745±.004	.799±.002	.815±.001	.883±.003	.899±.002	.901±.001	.900±.003	.929±.002	.942±.001
		PC-cubic	.498±.002	.530±.001	.540±.001	.745±.004	.798±.003	.817±.001	.882±.003	.901±.002	.905±.001	.900±.003	.929±.002	.946±.002
	3	PC-linear	.500±.002	.528±.001	.534±.001	.740±.004	.793±.002	.811±.001	.881±.002	.896±.002	.900±.001	.899±.003	.926±.002	.936±.001
		PC-quadratic	<b>.504</b> ±.002	.534±.001	.541±.001	.742±.004	.800±.002	.817±.001	.881±.003	.899±.002	.903±.001	.898±.003	.929±.002	.943±.001
		PC-cubic	.501±.002	.534±.001	.544±.001	.742±.004	.799±.003	<b>.822</b> ±.001	.880±.003	.900±.002	<b>.905</b> ±.002	.898±.003	.928±.002	.946±.002
0.50	1	PC-linear	.489±.002	.524±.001	.540±.001	.728±.003	.773±.003	.805±.002	.886±.002	.900±.001	.900±.000	<b>.906</b> ±.003	.931±.002	.935±.001
		PC-quadratic	.494±.002	.531±.001	.541±.001	.729±.003	.779±.003	.809±.001	.885±.002	.899±.001	.900±.000	.906±.003	<b>.932</b> ±.002	.938±.001
		PC-cubic	.493±.002	.532±.001	.541±.001	.729±.004	.780±.003	.810±.001	.885±.002	.898±.002	.900±.001	.904±.003	.931±.002	.939±.001
	2	PC-linear	.492±.002	.527±.001	.535±.001	.727±.003	.776±.003	.805±.002	.883±.002	.900±.001	.900±.000	.891±.003	.924±.002	.931±.001
		PC-quadratic	.496±.002	.533±.001	.542±.001	.727±.004	.780±.003	.809±.001	.880±.003	.900±.002	.900±.000	.888±.003	.924±.002	.933±.001
		PC-cubic	.495±.002	.532±.001	.545±.001	.726±.004	.779±.003	.807±.001	.880±.003	.898±.002	.901±.001	.885±.003	.922±.002	.935±.001
	3	PC-linear	.493±.002	.530±.001	.541±.001	.721±.004	.773±.003	.801±.002	.881±.003	.900±.001	.900±.000	.889±.003	.924±.002	.932±.001
		PC-quadratic	.499±.002	.535±.001	.539±.001	.720±.004	.779±.003	.807±.001	.880±.003	.899±.002	.900±.001	.884±.003	.923±.002	.935±.001
		PC-cubic	.500±.002	.537±.001	.548±.001	.719±.004	.778±.003	.806±.002	.879±.003	.895±.002	.900±.001	.883±.003	.919±.002	.937±.001
0.25	1	PC-linear	.487±.002	.527±.001	.538±.001	.721±.003	.765±.003	.798±.002	.880±.002	.896±.001	.900±.000	.897±.003	.925±.002	.933±.001
		PC-quadratic	.494±.002	.537±.001	.547±.001	.723±.003	.773±.003	.807±.002	.879±.002	.894±.001	.899±.000	.899±.003	.927±.002	.934±.001
		PC-cubic	.496±.002	.542±.001	.551±.001	.723±.004	.774±.003	.812±.001	.879±.002	.891±.002	.897±.001	.898±.003	.927±.002	.935±.001
	2	PC-linear	.495±.002	.538±.001	.549±.001	.714±.004	.761±.003	.790±.002	.879±.002	.894±.001	.900±.000	.897±.003	.928±.002	.933±.001
		PC-quadratic	.500±.002	.544±.001	.550±.001	.715±.004	.762±.003	.798±.002	.877±.002	.892±.001	.899±.001	.893±.003	.927±.002	.933±.001
		PC-cubic	.500±.002	<b>.548</b> ±.001	.554±.001	.716±.004	.762±.003	.802±.002	.877±.002	.888±.002	.896±.001	.891±.003	.926±.002	.933±.000
	3	PC-linear	.488±.002	.535±.001	.549±.001	.707±.004	.761±.003	.793±.002	.876±.003	.895±.001	.900±.000	.887±.003	.924±.002	.930±.001
		PC-quadratic	.493±.002	.544±.001	.553±.001	.708±.004	.761±.003	.795±.002	.875±.003	.893±.001	.899±.001	.883±.003	.923±.002	.931±.001
		PC-cubic	.493±.002	.547±.001	<b>.562</b> ±.001	.709±.004	.761±.003	.794±.002	.874±.003	.890±.002	.896±.001	.882±.003	.921±.002	.931±.001

Table 16: **Reproduction rates (%) across truncation fractions  $\tau \in \{0.75, 0.50, 0.25\}$  at  $K=1$ , GPT-OSS-20B (larger  $D$  is better).** Column symbols  $(r_C, r_W, D)$  follow Table 1, with  $\overline{\text{AUROC}} = (1 + D)/2$  at  $K=1$ . Macro-averaged over problems with at least one correct and one wrong initial sample.

Model	Benchmark	$\tau$	$r_C$	$r_W$	$D$	$\overline{\text{AUROC}}$
GPT-OSS-20B	FrontierScience-Olympiad	0.75	<b>55.4</b>	<b>14.0</b>	<b>41.4</b>	0.707
		0.50	<b>48.1</b>	<b>8.6</b>	<b>39.5</b>	0.697
		0.25	<b>45.0</b>	<b>5.9</b>	<b>39.1</b>	0.696
GPT-OSS-20B	HMMT Feb 2026	0.75	<b>78.3</b>	<b>29.7</b>	<b>48.6</b>	0.743
		0.50	<b>67.8</b>	<b>18.1</b>	<b>49.7</b>	0.748
		0.25	<b>60.2</b>	<b>12.3</b>	<b>47.9</b>	0.740
GPT-OSS-20B	AIME 2025	0.75	<b>87.8</b>	<b>42.6</b>	<b>45.2</b>	0.726
		0.50	<b>78.6</b>	<b>28.6</b>	<b>50.0</b>	0.750
		0.25	<b>73.0</b>	<b>17.1</b>	<b>55.9</b>	0.780
GPT-OSS-20B	Brumo 2025	0.75	<b>82.8</b>	<b>39.0</b>	<b>43.7</b>	0.719
		0.50	<b>74.8</b>	<b>18.3</b>	<b>56.5</b>	0.782
		0.25	<b>67.6</b>	<b>16.5</b>	<b>51.1</b>	0.756

Table 17 reports PC-linear, PC-quadratic, and PC-cubic accuracy across all  $(\tau, K)$  configurations on the four GPT-OSS-20B benchmarks at budgets  $B \in \{250k, 1M, 5M\}$ , with Standard MV at the top for reference. The main paper fixes  $\tau=0.75, K=1$  (Section 4) as a minimal default that preserves most of the trace and uses a single regeneration per sample. We use the sweep below to characterize how PC-WMV accuracy varies with  $(\tau, K)$ , not to select the operating point.

Two observations follow. At 250k tokens, high-cost configurations (large  $K$  and small  $\tau$ ) underperform Standard MV because each regeneration eats into the budget for new groups:  $\tau=0.25, K=3$  PC-cubic (cost  $\approx 3.25\times$ ) reaches .493, .709, .874, and .882 on FrontierScience-Olympiad, HMMT, AIME, and Brumo, underperforming Standard MV on the latter three (.736, .881, .901), while the

low-cost  $\tau=0.75$ ,  $K=1$  (cost  $\approx 1.25\times$ ) outperforms Standard MV on all four. At 1M–5M budgets, the default  $\tau=0.75$ ,  $K=1$  stays close to the per-cell best on the three math benchmarks (HMMT, AIME, Brumo). FrontierScience-Olympiad is the exception, where the larger discrimination gap at deeper truncation repays the higher per-group cost (PC-cubic at  $\tau=0.25$ ,  $K=3$  reaches .547 at 1M and .562 at 5M on FrontierScience-Olympiad, against .537 and .545 at  $\tau=0.75$ ,  $K=1$ ).  $K=1$  is sufficient on the math benchmarks at 1M, while  $K=3$  yields modest improvements on HMMT at 5M (PC-cubic .822 at  $K=3$  vs. .814 at  $K=1$ , both at  $\tau=0.75$ ). Overall, the default  $\tau=0.75$ ,  $K=1$  remains effective across the four benchmarks without being tuned to them, and the results of the main paper in Table 3 are therefore not sensitive to a particular choice of  $(\tau, K)$ .

### D.6 Robustness to Judge Choice

We show that PC’s per-cell advantage over the best baseline holds regardless of whether answer equivalence is evaluated by the model itself or by a stronger external grader.

The main paper uses each evaluated model itself to determine answer equivalence (Appendix H.2). One possible concern is that the evaluation may be biased by the limited capability of the model itself. As a robustness check, this section reports results using a stronger external grader. Namely, we re-scored the released pool with Claude Sonnet 4.6 [Anthropic, 2026] on four models (GPT-OSS-120B, GPT-OSS-20B, Nemotron3-30B, Nemotron2-9B) across the three LLM-judged benchmarks (Brumo 2025, HMMT Feb 2026, FrontierScience-Olympiad), giving 12 cells. AIME 2025 is exact-match and is therefore judge-free.

We re-cluster the released generation pool using the external judge’s YES/NO equivalence judgments instead of the model’s own, then recompute per-sample correctness labels along with  $\overline{\text{AUROC}}$ , PC-WMV accuracy, and the baseline accuracies. No new samples are drawn from the model.

**PC’s  $\overline{\text{AUROC}}$  advantage is preserved on every cell.** Figure 9 plots, per cell, the gap  $\Delta\overline{\text{AUROC}} := \overline{\text{AUROC}}_{\text{PC}} - \overline{\text{AUROC}}_{\text{best baseline}}$  under self-judge ( $x$ ) against the same quantity under the external judge ( $y$ ). All 12 points fall in the same quadrant under both judges: 9 cells with  $\Delta\overline{\text{AUROC}} > 0$  (PC ahead of the best baseline) and 3 cells with  $\Delta\overline{\text{AUROC}} < 0$ . No cell flips. Per-cell numbers are in Table 18.

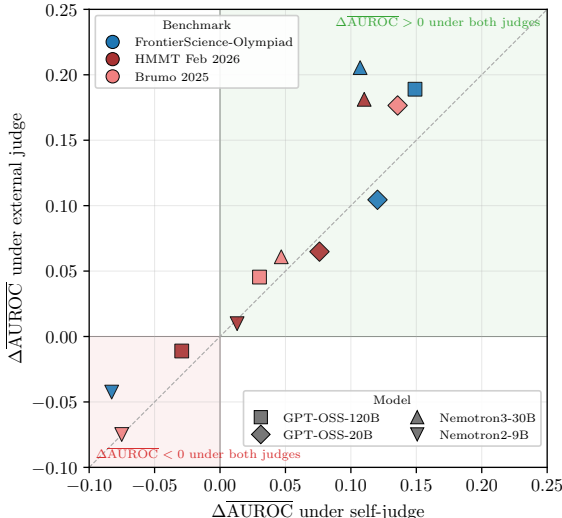


Figure 9: **PC’s  $\overline{\text{AUROC}}$  advantage is preserved across judges.** Each axis is  $\Delta\overline{\text{AUROC}} := \overline{\text{AUROC}}_{\text{PC}} - \overline{\text{AUROC}}_{\text{best baseline}}$ , under self-judge ( $x$ ) and an external judge (Claude Sonnet 4.6,  $y$ ); one point per cell (12 cells), and the dashed line is  $y=x$ . All 12 points lie in the top-right or bottom-left quadrant; no cell crosses an axis.

**WMV cost–accuracy curves under both judges nearly overlap.** Figure 10 overlays the WMV cost–accuracy curves under self-judge (faded) and the external judge (saturated) for the four primary

Table 18: **Per-cell PC and best-baseline  $\overline{\text{AUROC}}$  under self-judge vs. an external judge (Claude Sonnet 4.6).** Bold marks the higher of PC and the best baseline within each cell, with the best baseline’s identity in parentheses. AIME 2025 is exact-match (judge-free) and is omitted.

Model	Benchmark	PC		best baseline	
		self	external	self	external
GPT-OSS-120B	FrontierScience-Olympiad	<b>0.719</b>	<b>0.778</b>	0.570 (Self-certainty)	0.589 (Self-certainty)
	HMMT Feb 2026	0.698	0.711	<b>0.728</b> (DeepConf tail)	<b>0.722</b> (DeepConf tail)
	Brumo 2025	<b>0.636</b>	<b>0.660</b>	0.606 (DeepConf tail)	0.615 (DeepConf tail)
GPT-OSS-20B	FrontierScience-Olympiad	<b>0.707</b>	<b>0.718</b>	0.587 (P(True))	0.613 (P(True))
	HMMT Feb 2026	<b>0.743</b>	<b>0.740</b>	0.667 (P(True))	0.675 (P(True))
	Brumo 2025	<b>0.719</b>	<b>0.736</b>	0.583 (P(True))	0.559 (P(True))
Nemotron3-30B	FrontierScience-Olympiad	<b>0.631</b>	<b>0.733</b>	0.524 (Verbal 0–100)	0.527 (Verbal 0–100)
	HMMT Feb 2026	<b>0.698</b>	<b>0.766</b>	0.588 (DeepConf tail)	0.584 (P(True))
	Brumo 2025	<b>0.801</b>	<b>0.823</b>	0.755 (DeepConf tail)	0.762 (DeepConf tail)
Nemotron2-9B	FrontierScience-Olympiad	0.537	0.603	<b>0.620</b> (P(True))	<b>0.646</b> (P(True))
	HMMT Feb 2026	<b>0.648</b>	<b>0.648</b>	0.635 (P(True))	0.639 (P(True))
	Brumo 2025	0.633	0.633	<b>0.708</b> (P(True))	<b>0.708</b> (P(True))

methods (PC-cubic, Standard MV, DeepConf tail, P(True)). On Brumo and HMMT, the two layers are essentially indistinguishable. On FrontierScience-Olympiad, the external-judge curves sit above their self-judge counterparts by a roughly uniform vertical offset; PC-cubic stays the top (or tied-top) curve in every panel where it leads under self-judge, and stays below where it trails. The per-cell ordering of methods at any operating point is therefore preserved.

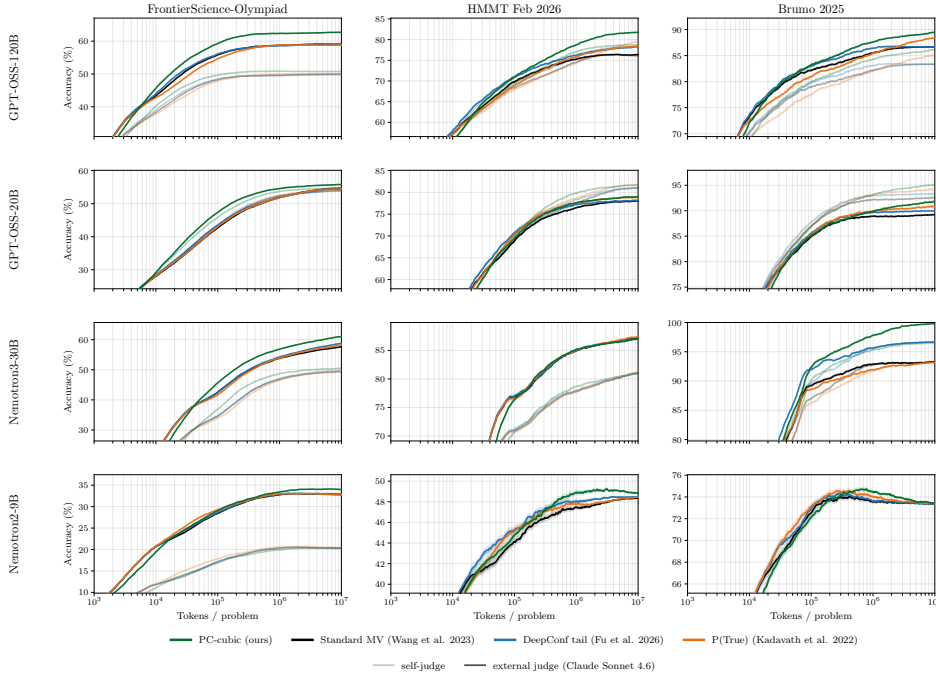


Figure 10: **WMV cost–accuracy curves are stable across judges.** 4 models  $\times$  3 benchmarks; faded curves use the model’s own judge, saturated curves use an external judge (Claude Sonnet 4.6). The four methods (PC-cubic, Standard MV, DeepConf tail, P(True)) match Figure 5. The relative ordering of methods is preserved in every panel; the largest absolute shifts between the two judges are in the FrontierScience-Olympiad column.

**Pool-level shifts are concentrated on FrontierScience-Olympiad.** On Brumo and HMMT, the two judges disagree on fewer than 4% of per-sample correctness labels per cell, and Pass@1 differs

by at most 0.06. On FrontierScience-Olympiad the per-sample flip rate is higher (9% to 17%) and Pass@1 rises by up to 0.09 on three of the four cells; the fourth (GPT-OSS-20B) has compensating up- and down-flips that leave Pass@1 within 0.01 despite an 8.6% flip rate. The shift reflects the external judge recognizing more equivalent surface forms than the model’s own. The added equivalences strengthen PC’s relative position rather than weaken it: in Figure 9, three of the four FrontierScience-Olympiad points (blue) sit above the  $y=x$  diagonal, and the leftmost column of Figure 10 shows PC’s gap over the baselines widening on those cells under the external judge.

### D.7 Reliability Signals vs. Pass@1

This subsection backs the analysis of Section 4.4 (rising  $r_C$  and a smaller, problem-dependent  $r_W$  slope within each category) with full panels and slope tables for the reproduction rates  $r_C, r_W$  under the GLM estimator (Appendix D.7.1), verifies that the qualitative pattern survives per-benchmark refits (Appendix D.7.2) and two alternative estimators (Appendix D.7.3), and reports the corresponding Pass@1 view for the per-sample baseline signals (Appendix D.7.4).

#### D.7.1 GLM Panels and Slopes

Figure 11 adds GLM panels for the two models not shown in Figure 3 (GPT-OSS-20B, Nemotron2-9B), and Table 19 reports the slopes for all five. The qualitative pattern is consistent:  $r_C$  rises with Pass@1 on both categories, while  $r_W$  has a smaller, problem-dependent slope and sits at a lower level on Science than on Math. The GLM fit kernel and cluster-bootstrap inference protocol below are shared with the alternative estimators of Appendix D.7.3.

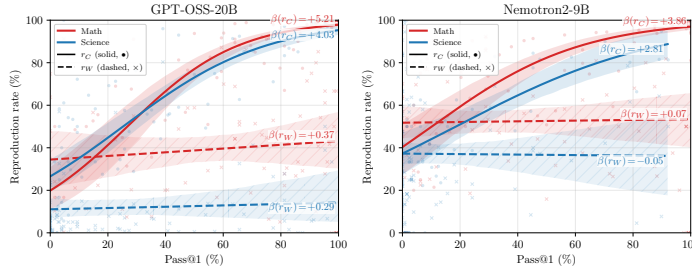


Figure 11: **Per-problem reproduction rates vs. Pass@1, remaining models.** GLM fits for GPT-OSS-20B and Nemotron2-9B, complementing Figure 3. Curves and overlays follow the same convention.

Table 19: **Logistic GLM slope estimates on  $\text{logit}(r) = \beta_0 + \beta \cdot \text{Pass@1}$  per (model, category).**  $2\sigma$  CIs are from cluster bootstrap over problems (1000 replicates). The  $p$ -column gives the two-sided bootstrap  $p$ -value for  $H_0 : \beta = 0$ , with “<.001” indicating that no replicate crossed zero.

Model	Category	$\beta(r_C)$		$\beta(r_W)$	
		$\hat{\beta}$ [2 $\sigma$ CI]	$p$	$\hat{\beta}$ [2 $\sigma$ CI]	$p$
GPT-OSS-120B	Science	+4.28 [+3.51, +5.14]	<.001	-0.06 [-1.20, +0.99]	0.96
	Math	+5.10 [+4.05, +6.26]	<.001	+1.14 [+0.04, +2.30]	0.034
GPT-OSS-20B	Science	+4.03 [+3.36, +4.77]	<.001	+0.29 [-1.05, +1.41]	0.66
	Math	+5.21 [+4.38, +6.25]	<.001	+0.37 [-0.67, +1.56]	0.48
Nemotron3-30B	Science	+3.67 [+2.90, +4.37]	<.001	+0.14 [-1.03, +1.20]	0.8
	Math	+3.18 [+2.17, +4.37]	<.001	-0.20 [-1.40, +0.79]	0.67
Nemotron2-9B	Science	+2.81 [+1.89, +4.07]	<.001	-0.05 [-1.25, +0.90]	0.89
	Math	+3.86 [+3.21, +4.69]	<.001	+0.07 [-0.69, +0.74]	0.85
Ministral3-14B	Science	+2.66 [+1.27, +4.09]	0.002	-0.61 [-1.98, +0.55]	0.27
	Math	+2.94 [+2.22, +3.67]	<.001	-0.75 [-1.45, -0.08]	0.022

**GLM fit kernel.** For each outcome  $Y \in \{C, W\}$  (regenerations seeded from a correct ( $C$ ) or wrong ( $W$ ) trace, matching  $r_C$  and  $r_W$  in Section 3.1), fit a logistic regression  $\Pr(Y_j = 1 \mid \text{Pass@1}_j) =$

$\sigma(\beta_{0,Y} + \beta_Y \cdot \text{Pass}@1_j)$  on trial-level data, where each trial  $j$  inherits the  $\text{Pass}@1$  of its problem, by maximum likelihood (`statsmodels.GLM`, Binomial family, default iteratively reweighted least squares (IRLS) solver). Reported quantities are the slope  $\beta_Y$  and the predicted curve on a fixed  $\text{Pass}@1$  grid, masked to the cell’s observed support.

**Inference protocol.** A (model, category) cell consists of  $N$  per-problem records, each carrying its  $\text{Pass}@1$  and two Bernoulli trial streams:  $r_{C,i,j} \in \{0, 1\}$  for the  $n_{C,i}$  regenerations seeded from a correct trace and  $r_{W,i,j}$  for the  $n_{W,i}$  from a wrong trace ( $r = 1$  if the regenerated answer matches the seed, 0 otherwise). Each problem  $i$  contributes  $n_{C,i}$  trials ( $\text{Pass}@1_i, r_{C,i,j}$ ) to the  $r_C$  regression (and  $n_{W,i}$  trials ( $\text{Pass}@1_i, r_{W,i,j}$ ) to  $r_W$ ), where the same  $\text{Pass}@1$  is shared across all trials from the same problem. We refer to this trial-level dataset as the expanded trials. Point estimates apply each estimator’s fit kernel  $\hat{f}_Y$  ( $Y \in \{C, W\}$ ) to the expanded trials.

Confidence intervals are derived using  $B = 1000$  cluster-bootstrap iterations. At iteration  $b$ , we resample  $N$  problem indices with replacement, then refit  $\hat{f}_C^{(b)}$  and  $\hat{f}_W^{(b)}$  on the corresponding trial set. Within-problem correlation among regenerations that share a prefix is corrected for by resampling problems rather than trials; trial-level Bernoulli standard errors would otherwise be underestimated by a factor of 2 to 4 on these data. Because  $\hat{f}_C^{(b)}$  and  $\hat{f}_W^{(b)}$  share the same resample within an iteration, the difference  $D^{(b)} = \hat{f}_C^{(b)} - \hat{f}_W^{(b)}$  inherits the correct joint distribution, and CIs for  $D$  are read off  $\{D^{(b)}\}$  directly rather than summed from per-fit half-widths.

Pointwise  $2\sigma$  CIs are percentile intervals at level  $2(1 - \Phi(2)) \approx 0.0455$ , taken per  $\text{Pass}@1$  grid point for continuous estimators and per bin for the binned estimator. The two-sided bootstrap  $p$ -value for  $H_0 : \beta = 0$  in Table 19 is  $p = \min\{1, 2 \min(\Pr_b[\beta^{(b)} \leq 0], \Pr_b[\beta^{(b)} \geq 0])\}$ , with “<.001” indicating no replicate crossed zero. The seed is fixed at 0. A small convergence check (3 seeds, several  $B$ , GPT-OSS-120B Math  $r_W$ ) confirmed stability from  $B = 1000$ .

### D.7.2 Robustness under Per-Benchmark Pooling

Section 4.4 pools the three Math benchmarks (HMMT Feb 2026, AIME 2025, Brumo 2025) into a single Math curve per model. Since the three span different  $\text{Pass}@1$  ranges within a fixed model, the pooled slope could in principle reflect between-benchmark  $\text{Pass}@1$  differences rather than a within-benchmark  $\text{Pass}@1$  effect. To check for this confound we refit the same logistic GLM on each (model, benchmark) cell separately, with the fit kernel and cluster-bootstrap protocol of Appendix D.7.1. Figure 12 plots the four per-benchmark curves per model in a single panel, and Table 20 reports the slopes.

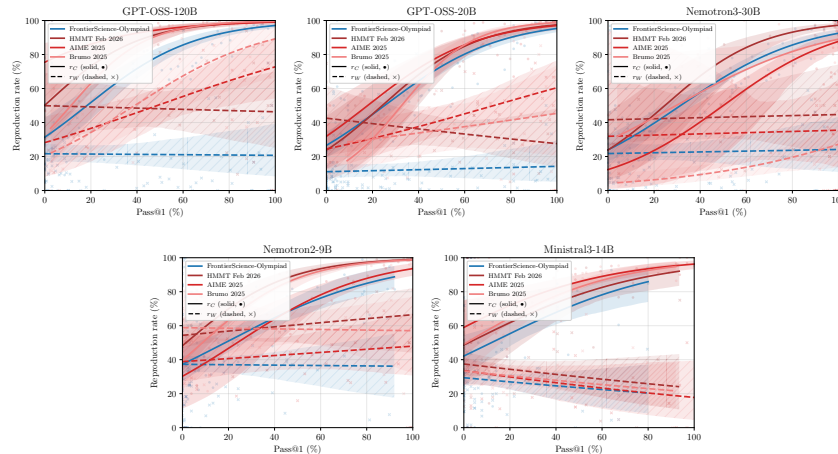


Figure 12: **Per-problem reproduction rates vs.  $\text{Pass}@1$ , per benchmark.** One panel per model. Solid lines with  $\bullet$  are  $r_C$  and dashed lines with  $\times$  are  $r_W$ , both logistic-regression fits per benchmark with shaded  $2\sigma$  cluster-bootstrap CIs over problems. Scatter overlays are per-problem empirical rates. Companion to Figure 3, with Math (HMMT Feb 2026, AIME 2025, Brumo 2025) split into separate curves rather than pooled.

Table 20: **Per-(model, benchmark) GLM slope estimates on  $\text{logit}(r) = \beta_0 + \beta \cdot \text{Pass@1}$ .** Per-benchmark variant of Table 19, fit on each (model, benchmark) cell separately.  $2\sigma$  CIs from a cluster bootstrap over problems (1000 replicates), and two-sided bootstrap  $p$ -values for  $H_0 : \beta = 0$  (“ $<.001$ ” indicates that no replicate crossed zero).

Model	Benchmark	$\beta(r_C)$		$\beta(r_W)$	
		$\hat{\beta}$ [ $2\sigma$ CI]	$p$	$\hat{\beta}$ [ $2\sigma$ CI]	$p$
GPT-OSS-120B	FrontierScience-Olympiad	+4.28 [+3.51, +5.14]	<.001	-0.06 [-1.20, +0.99]	0.96
	HMMT Feb 2026	+4.97 [+3.76, +6.45]	<.001	-0.14 [-1.58, +1.65]	0.83
	AIME 2025	+3.50 [+2.01, +5.80]	<.001	+1.92 [+0.67, +4.50]	0.002
	Brumo 2025	+6.21 [+4.53, +8.34]	<.001	+3.46 [+1.25, +5.75]	0.004
GPT-OSS-20B	FrontierScience-Olympiad	+4.03 [+3.36, +4.77]	<.001	+0.29 [-1.05, +1.41]	0.66
	HMMT Feb 2026	+4.82 [+3.61, +6.83]	<.001	-0.66 [-2.01, +1.17]	0.4
	AIME 2025	+4.24 [+3.05, +6.08]	<.001	+1.55 [+0.45, +2.91]	0.006
	Brumo 2025	+6.55 [+5.28, +8.25]	<.001	+0.81 [-1.34, +3.16]	0.42
Nemotron3-30B	FrontierScience-Olympiad	+3.67 [+2.90, +4.37]	<.001	+0.14 [-1.03, +1.20]	0.8
	HMMT Feb 2026	+4.72 [+3.48, +6.71]	<.001	+0.13 [-1.75, +1.68]	0.85
	AIME 2025	+3.93 [+2.59, +6.97]	<.001	+0.16 [-4.10, +3.47]	0.86
	Brumo 2025	+2.97 [+0.40, +5.26]	0.016	+2.14 [+0.68, +3.59]	0.018
Nemotron2-9B	FrontierScience-Olympiad	+2.81 [+1.89, +4.07]	<.001	-0.05 [-1.25, +0.90]	0.89
	HMMT Feb 2026	+4.57 [+3.43, +5.93]	<.001	+0.51 [-0.49, +1.45]	0.26
	AIME 2025	+3.52 [+2.30, +5.31]	<.001	+0.37 [-0.74, +1.40]	0.42
	Brumo 2025	+4.83 [+3.96, +6.00]	<.001	-0.07 [-2.18, +1.47]	1
Ministral3-14B	FrontierScience-Olympiad	+2.66 [+1.27, +4.09]	0.002	-0.61 [-1.98, +0.55]	0.27
	HMMT Feb 2026	+2.68 [+0.87, +4.48]	0.006	-0.68 [-1.84, +0.49]	0.2
	AIME 2025	+2.88 [+1.71, +4.13]	<.001	-0.85 [-2.44, +0.42]	0.22
	Brumo 2025	+3.19 [+2.01, +4.98]	<.001	-0.65 [-1.69, +0.56]	0.28

The two claims in Section 4.4 both survive the per-benchmark refit. (i)  $\beta(r_C) > 0$  on all 20 (model, benchmark) cells with  $p < 0.05$  (in fact  $p < 0.001$  on 17 of 20 cells), so the rising- $r_C$  pattern is within-benchmark and not a pooling artefact. (ii)  $|\beta(r_W)| < \beta(r_C)$  on all 20 cells, so the smaller-magnitude statement is also within-benchmark.

The per-benchmark view further clarifies the two non-zero pooled  $\beta(r_W)$  values from Section 4.4. The GPT-OSS-120B Math value +1.14 is driven by AIME 2025 (+1.92,  $p = 0.002$ ) and Brumo 2025 (+3.46,  $p = 0.004$ ), with HMMT Feb 2026 separately null (-0.14,  $p = 0.83$ ): the pooled value reflects a real within-benchmark Pass@1 effect on AIME and Brumo, but the effect is benchmark-specific rather than uniform across Math. The Ministral3-14B Math value -0.75 is uniform across all three benchmarks (-0.85, -0.68, -0.65), i.e. a within-benchmark effect that holds Math-wide. In neither case is the pooled slope a between-benchmark artefact.

### D.7.3 Robustness under Alternative Estimators

In Figure 3, we fit a logit-linear model. To verify that the conclusions in the main paper (that is, rising  $r_C$ , a smaller and problem-dependent  $r_W$  slope within each category, and lower  $r_W$  on Science than on Math) do not depend on that form, we rerun the same plot for all five models under two alternative estimators, sharing the cluster-bootstrap protocol of Appendix D.7.1.

**Trial-pooled binned estimator (Figure 13).** This estimator reads reproduction rates directly off the data, removing the GLM’s logit-linear assumption at the cost of bin-edge sensitivity. Bin edges come from the full-data Pass@1 quantiles, with 5 equal-count bins per category deduplicated by `np.unique`. A Pass@1 mass at zero can collapse adjacent edges, e.g. Ministral3-14B Science with 53 problems at zero resolves to 3 effective bins. Each bootstrap iteration assigns problems to those fixed edges and reports the trial-pooled rate  $\sum_{i \in \text{bin}} k_{Y,i} / \sum_{i \in \text{bin}} n_{Y,i}$ , where  $k_{Y,i}$  and  $n_{Y,i}$  count reproductions and trials.

**LOWESS smoother (Figure 14).** Because this estimator does not assume a monotone or parametric relationship, it can reveal any non-monotonic structure in  $r_W$  that a logit-linear model would inadvertently hide. We use `statsmodels.nonparametric.smoothers_lowess` on trial-level

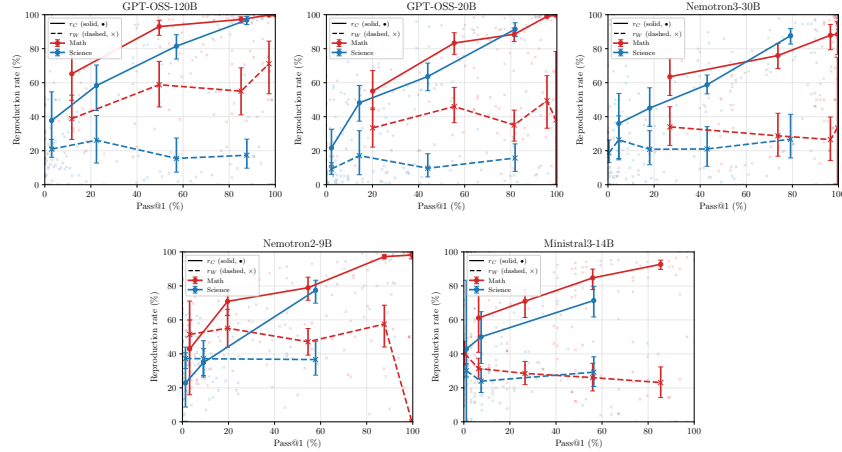


Figure 13: **Binned view of Figure 3, all five models.** Trial-pooled  $r_C$  (solid,  $\bullet$ ) and  $r_W$  (dashed,  $\times$ ) over five Pass@1 quantile bins per category, with  $2\sigma$  cluster-bootstrap CIs (1000 replicates, same inference protocol as the GLM in the main paper).

$(\text{Pass}@1_j, Y_j)$  pairs with span frac = 0.5 and robustness iterations it = 0. The default it = 3 uses bisquare residual weights designed for continuous residuals, which collapse Bernoulli outcomes to degenerate 0 or 100% curves (verified empirically on Science). The fit is linearly interpolated onto the GLM’s Pass@1 grid and masked to the observed support.

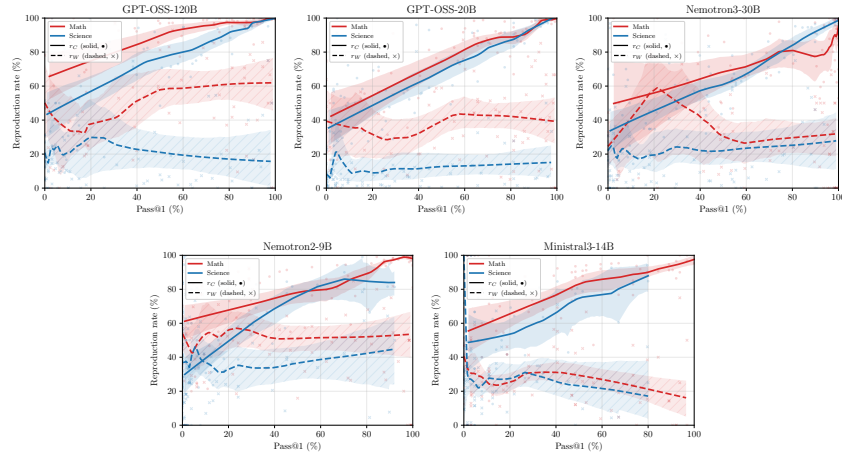


Figure 14: **LOWESS smoother view of Figure 3, all five models.**  $r_C$  (solid) and  $r_W$  (dashed) from trial-level LOWESS (span = 0.5, no robustness reweightings) per category, with  $2\sigma$  pointwise CIs from cluster bootstrap over problems (1000 replicates).

All three estimators agree qualitatively across all five models:  $r_C$  rises across Pass@1 on every (model, category) pair, and  $r_W$  has a smaller, problem-dependent slope with the category-specific levels described in Section 4.4.

#### D.7.4 Baseline Confidence Signals vs. Pass@1

For comparison with Figure 3, we repeat the per-class, Pass@1-conditioned view on the two baseline confidence signals named in the caption of Figure 2: DeepConf tail (Figure 15) and P(True) (Figure 16). For each signal, we split per-trial values by whether the trace’s answer matches gold (Correct, solid) or not (Wrong, dashed), and fit each class per category with a Gaussian linear model  $s = \beta_0 + \beta \cdot \text{Pass}@1$ , replacing the Bernoulli logistic GLM of Appendix D.7.1 since the response is now a continuous score. The cluster-bootstrap protocol ( $B = 1000$  resamples over problems,

$2\sigma$  percentile CIs) is unchanged. Scatter overlays show per-problem mean confidence (one dot per problem per class), the continuous-signal analogue of the per-problem rate  $k/n$  in Figure 3.

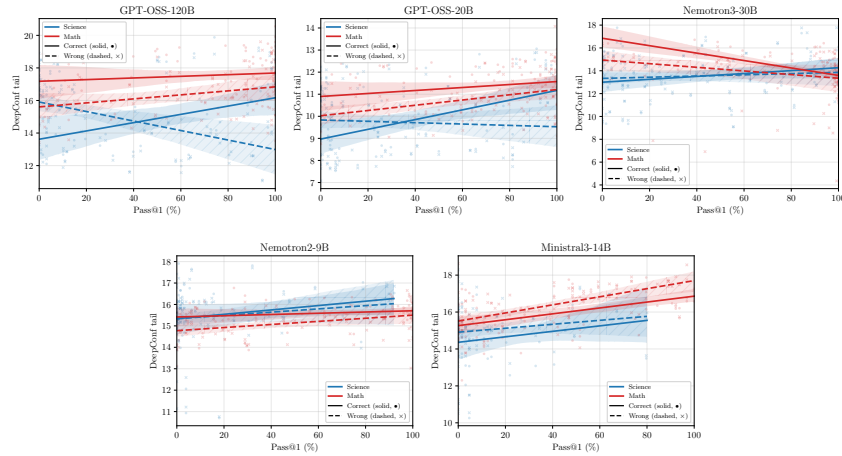


Figure 15: **DeepConf tail vs. Pass@1, all five models.** Per-class Gaussian linear fits with  $2\sigma$  cluster-bootstrap CIs over problems. Scatter overlays are per-problem mean confidence.

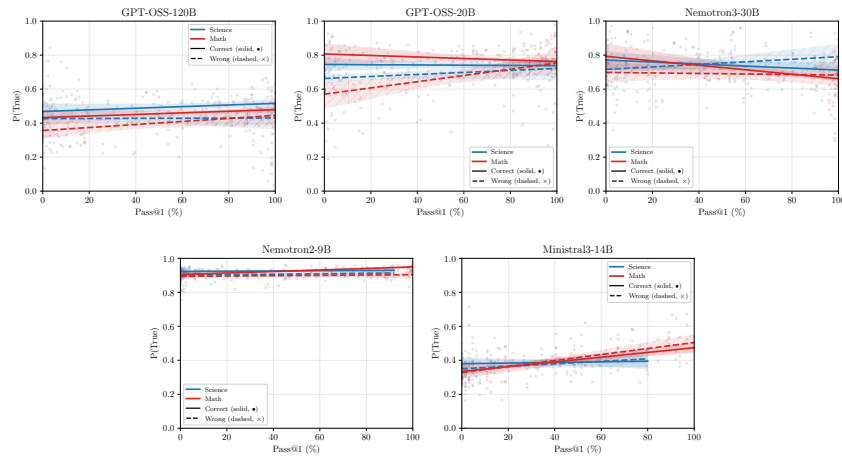


Figure 16: **P(True) vs. Pass@1, all five models.** Same protocol as Figure 15.

## E Baseline Implementation Details

We document here the exact confidence scores and voting rules used for each baseline, since different papers use slightly different weighting conventions.

**Glossary of baseline labels.** The baselines summarized in Section 4 appear under the following labels in our tables and figures (e.g. Table 3 and the per-model tables of Appendix D.3). The per-baseline paragraphs below give the full implementation details.

- *DeepConf* [Fu et al., 2026]: a family of trace-level log-probability scores (*first-token*, *Mean* (the *Self-certainty* signal of Kang et al. [2025]), *bottom-10%*, *block-min*, *tail*). Each is plugged into Eq. (3) with  $w$  as the identity. Filtered variants (*top-10%*, *top-90%*) keep only the top- $\eta\%$  of traces by the same score before voting.
- *CISC* [Taubenfeld et al., 2025]: Confidence-Informed Self-Consistency, a per-sample weighting scheme that draws its raw confidence from one of four sources: *Response probability* [Wang et al., 2023b] (length-normalized geometric mean of per-token probabilities), *Verbal binary* [Lin

et al., 2022] (a 0/1 self-rating parsed from a follow-up call), *Verbal 0–100* [Lin et al., 2022] (a percentage self-rating parsed from a follow-up call), and  $P(\text{True})$  [Kadavath et al., 2022] (the renormalized softmax probability of the “1” token versus “0” at the rating-call confidence position).

- *Adaptive stopping*: cost–accuracy curves traced by sweeping the early-stopping hyperparameter of Adaptive Consistency (*AC sweep* [Aggarwal et al., 2023]) and Early-Stopping Self-Consistency (*ESC sweep* [Li et al., 2024]) over the same initial pool.
- *SubthoughtReasoner* [Hammoud et al., 2025]: a single-trace refinement baseline that segments each trace at linguistic cues and votes over per-subthought regenerations. It appears only in the GPT-OSS-20B all-baselines tables (Tables 7 and 12).
- *PC-linear, PC-quadratic, PC-cubic*: PC-WMV (Algorithm 1) instantiated with the power-family weighting  $w^{(n)}(c) = c^n$  at  $n = 1, 2, 3$ . We use “PC-cubic” as shorthand for PC-WMV with  $n=3$ .

**Deep Think with Confidence (DeepConf) [Fu et al., 2026].** We compute five trace-level confidence scores from the top-20 token log-probabilities saved at generation, following the original implementation.<sup>3</sup> For a trace  $y_i$ , let  $P_{t,j}$  be the  $j$ -th largest token probability at position  $t \leq |y_i|$ . The readout  $\ell_i = \{P_{t,j}\}_{t \leq |y_i|, j \leq 20}$  is the top-20 log-probability record along  $y_i$ . Write  $C_t = -\frac{1}{20} \sum_{j=1}^{20} \log P_{t,j}$  for the negative top-20 mean at position  $t$ . The five trace-level signals  $s(y_i, \ell_i)$  are:

Score	Definition
First-token	KL divergence between the normalized top-20 distribution at the first generated token and the uniform distribution.
Mean	$\frac{1}{ y_i } \sum_t C_t$ , the average token-level confidence over the trace.
Bottom-10%	Mean of the lowest 10% of moving averages over $C_t$ (window length 1024, stride 1).
Block-min	Minimum block-level mean $C_t$ , after splitting the trace at double-newline boundaries.
Tail	Mean $C_t$ over the last 2,024 tokens of the trace.

The Mean score above is a top-20 implementation of the self-certainty signal originally proposed by Kang et al. [2025] on the full vocabulary. We adopt it as our *Self-certainty* baseline and report it under that label throughout the paper. DeepConf is the case of Eq. (3) where  $s(y_i, \ell_i)$  is one of the five signals above and  $w$  is the identity, giving  $v_i(a) = s(y_i, \ell_i) \cdot \mathbf{1}[a_i = a]$ , where  $a_i$  is the answer extracted from trace  $i$ . Confidence filtering (Section 3.2 of their paper) optionally restricts the sum to the top- $\eta\%$  of traces by  $s(y_i, \ell_i)$  before aggregation. The unfiltered variant (DeepConf-`<score>`) sums  $v_i(a)$  over all traces, for each of the five scores above. In addition, we evaluate four filtered variants that combine the two stronger scores with the two retention levels proposed in the paper:

Score	$\eta$	Aggregation
Bottom-10%	10%	Keep top-10% by bottom-10% confidence, then sum $s(y_i, \ell_i) \cdot \mathbf{1}[a_i = a]$ over retained.
Bottom-10%	90%	Same with $\eta = 90\%$ .
Tail	10%	Keep top-10% of traces by tail confidence, then sum $s(y_i, \ell_i) \cdot \mathbf{1}[a_i = a]$ over retained.
Tail	90%	Same with $\eta = 90\%$ .

The DeepConf online early-termination mechanism is not used: our evaluation is offline over a pre-generated pool under a shared token budget.

**Confidence-Informed Self-Consistency (CISC) [Taubenfeld et al., 2025].** CISC (Definition 3.1 of their paper) extracts a per-sample raw confidence  $s_i = s(y_i, \ell_i)$  from one of four sources drawn from prior work, then applies a softmax weighting  $w(s_i) = \exp(s_i/T) / \sum_j \exp(s_j/T)$  (over samples) with tunable temperature  $T$ :

<sup>3</sup><https://github.com/facebookresearch/deepconf>

Source	$\ell_i$	Raw confidence $s_i$
Response probability [Wang et al., 2023b]	per-token log-probabilities of $y_i$	Length-normalized geometric mean of token probabilities, $\exp(\frac{1}{ y_i } \sum_t \log P_t)$ where $P_t$ is the probability of the generated token at position $t$ .
Verbal binary [Lin et al., 2022]	$\emptyset$ (verbalized)	$\{0, 1\}$ self-rating parsed from text, a simplification of the verbalized paradigm.
Verbal 0–100 [Lin et al., 2022]	$\emptyset$ (verbalized)	Post-hoc percentage-confidence self-rating parsed from text.
P(True) [Kadavath et al., 2022]	top-20 logprobs at the rating-call confidence token	Renormalized softmax probability of “1” versus “0” computed from the top-20 logprobs at the rating-call confidence token, $\exp(\ell_1)/(\exp(\ell_0) + \exp(\ell_1))$ when both are present (with single-side fallbacks otherwise).

The original CISC release<sup>4</sup> targets non-reasoning models and forces a single-token response (`temperature=0, max_tokens=1`). This setting is incompatible with our reasoning models, whose chat template (e.g., Harmony for GPT-OSS) leaves the final channel open at the end of the saved trace: the appended rating suffix sits inside that open channel, and the model may emit channel-control tokens or brief reasoning before producing the digit, and occasionally reopens an analysis or commentary channel after the digit. For our reasoning models we therefore make a separate completions call per initial sample, continuing from the saved trace  $y_i$  appended with a short rating suffix and using each model’s recommended sampling parameters. Verbal binary and P(True) share the binary suffix “*Now I will rate my confidence in the proposed answer as either 0 or 1. Proposed confidence:* (”, and the Verbal 0–100 suffix is “*Now I will rate my confidence in the proposed answer on a scale of 0–100. Proposed confidence:* (” (with leading newline). The follow-up call is allowed to reason. We then detect the CoT-to-final delimiter and read the confidence from the final portion (first token whose top-20 candidates contain “0” or “1” for Verbal binary and P(True), first integer up to “)”) for Verbal 0–100). A single binary call serves both Verbal binary (text parse of the digit) and P(True) (top-20 logprob softmax of “1” versus “0” at the same token). The suffix wording mirrors the CISC public release. Parse failures are imputed with the per-problem median of the non-missing scores, which keeps the answer in the vote at a neutral weight (Appendix H.1 discusses why this is preferred over dropping the sample from the pool). To avoid a baseline-specific  $T$  search that could over-fit our benchmarks, we report the untuned linear weighting  $w(s) = s$  for each source (verbal 0–100 rescaled to  $[0, 1]$ ), so  $v_i(a) = s(y_i, \ell_i) \cdot \mathbb{1}[a_i = a]$ . Softmax with  $T=1$  is also computed by our pipeline but omitted from the tables because it consistently underperforms the linear variant. A full  $T$  sweep is left to future work.

Under the budget accounting defined in Appendix G.1, we charge Verbal binary, Verbal 0–100, and P(True) a per-sample token cost of  $|y_i|$  plus the length of the secondary-call output up to and including the parsed digit (or its enclosing “)”). Here, we charge this minimum-parse length rather than the full secondary-call length because the model occasionally continues with extra reasoning after the digit that the parser ignores. Charging that overflow would overstate the unavoidable cost of these baselines. A tighter `max_tokens` cap on the secondary call would bound the overflow at the source, but we leave the secondary call’s maximum output length matched to the initial generation budget (Appendix I) to avoid baseline-specific tuning, and rely on the parser-anchored cost above to keep the budget accounting honest. Response probability has no secondary call: the per-token log-probabilities of  $y_i$  are saved at initial generation and read for free.

**Adaptive Consistency (AC)** [Aggarwal et al., 2023]. AC consumes the initial pool one sample at a time and stops at the first  $k$  for which a Beta-binomial posterior favors the running top answer over the runner-up by at least  $C_{\text{thresh}}$ . Let  $n_1$  and  $n_2$  be the top-1 and top-2 answer counts after  $k$  samples. The closed-form stopping criterion is

$$1 - I_{1/2}(n_1 + 1, n_2 + 1) \geq C_{\text{thresh}},$$

where  $I_x(\alpha, \beta)$  is the regularized incomplete beta function. This is the analytic equivalent of the Monte Carlo integral implemented in the official release.<sup>5</sup> At the stop time, the prediction is the running mode, so AC adds no per-sample weighting: it is Standard MV truncated at a natural stopping point. The original paper reports  $C_{\text{thresh}} = 0.95$  as the default and sweeps  $[0.5, 1)$  in Figure 2 to trace

<sup>4</sup><https://github.com/google-research/google-research/tree/master/cisc>

<sup>5</sup><https://github.com/Pranjal2041/AdaptiveConsistency>

a cost–accuracy frontier. We sweep  $C_{\text{thresh}} \in \{0.5, 0.6, 0.7, 0.8, 0.9, 0.95, 0.97, 0.99, 0.995, 0.999\}$ . Each value yields a single (cost, accuracy) point at its natural stopping cost, and we label the resulting curve “AC sweep”.

**Early-Stopping Self-Consistency (ESC)** [Li et al., 2024]. ESC consumes the initial pool in fixed-size windows of  $W$  samples. When a window is unanimous, ESC locks that answer as the final prediction and stops. Otherwise, the window’s votes are added to a running counter and a new window is drawn. Before any lock, the intermediate prediction is the mode of the running counter. The paper recommends  $W = 5$  for most tasks and  $W = 8$  for MATH. Our streaming reformulation reproduces the lock semantics of the official batch release.<sup>6</sup> We sweep  $W \in \{2, 3, \dots, 10\}$  and label the resulting natural-stopping curve “ESC sweep”. Like AC, ESC is Standard MV with a window-based stopping rule and adds no per-sample weight.

**Cost accounting for AC and ESC.** Both methods consume only initial samples. Their per-trial budget is the cumulative generated-token length of the consumed initial samples, the same cost accounting used by Standard MV, Self-certainty, DeepConf, and Response probability. Because each hyperparameter value yields one (cost, accuracy) point at its natural stopping cost rather than a curve over a shared budget grid, we treat the points across the swept hyperparameter as the method’s cost–accuracy curve and interpolate it for any required budget. The pool size  $N$  bounds how many tokens AC and ESC can spend, so their plateaus are bounded by  $N$ -sample Standard MV.

**SubthoughtReasoner** [Hammoud et al., 2025]. At the time of writing, no official implementation was available, so we reimplemented the method based on the description provided in the original paper. Our implementation segments each reasoning trace into sequential subthoughts at the linguistic cues described in Section 3 of their paper, regenerates a continuation from the end of each subthought, and takes an unweighted majority vote over the resulting pool of answers. To bound the per-problem cost of constructing this pool, we process initial samples in order, accumulating each sample’s initial tokens together with its subthought-regenerated continuations, and stop once the cumulative cost reaches that of the  $N$  initial samples for that problem. Otherwise, the per-problem cost of regenerating subthought continuations from all  $N$  initial samples would be several times that of the initial generation alone. We evaluated this baseline on only a small subset of (model, benchmark) conditions.

**Prefix consistency (ours).** For prefix consistency,  $\ell_i = \emptyset$ : it reads only generated tokens and regenerated answers, with no log-probability access. Unlike the per-sample signal  $s(y_i, \ell_i)$  used by the baselines above, our signal  $c_i^{(\tau)}(a)$  is defined per distinct candidate  $a \in A_i^{(\tau)}$  (Section 3.1). Moreover, we use the power-family weighting  $w^{(n)}(c) = c^n$  for  $n \in \{1, 2, 3\}$  (PC-linear, PC-quadratic, PC-cubic). PC-linear ( $n=1$ ) admits a simple interpretation: substituting  $w(c) = c$  and Eq. (7) into the PC-WMV vote gives  $\sum_i v_i(a) = \frac{1}{K+1} \sum_i |\{a' \in A_i^{(\tau)} : a' = a\}|$ , which is proportional to the count of  $a$  in the combined pool of  $N$  initial answers and  $NK$  regenerations. PC-linear’s argmax therefore coincides with unweighted majority voting on this  $(K+1)N$  pool, treating each regeneration as one additional vote of equal weight. PC-quadratic and PC-cubic depart from this baseline by giving super-linear weight to candidates that the same group reproduces.

## F Examples of Prefix Consistency

Figure 17 shows two representative examples of how regeneration behaves after truncation. When the initial answer is correct, the regenerated continuation often recovers the same core reasoning structure and reproduces the correct answer. In contrast, when the initial reasoning is already flawed, regeneration typically does not repair it. Instead, it continues along a similar erroneous line of reasoning and may even produce a different wrong answer. These examples help illustrate why regeneration amplifies the consistency of correct traces while still failing to escape incorrect ones.

<sup>6</sup><https://github.com/Yiwei98/ESC>

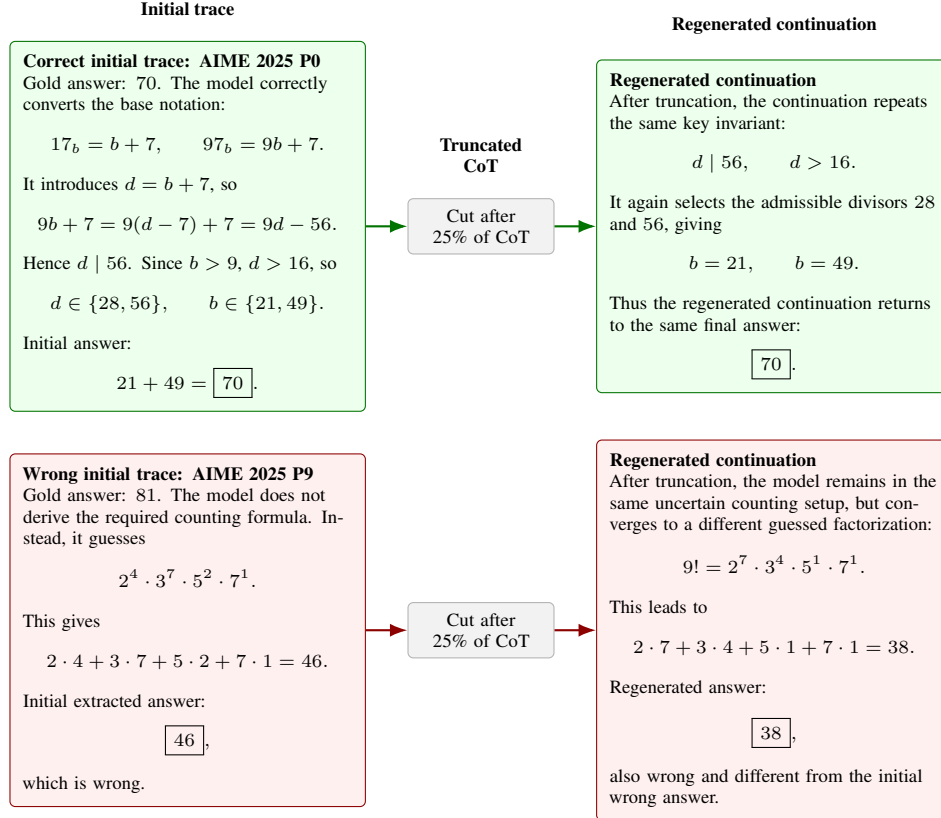


Figure 17: **Qualitative examples of CoT regeneration after truncation.** A correct initial trace (green, top) and a wrong initial trace (red, bottom) on AIME 2025, each truncated at 25% of its CoT and continued from the prefix.

## G Evaluation Protocol

This appendix consolidates the analysis pipeline shared across the experimental sections of the main paper. Implementation choices specific to each baseline are in Appendix E. Hardware and inference settings are in Appendix I.

### G.1 Setup

**Benchmarks.** We evaluate on one science benchmark (FrontierScience-Olympiad) and three math benchmarks (HMMT Feb 2026, AIME 2025, Brumo 2025). Table 21 lists the problem count, answer format, and scoring rule of each. We use the full released test split for every benchmark. Answers are extracted from the boxed expression, then math-normalized for the math benchmarks (fraction unification, degree-marker removal) or used with minimal normalization for FrontierScience-Olympiad. Equivalence to the gold answer is decided by exact match for AIME 2025 and by an LLM judge for the other three benchmarks (Appendix H.2). HuggingFace URLs and licenses are in Table 24.

Table 21: **Evaluation benchmarks.**

Dataset	# Problems	Category	Answer format	Scoring
FrontierScience-Olympiad	100	Science	Free-form (expression, number, or short text)	LLM judge
HMMT Feb 2026	33	Math	Integer or closed-form expression	LLM judge
AIME 2025	30	Math	Integer in $[0, 999]$	Exact match
Brumo 2025	30	Math	Integer or closed-form expression	LLM judge

**Pre-generated pool and cost vectors.** For each (model, benchmark) cell we draw  $N=128$  initial generations per problem ( $N=64$  for Ministral3-14B, where the full  $N=128$  run had not completed at the time of writing), and for prefix-consistency methods we additionally draw  $K$  regenerations per initial sample at the chosen truncation fraction  $\tau$ . All voting and analysis read from this fixed pool, so the same generated tokens back every comparison and the only randomness in the reported numbers is from the analysis-side resampling described below. Each generation carries its actual recorded token count. For each method, the cost of a vote is the cumulative generated-token length of every sample it actually reads. Standard MV, Self-certainty, DeepConf, Response probability, AC, and ESC consume only the initial samples. CISC’s verbalized sources (Verbal binary, Verbal 0–100) and P(True) additionally consume the secondary verbal-rating completions call per sample described in Appendix E. PC additionally reads the regenerated continuations from each sample’s prefix. SubthoughtReasoner reads the continuations regenerated from each subthought boundary.

**Hyperparameter defaults.** Unless otherwise noted, every result in the main paper uses  $\tau=0.75$ ,  $K=1$ , and the power-family weighting  $w^{(n)}(c) = c^n$  for  $n \in \{1, 2, 3\}$ . Sensitivity to alternative choices of  $\tau$  and  $K$  is reported in Appendix D.5.

**Confidence intervals (CIs) and bootstrap conventions.** All CIs reported in this paper are  $2\sigma$ , taken as twice the standard deviation of the trial or bootstrap distribution. The trial Monte Carlo (Sections 4.2 and 4.3) draws  $M = 500$  replicates per (method, benchmark, budget) cell. The parametric ratio bootstrap (Section 4.3) and the cluster bootstrap over problems (Section 4.4) each use 1,000 resamples.

## G.2 $\overline{\text{AUROC}}$ for the Correctness-Predictor Evaluation (Section 4.1)

**Definition of  $\overline{\text{AUROC}}$ .** AUROC denotes the Area Under the Receiver Operating Characteristic curve. Let  $\mathcal{Q}' := \{q \in \mathcal{Q} : 0 < \text{Pass}@1_q < 1\}$  be the subset of problems on which  $\text{AUROC}_q$  and the per-problem rates  $r_{C,q}, r_{W,q}$  are defined, and set  $s_i = c_i(a_i)$  for prefix consistency and  $s_i = s(y_i, \ell_i)$  for the baselines (Appendix E). We score each signal by a per-problem AUROC and macro-average over  $\mathcal{Q}'$ :

$$\text{AUROC}_q := \Pr[s_i > s_j \mid a_i = a_q^*, a_j \neq a_q^*], \quad \overline{\text{AUROC}} := \frac{1}{|\mathcal{Q}'|} \sum_{q \in \mathcal{Q}'} \text{AUROC}_q, \quad (23)$$

where  $i, j$  are independent draws from the  $N$  initial samples on problem  $q$ , and the reported  $r_C, r_W, D$  are means of  $r_{C,q}, r_{W,q}, D_q$  over  $\mathcal{Q}'$ .

**AUROC computation.** For each problem  $q$  with at least one correct and one wrong initial sample, we score the per-problem AUROC (Eq. (23)) by computing the trapezoidal area under the empirical ROC of the signal  $s_i$  on the  $N$  initial samples. Ties contribute  $1/2$ . We exclude problems for which all  $N$  initial samples are correct or all  $N$  initial samples are wrong (the AUROC and per-problem rates  $r_{C,q}, r_{W,q}$  are undefined there) and macro-average over the surviving problems  $\mathcal{Q}'$ , weighting each problem equally rather than weighting by the number of cross-class pairs. Table 2 reports this macro  $\overline{\text{AUROC}}$ , and the per-problem rates  $r_C, r_W, D$  in Table 1 are macro-averaged over the same  $\mathcal{Q}'$ .

For prefix consistency, the binary score  $c_i(a_i) \in \{1/2, 1\}$  has only one non-trivial operating point on the false-positive/true-positive rate plane,  $(\text{FPR}, \text{TPR}) = (r_{W,q}, r_{C,q})$ , so the trapezoidal area gives  $\text{AUROC}_q = (1 + D_q)/2$ . Tables 1 and 2 therefore encode the same information for prefix consistency, and the  $\overline{\text{AUROC}}$  ordering across benchmarks matches the  $D$  ordering.

## G.3 Cost-Accuracy Evaluation (Sections 4.2 and 4.3)

**Sample-with-replacement trials.** At each token budget  $B$  we draw samples from the pool with replacement until the cumulative cost reaches  $B$ , then run each method’s voting rule on the drawn set and report the mean accuracy over the  $M$  trials. The trial-mean variance used to derive the CI is  $\sigma^2 = \frac{1}{M|\mathcal{Q}'|^2} \sum_q \hat{p}_q(1 - \hat{p}_q)$ , where  $\hat{p}_q$  is the trial-mean correctness on problem  $q$  and  $|\mathcal{Q}'|$  is the number of problems. This Monte Carlo CI is what is shown as “ $\pm$ ” in Table 3.

**Dense token-budget grid.** Token-efficiency ratios in Table 4 require evaluating the cost–accuracy curve at arbitrary target budgets, so we evaluate every method on the log-uniform grid

$$\mathcal{B} = \{10^{3+k/100} : k = 0, 1, \dots, 400\}.$$

The dense grid is used for all methods that admit a continuous budget (Standard MV, PC variants, DeepConf, CISC, P(True), Response probability). AC and ESC instead contribute their natural-stopping points (one per swept hyperparameter) as described in Appendix E.

**Standard MV plateau and Pass@1.** The Standard MV plateau is Standard MV’s bootstrap-saturated accuracy on the  $N$ -sample initial pool, taken as Standard MV’s stored accuracy at  $\max \mathcal{B} = 10^7$  tokens. We use this finite-budget anchor rather than the unbounded i.i.d. asymptote (which is pool-determined but, on slow-converging problems, can sit above what any finite budget reaches) so that the target stays reachable by Standard MV at every  $\alpha \in [0, 1]$ . Pass@1 is the closed-form expected accuracy of a single uniformly drawn pool sample, computed directly from the pool.

**Monotone envelope and log-budget interpolation.** Each method’s grid of (budget, accuracy) points is reduced to its running-max envelope along sorted budget (so accuracy is non-decreasing in budget). This gives the “min budget at which the method has ever reached this accuracy” semantics that the token-efficiency ratio is meant to compare. To read off the budget at a target accuracy  $\text{acc}_{\text{tgt}}$ , we find the first envelope segment  $(B^{(j-1)}, \text{acc}^{(j-1)}) \rightarrow (B^{(j)}, \text{acc}^{(j)})$  that brackets  $\text{acc}_{\text{tgt}}$  and linearly interpolate in (accuracy, log-budget):

$$\log B_{\text{tgt}} = \log B^{(j-1)} + \frac{\text{acc}_{\text{tgt}} - \text{acc}^{(j-1)}}{\text{acc}^{(j)} - \text{acc}^{(j-1)}} \cdot (\log B^{(j)} - \log B^{(j-1)}).$$

The same rule applies to AC and ESC, whose curves are the natural-stopping point lists.

**Parametric bootstrap for ratio CIs.** Confidence intervals on  $B_{\text{method}}/B_{\text{MV}}$  come from a parametric bootstrap with the same trial Monte Carlo noise model used by Table 3. Each draw perturbs every fixed-budget accuracy entry by independent  $\mathcal{N}(0, \sigma_{\text{acc}}^2)$  noise with  $\sigma_{\text{acc}} = \text{CI}_{\text{acc}}/2$  (one  $\sigma$  from the stored  $2\sigma$  CI), and additionally perturbs each natural-stopping operating point’s cost by  $\mathcal{N}(0, \sigma_{\text{cost}}^2)$  noise with  $\sigma_{\text{cost}} = \text{CI}_{\text{cost}}/2$  (the trial-MC standard error of the natural-stopping cost, which varies across operating points unlike the fixed-budget cost). The plateau is perturbed by an analogous draw using its own CI. Each replicate then recomputes the envelope, the target  $\text{acc}_{\text{tgt}} = \text{Pass@1} + \alpha \cdot (\text{plateau}' - \text{Pass@1})$  with the perturbed plateau  $\text{plateau}'$ , and the ratio. Pass@1 is closed-form over the pool (deterministic) and is held fixed across draws. Anchoring the plateau to Standard MV’s stored accuracy at  $\max \mathcal{B}$  rather than to the running-max envelope’s max breaks the upward extreme-value bias that an iid + running-max combination would otherwise inject near the plateau. Cells where the method’s monotone envelope does not reach the target on the point estimate are reported as “N/A”. The CI subscript is additionally suppressed (point estimate shown alone) when fewer than 50% of bootstrap draws reach the target.

#### G.4 Reproduction-Rate GLM (Section 4.4)

**Logistic GLM and cluster bootstrap.** The slopes  $\beta(r_C)$  and  $\beta(r_W)$  in Section 4.4 and Table 19 are the Pass@1 coefficients of a per-(model, category) logistic GLM fit on the expanded per-trial Bernoulli outcomes:  $\text{logit } r_C$  (and separately  $\text{logit } r_W$ ) is fit as an affine function of Pass@1, where each (correct initial sample, regeneration) pair contributes one trial to the  $r_C$  fit, each (wrong initial sample, regeneration) pair contributes one trial to the  $r_W$  fit, and every trial carries the source problem’s Pass@1 as its covariate. The fit uses statsmodels’ GLM with a binomial family. CIs and  $p$ -values come from a joint cluster bootstrap over whole problems: each resample draws problems with replacement (preserving each problem’s full set of trials) and refits the GLM. We report band-widths from the bootstrap distribution and two-sided  $p$ -values from the empirical sign distribution.

## H Answer Extraction and Equivalence Judging

Final answers are extracted from `\boxed{\}` via regex and normalized.

## H.1 Answer Extraction

**Boxed-answer parses.** Failed boxed responses receive no vote in any aggregator (Standard MV, PC, DeepConf, CISC), so they only ever lower the effective sample count, never bias the vote distribution toward a wrong answer. Seventeen of the twenty cells stay below 1% on both Generations and Continuations (Table 22). The three cells that exceed 1% on continuations all involve Nemotron3-30B: FrontierScience-Olympiad (0.17%  $\rightarrow$  1.62%), AIME 2025 (0.00%  $\rightarrow$  1.17%), and Brumo 2025 (4.14%  $\rightarrow$  1.25%, the only cell with generations also above 1%). We treat boxed parse failures as missing votes rather than as a separate signal because the rate is small enough that it does not move the relative comparisons reported in the paper.

Table 22: **Extraction failure rate.** Boxed columns: percentage of generated answers for which the parser found neither a `\boxed{...}` expression nor a usable numeric fallback. Generations pools over (problem, sample) on the original full generation; Continuations pools over (problem, sample, regen) on  $K=1$  completions from the truncation point onward ( $\tau=0.75$ ). Verbal columns: percentage of secondary completions whose confidence value could not be extracted (0–100 = CISC value, Binary = “Is your answer correct? 0/1” verdict, P(True) = logprob of the binary call’s “1” token; the latter two share the same secondary call). Failure handling in downstream aggregators is described in Appendix H.1. Pooled totals across all 20 cells: 0.25% (Generations), 0.42% (Continuations), 12.82% (Binary), 27.31% (0–100), 0.01% (P(True)). Boxed-extraction rates are flat across  $\tau \in \{0.25, 0.50, 0.75\}$  (within 0.05 pp) on the cells where multiple  $\tau$  are available.

Model	Dataset	$N$	Boxed extraction (%)		Verbal queries (%)		
			Generations	Continuations	0–100	Binary	P(True)
GPT-OSS-120B	FrontierScience-Olympiad	128	0.08	0.05	42.99	12.04	0.00
	HMMT Feb 2026	128	0.00	0.02	47.61	25.14	0.00
	AIME 2025	128	0.00	0.00	48.07	21.59	0.00
	Brumo 2025	128	0.00	0.00	44.87	19.92	0.00
GPT-OSS-20B	FrontierScience-Olympiad	128	0.31	0.35	19.38	8.21	0.00
	HMMT Feb 2026	128	0.00	0.05	26.07	24.76	0.00
	AIME 2025	128	0.03	0.03	55.65	30.60	0.00
	Brumo 2025	128	0.00	0.00	51.67	29.19	0.00
Nemotron3-30B	FrontierScience-Olympiad	128	0.17	1.62	48.77	18.92	0.00
	HMMT Feb 2026	128	0.54	0.59	44.06	18.73	0.00
	AIME 2025	128	0.00	1.17	47.53	20.34	0.00
	Brumo 2025	128	4.14	1.25	42.57	18.90	0.00
Nemotron2-9B	FrontierScience-Olympiad	128	0.03	0.38	0.00	0.03	0.00
	HMMT Feb 2026	128	0.00	0.33	0.00	0.24	0.00
	AIME 2025	128	0.00	0.21	0.00	0.00	0.00
	Brumo 2025	128	0.16	0.08	0.16	0.23	0.16
Ministral3-14B	FrontierScience-Olympiad	64	0.28	0.27	0.02	7.41	0.00
	HMMT Feb 2026	64	0.05	0.05	0.28	6.01	0.00
	AIME 2025	64	0.00	0.00	0.21	10.10	0.00
	Brumo 2025	64	0.00	0.05	0.05	6.98	0.00

**Verbal score handling.** For the verbal-confidence calls used by CISC, Verbal binary, and P(True), the parser fails when the secondary completion does not yield an integer in the requested range (a 0–100 value for CISC, a 0/1 verdict for Verbal binary). P(True) reads the logprob of the binary call’s “1” token directly, so it is essentially never missing. Verbal failure rates show wide model spread, under 1% for Nemotron2-9B and Ministral3-14B versus 19%–56% for GPT-OSS and Nemotron3-30B on Verbal 0–100 (Table 22). The two analyses that consume verbal scores handle parse failures charitably to the verbal baselines: the AUROC table (Table 2) drops failures, while the WMV pipeline imputes the per-problem median (Appendix E). Dropping the sample from the WMV pool would bias the per-problem answer distribution if failures correlate with the boxed answer, and would also hide the parser-failure rate from the evaluation. Keeping each failure at its natural pool frequency instead mirrors the deployment-time behavior in which a fresh draw would re-incur the same parse error rate. We therefore treat parser fragility as an intrinsic property of the baseline, with each failure contributing a neutrally-weighted vote. Table 23 reports AUROC under both modes side-by-side. The gap is at most 0.031 on every cell, so failure handling does not change the best signal on any cell.

Table 23: **Verbal-confidence AUROC sensitivity to failure handling.** For Verbal 0–100 and Verbal binary, macro-averaged AUROC under (i) *drop*, the convention used by Table 2 that excludes samples whose verbal score failed to parse, and (ii) *imputed*, the convention used by the WMV pipeline that substitutes the per-problem median of the non-missing scores so the parsed answer still casts a neutrally-weighted vote (Appendix E). Per-cell verbal-extraction failure rates are shown for context. Cells where every sample fails (fail = 100%) leave both modes undefined (“–”).

Signal / mode	GPT-OSS-120B				GPT-OSS-20B				Nemotron3-30B				Nemotron2-9B				Ministral3-14B			
	FSci	HMMT	AIME	Brumo	FSci	HMMT	AIME	Brumo	FSci	HMMT	AIME	Brumo	FSci	HMMT	AIME	Brumo	FSci	HMMT	AIME	Brumo
<i>Verbal 0–100</i>																				
drop	.516	.552	.505	.436	.516	.574	.561	.511	.524	.489	.606	.532	.571	.563	.584	.548	.505	.525	.525	.450
imputed	.510	.536	.501	.448	.514	.559	.550	.506	.520	.491	.579	.534	.571	.563	.584	.548	.505	.525	.525	.450
fail (%)	43.0	47.6	48.1	44.9	19.3	26.1	55.6	51.7	48.7	44.1	47.5	42.4	0.0	0.0	0.0	0.0	0.0	0.3	0.2	0.1
<i>Verbal binary</i>																				
drop	.530	.591	.583	.554	.542	.573	.561	.526	.515	.524	.536	.477	.496	.504	.505	.504	.470	.457	.474	.495
imputed	.527	.560	.555	.529	.542	.564	.549	.523	.515	.520	.544	.478	.496	.504	.505	.504	.475	.458	.471	.496
fail (%)	12.0	25.1	21.6	19.9	8.2	24.8	30.6	29.2	18.9	18.7	20.3	18.3	0.0	0.2	0.0	0.1	7.4	6.0	10.1	7.0

Abbreviations: FSci = FrontierScience-Olympiad, HMMT = HMMT Feb 2026, AIME = AIME 2025, Brumo = Brumo 2025.

The secondary-call token cost is charged regardless of parse success, so a high failure rate raises the per-vote cost rather than reducing the effective sample count.

**Verbal 0–100 parser fragility.** The parser splits the model’s response on the first “)” and scans for any digit before it, expecting a near-immediate “<digit>” completion (the prompt suffix already opens an explicit “Proposed confidence: (”). The dominant failure pattern is a parenthetical or commentary token landing before the digit, for example “score) 70”, “analysis) 87 (commentary?) (final) 93”, “rating)\n\n\*\*70\*\*.”, “(C) 80%”, and “value). \n(If you think...).”. A smaller share of failures is completions with no digit at all, such as “score). That is this answer: \*\*safe\*\*.”. The model that does not fail at all, Nemotron2-9B, has a median successful response length of just 5 tokens, indicating that it emits “<digit>” and stops. The failing models have median successful lengths of 30–200 tokens, meaning even their successful completions wander past the digit and leave many opportunities for parenthetical content to land before any number. This fragility illustrates a broader challenge of porting verbalized-confidence baselines, originally designed for instruction-following models that snap to a strict response template, to reasoning models that interleave thinking, commentary, and LaTeX before committing to a structured output. The original CISC and P(True) papers validated these methods only on instruction-tuned (non-reasoning) models that reliably follow the structured response template. We extend the same prompt and parser to reasoning models without modification, and a fully robust implementation in this regime would require redesigning both the elicitation prompt and the parser.

## H.2 Equivalence Judging

**Judge configuration.** AIME 2025 is scored by exact match on the normalized answer (integer). For benchmarks where multiple surface forms can denote the same answer (HMMT Feb 2026, Brumo 2025, and FrontierScience-Olympiad), equivalence is determined by an LLM judge: the FrontierScience-Olympiad prompt follows the official grader released with the benchmark [Wang et al., 2025, Appendix B], and the math prompt follows the format used in MathArena [Balunović et al., 2025] and similar competition-math evaluations. Both prompts return a single-token “YES”/“NO” verdict which is mapped to an equivalence edge. Transitive closure over these edges yields canonical answer clusters for each problem.

Using the evaluated model as its own judge is a known limitation: a stronger external grader could shift absolute accuracies. We verify in Appendix D.6 that this does not change the relative comparisons reported here: re-scoring the pool with Claude Sonnet 4.6 on a 4-model, 3-benchmark subset (12 cells) preserves the sign of  $\overline{\text{AUROC}}_{\text{PC}} - \overline{\text{AUROC}}_{\text{best baseline}}$  on all 12 cells (no cell flips), and the per-cell ordering of WMV methods is preserved at every operating point.

The full prompts used are:

### FrontierScience-Olympiad.

You are grading an attempted answer to a science olympiad problem. You will be given the attempted answer and the reference answer. Evaluate strictly, but fairly. The reference answer is either a single number or expression in latex formatting, a chemical formula, a compound name, or a phrase referring to a specific name, entity, or method. Mark the attempted answer as correct if it fully matches the reference answer or is otherwise equivalent (e.g., an equivalent algebraic expression, a numerical number within 1 decimal place rounding of the reference answer (e.g.,  $6.69 \approx 6.7$ ), an equivalent name for a compound/formula, equivalent when accounting for units, etc.). Mark it as incorrect if it is not equivalent to the reference answer.

Attempted answer: {answer1}

Reference answer: {answer2}

Answer only ‘YES’ if correct or ‘NO’ if incorrect.

### HMMT Feb 2026, Brumo 2025.

Determine whether two mathematical answers are numerically identical.

Answer 1: {answer1}

Answer 2: {answer2}

Criteria:

- If they represent exactly the same numerical value, respond ‘YES’
- If they represent different values or one is not numerical, respond ‘NO’
- Different formats (fractions, decimals, radicals, exponential notation) are acceptable if numerically equivalent

Examples: ‘1/2’ and ‘0.5’ → YES; ‘ $\sqrt{4}$ ’ and ‘2’ → YES; ‘ $2^3$ ’ and ‘8’ → YES; ‘3.14’ and ‘ $\pi$ ’ → NO; ‘x+1’ and ‘1+x’ → YES; ‘ $x^2$ ’ and ‘2x’ → NO.

Answer only ‘YES’ or ‘NO’.

## I Reproducibility Statement

**Code and data.** The analysis pipeline and reproduction scripts are released at <https://github.com/naoto-iwase/prefix-consistency>, and the answer pool used to reproduce all reported numbers is released at <https://doi.org/10.5281/zenodo.20082164>.

Models and datasets are publicly available (Table 24). Initial generation is stochastic (no vLLM seed), but aggregation and voting use seed 42, so every reported number is bitwise reproducible from the pool.

**Inference and sampling.** Each model is served through a vLLM OpenAI-compatible endpoint on  $4 \times$  NVIDIA A100 80GB GPUs, with context window 131,072 and a maximum output length of 100,000 tokens. Sampling uses each model’s recommended settings (Table 25).

Table 26 reports per-generation token counts at the default  $\tau=0.75$  for all models, with the additional  $\tau \in \{0.50, 0.25\}$  values reported for GPT-OSS-20B (the model used in the  $\tau$ -sensitivity sweep of Appendix D.5).

**Generation prompts.** For the three math benchmarks (HMMT Feb 2026, AIME 2025, Brumo 2025) the system prompt is “*You are a helpful assistant specialized in solving mathematical problems.*” For FrontierScience-Olympiad it is “*You are an expert scientist solving olympiad-level problems in physics, chemistry, and biology.*” Both append “*Please reason step by step, and put your final answer within `\boxed{\}`.*” to each problem statement. Initial samples and the regenerated continuations from each truncation point share the same prompt.

Table 24: **Models and datasets used in the experiments.** License names follow the original release pages. Please verify before redistribution.

Name	Reference	License
<i>Models</i>		
GPT-OSS-120B [OpenAI, 2025]	<a href="https://huggingface.co/openai/gpt-oss-120b">https://huggingface.co/openai/gpt-oss-120b</a>	Apache 2.0
GPT-OSS-20B [OpenAI, 2025]	<a href="https://huggingface.co/openai/gpt-oss-20b">https://huggingface.co/openai/gpt-oss-20b</a>	Apache 2.0
Nemotron3-30B [NVIDIA, 2025a]	<a href="https://huggingface.co/nvidia/NVIDIA-Nemotron-3-Nano-30B-A3B-BF16">https://huggingface.co/nvidia/NVIDIA-Nemotron-3-Nano-30B-A3B-BF16</a>	NVIDIA Open Model License
Nemotron2-9B [NVIDIA, 2025b]	<a href="https://huggingface.co/nvidia/NVIDIA-Nemotron-Nano-9B-v2">https://huggingface.co/nvidia/NVIDIA-Nemotron-Nano-9B-v2</a>	NVIDIA Open Model License
Ministral3-14B [Mistral AI, 2026]	<a href="https://huggingface.co/mistralai/Ministral-3-14B-Reasoning-2512">https://huggingface.co/mistralai/Ministral-3-14B-Reasoning-2512</a>	Apache 2.0
<i>Datasets</i>		
AIME 2025 [Balunović et al., 2025]	<a href="https://huggingface.co/datasets/MathArena/aime_2025">https://huggingface.co/datasets/MathArena/aime_2025</a>	CC BY-NC-SA 4.0
HMMT Feb 2026 [Balunović et al., 2025]	<a href="https://huggingface.co/datasets/MathArena/hmmt_feb_2026">https://huggingface.co/datasets/MathArena/hmmt_feb_2026</a>	CC BY-NC-SA 4.0
Brumo 2025 [Balunović et al., 2025]	<a href="https://huggingface.co/datasets/MathArena/brumo_2025">https://huggingface.co/datasets/MathArena/brumo_2025</a>	CC BY-NC-SA 4.0
FrontierScience-Olympiad [Wang et al., 2025]	<a href="https://huggingface.co/datasets/openai/frontierscience">https://huggingface.co/datasets/openai/frontierscience</a>	Apache 2.0

Table 25: **Sampling settings per model.** Values follow each model’s recommended configuration on its release page.

Model	temperature	top_p	top_k	reasoning_effort
GPT-OSS-120B	1.0	1.0	40	medium
GPT-OSS-20B	1.0	1.0	40	medium
Nemotron3-30B	1.0	1.0	20	–
Nemotron2-9B	0.6	0.95	20	–
Ministral3-14B	0.7	0.95	20	–

Table 26: **Average output tokens per generation.** Generations is the original full generation. Continuations are completions from the truncation point onward ( $K=1$ ). Verbal queries are secondary completions on each init sample: 0–100 elicits the CISC confidence value, Binary elicits a 0/1 verdict (the binary completion’s logprob is also the P(True) signal). All values are means of actual generated tokens over every (problem, sample) pair.  $N$  is the number of answers per problem.

Model	Dataset	$N$	Generations	Continuations			Verbal queries	
				$\tau=0.75$	$\tau=0.50$	$\tau=0.25$	0–100	Binary
GPT-OSS-120B	FrontierScience-Olympiad	128	3,341	945	–	–	322	196
	HMMT Feb 2026	128	6,925	2,199	–	–	246	182
	AIME 2025	128	5,442	1,668	–	–	262	220
	Brumo 2025	128	4,782	1,493	–	–	246	190
GPT-OSS-20B	FrontierScience-Olympiad	128	7,813	2,631	4,426	5,906	230	210
	HMMT Feb 2026	128	13,707	4,621	7,992	10,941	295	290
	AIME 2025	128	11,159	3,598	6,232	8,564	273	388
	Brumo 2025	128	9,208	3,056	5,323	7,151	277	308
Nemotron3-30B	FrontierScience-Olympiad	128	29,064	8,333	–	–	1,419	103
	HMMT Feb 2026	128	39,816	12,618	–	–	308	149
	AIME 2025	128	28,941	7,313	–	–	281	119
	Brumo 2025	128	22,243	5,859	–	–	1,158	274
Nemotron2-9B	FrontierScience-Olympiad	128	10,124	3,016	–	–	13	3
	HMMT Feb 2026	128	14,216	4,172	–	–	8	4
	AIME 2025	128	11,715	3,498	–	–	10	3
	Brumo 2025	128	9,634	3,125	–	–	10	5
Ministral3-14B	FrontierScience-Olympiad	64	9,671	5,834	–	–	1,940	1,778
	HMMT Feb 2026	64	8,388	4,560	–	–	2,161	1,768
	AIME 2025	64	7,590	3,735	–	–	1,735	1,451
	Brumo 2025	64	7,739	3,994	–	–	1,802	1,277